

Alma Mater Studiorum – Università di Bologna

DOTTORATO DI RICERCA IN

Scienze Farmaceutiche

Ciclo XXIV

Settore Concorsuale di afferenza: CHIM/06

**SYNTHESIS AND SUPRAMOLECULAR ARCHITECTURES
OF LIPOPHILIC DERIVATIVES OF GUANINE**

▪

Presentata da: **ROSARIA CARMELA PERONE**

Coordinatore Dottorato

Relatore

Prof.Maurizio Recanatini

Prof.Gian Piero Spada

Esame finale anno 2012

Abstract

L'auto-assemblaggio è descritto come il processo mediante il quale un sistema disordinato di componenti pre-esistenti forma una struttura supramolecolare, in conseguenza di specifiche interazioni deboli tra i componenti del sistema stesso. Studi precedenti, hanno evidenziato la capacità di auto-assemblaggio di derivati lipofili delle guanosine; tali composti sono capaci di estrarre degli ioni dalla fase acquosa e trasportarli in fase organica mediante la formazione di specifiche strutture supramolecolari. In presenza di cationi le guanosine lipofile formano aggregati colonnari mentre in loro assenza generano delle strutture nastriformi. Lo scopo principale della seguente tesi è stato la sintesi di derivati lipofili della guanina, in particolare di derivati della guanina alchilati in posizione N9 e di un derivato della guanosina funzionalizzato con un sostituito perclorotrifenilmetilico (PTM). Lo scopo principale era osservare in che modo l'assenza dello zucchero, in un caso, e la presenza di un sostituito chirale con un elevato ingombro sterico (Gace α HPTM) nell'altro, potessero influenzare il comportamento supramolecolare delle molecole sintetizzate. Utilizzando le guanine invece delle guanosine, non solo vengono conservati tutti i gruppi donatori e accettori di legami a idrogeno richiesti per l'aggregazione supramolecolare, ma viene ridotto l'ingombro sterico che in alcuni casi ostacola la formazione di aggregati (guanine con sostituiti in N9 diversi dallo zucchero possiedono una maggiore libertà conformazionale anche in presenza di un gruppo ingombrato in posizione C8 della guanosina). L'auto-assemblaggio di derivati lipofili della guanina è stato studiato in soluzione mediante spettroscopia NMR e dicroismo circolare mentre su superficie lo studio è stato effettuato mediante STM (scanning tunneling microscopy). Allo stesso modo dei derivati lipofili della guanosina, i seguenti derivati formano strutture nastriformi e colonnari variando le condizioni sperimentali.

Abstract

Self-assembly relies on the association of pre-programmed building blocks through non-covalent interactions to give complex supramolecular architectures. Previous studies provided evidence for the unique self-assembly properties of semi-synthetic lipophilic guanosine derivatives which can sequester ions from an aqueous phase, carry them into an organic phase where they promote the generation of well-defined supramolecular assemblies. In the presence of cations lipophilic guanosines form columnar aggregates while in their absence they generate supramolecular ribbons. The aim of this thesis has been the synthesis of guanine derivatives, in particular N9-alkylated guanines and a guanosine functionalized as a perchlorotriphenylmethyl moiety (Gace α HPTM) in order to observe their supramolecular behaviour in the absence of sugar (ribose or deoxyribose) and in the presence of a bulky and chiral substituent respectively. By using guanine instead of guanosine, while maintaining all the hydrogen bond acceptor and donor groups required for supramolecular aggregation, the steric hindrance to supramolecular aggregation is notably reduced because (i.e. guanines with groups in N9 different from sugar are expected to have a greatest conformational freedom even in presence of bulky groups in C8). Supramolecular self-assembly of these derivatives has been accomplished in solutions by NMR and CD spectroscopy and on surface by STM technique. In analogy with other guanosine derivatives, also N9-substituted guanines and GAcce α HPTM form either ribbon-like aggregates or cation-templated G-quartet based columnar structures.

Table of contents

Chapter 1. Introduction

1.1 Concepts	2
1.2 Supramolecular chemistry	2
1.3 Self-assembly in supramolecular system	4
1.4 Guanine and G-quartet	5
1.5 DNA G-quadruplexes and their functions	7
1.5.1 Telomers and telomerases	9
1.5.2 Transcription	11
1.5.3 G-quadruplexes ligands	12
1.5.4 Methods for studying G-quadruplexes	14
1.6. Conclusions	19
References	20

Chapter 2. Supramolecular organization of guanosine derivative

2.1 Concepts	24
2.2 G-quartet based assemblies	24
2.3 Linear ribbon of guanosine	29
2.4 Switching between supramolecular assemblies of Lipo-G.	33
2.4.1 Addition/removal of cations	34
2.4.2 Variation of solvent polarity	36
2.4.3 UV-VIS irradiation	37
2.5 Conclusions	39
References	40

Chapter 3. N⁹-alkyl guanines	
3.1 Concepts	44
3.2 Synthetic approaches	45
3.3 Supramolecular studies in solution	49
3.4 N ⁹ -alkylated guanines: STM study	55
3.4.1 Introduction	55
3.4.2 Results and discussions	59
3.4.3 Conclusions	64
3.5 Reversible assembly/ Reassembly process	65
References	69
Chapter 4. Synthesis of a guanosine functionalized as PTM derivatives	
4.1 Concepts	73
4.2 Overview on PTM derivatives	75
4.2.1 Synthesis of PTM radicals	77
4.2.2 PTM properties	78
4.3 α HPTM-GACE: synthetic approaches	83
4.4 α HPTM-GACE: studies in solution	89
References	98
Chapter 5. Experimental part	102
References	127

As the wind of time blows into the sails of space, the unfolding of the universe nurtures the evolution of matter under the pressure of information. From divided to condensed and on to organized, living, and thinking matter, the path is toward an increase in complexity through self-organization. (J.M.Lehn)

1 Introduction

1.1 Concepts

Molecular chemistry has created a wide range of ever more sophisticated molecules and materials. Supramolecular chemistry aims at developing highly complex chemical systems from molecular components interacting via non-covalent intermolecular forces. Through the appropriate manipulation of these interactions, it became progressively the chemistry of molecular information at molecular level.^[1]

1.2 Supramolecular Chemistry

Supramolecular chemistry is often defined as being “*chemistry beyond the molecule*”, which is rather vague expression. Therefore, in order to get across the basic concepts of *supramolecules* and *supramolecular chemistry*, it could be worth using an analogy of daily life. Many sports involve teams of players, one of the main objectives in such sports is to organize the team such that the performance of team is significantly greater than the sum of the performances of each team –member. This concept of a good team being greater than the sum of its part can also be applied to a supermolecule. Indeed according to Dr. Lehn , a supermolecule is an organized, complex entity that is created from the association of two or more chemical species held together by intermolecular forces. Supramolecular structures are the result of not only additive but also cooperative interactions, including electrostatic interactions, hydrogen bonding, π – π interactions ,dispersion and hydrophobic interactions, and their properties are different than the sum of the properties of each individual component.

Supramolecular chemistry can be classified into three categories:

- chemistry associated with a molecule recognizing a partner molecule
- chemistry of molecules built to specific shape
- chemistry of molecular assembly from numerous molecule.

This classification is deeply related to the size of target molecular system. Molecular recognition chemistry generally deals with the smallest supramolecular systems and encompasses interaction between just a few molecules. In contrast, the chemistry of molecular assemblies can include molecular systems made from countless number of

molecules.^[2] Molecular recognition can be regarded in many ways as the most fundamental kind of supramolecular chemistry. Its importance came to light in the middle of nineteenth century before the concept of supramolecules was established. During microscopic observation Pasteur noticed that crystals of tartaric acid occurred in two types, that were mirror images of each other, and found that mold and yeast recognize and utilize only one of this types. In 1894 Emil Fischer proposed *the lock and key* mechanism, this concept proposed that the mechanism by which an enzyme recognizes and interacts with a substrate can be likened to a lock and key system. In 1967 Cram established a new field of chemistry *host-guest chemistry*, where the host component is defined as an organic molecule or ion whose binding sites converge in the complex and the guest component is any molecule or ion whose binding sites diverge in the complex.^[3] Only in 1978 J.M. Lehn attempted to organize these novel chemistries and proposed the term *supramolecular chemistry*.

Such supramolecules have geometrically specific shapes for example rotaxane which contains molecules that are threaded by linear molecules or catenane which contains entangled molecular rings. These molecules can be obtained introducing a strategy based on supramolecular chemistry. Controlled molecular association results in the spontaneous formation of supramolecules with specific shape and characteristics. This process is called *self-assembly or self-organization*. This process can be distinguished in two types: *strict* or *looser*. The first type involves associations formed through hydrogen bonds, in the other type the main binding forces come from hydrophobic interactions in aqueous media.

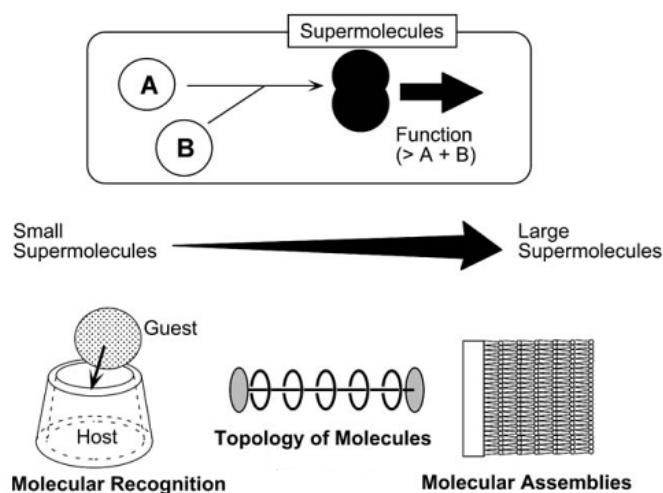


Figure 1: World of supramolecules

1.3 Self-assembly in supramolecular system

Self-assembly may be defined as the process by which a supramolecular species forms spontaneously from its components. Generally we can make two distinctions between static self-assembly (SSA) and dynamic self-assembly (DySA) by considering the thermodynamic description of the resulting assemblies (fig.1 2)^[4].

SSA refers to a stable *equilibrium* structures by a maximum(local or global) in the system's entropy and no systematic energy flows, examples are organic and inorganic crystals, block copolymer assemblies and supramolecular system.

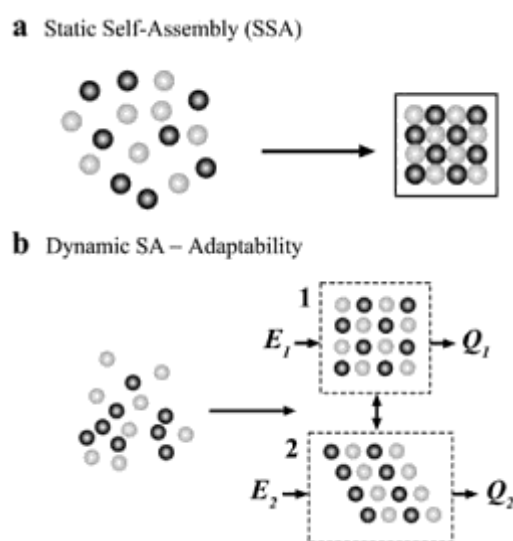


Figure 1.2. Schematic representations of (a) static and dynamic self-assembly (b). (a) In static self-assembly, components form an ordered, thermodynamically isolated aggregate whose structure does not change in time. (b) Dynamic self-assembly involves a disordered collection of components in an ordered structure through input of energy from an external source and dissipates this energy on the environment.

Biological system aside, self-assembly is also a common place throughout chemistry: the growth of crystals, the formation of liquid crystals, the spontaneous generation of synthetic lipid bilayers, the synthesis of metal co-ordination complexes and the alignment of molecules on surfaces are but a few of the many manifestation of self-assembly in chemical systems. Whereas self-assembly may be taken as a simple collection and aggregation of components into a confined entity, we shall considered self-organization as the spontaneous but information-directed generation of organized functional structures in equilibrium conditions.^[1] These structures are held together by a variety of

weak non covalent interactions as: hydrogen bonding, π - π stacking, dipolar interactions, van der Waals forces and hydrophobic interactions. A distinctive feature of using this weak forces in molecular assemblies is that such interactions are normally readily reversible, so that the final product is in thermodynamic equilibrium with its components. This leads to an additional property of most supramolecular systems: they have an built-in capacity of *error-correction* not available to covalent systems. Among non-covalent interactions the use of hydrogen bonding and π - π interactions have tended to receive most attention in the design of supramolecular system but van der Waals considerations are often also of crucial importance. A self-organization process may be considered to involve three main stages :

- Molecular recognition for the selective binding of the basic components.
- Growth through sequential binding of multiple components in the correct relative disposition.
- Termination of the process, requiring a built-in feature, a stop signal, that specifies the end point.

Suitable encoding by manipulation of structural subunits and processing through interactional algorithms should give access to a variety of systems.

1.4 Guanine and G-quartets

Nucleobases have been proposed as basic units of supramolecular motifs due to the potential non-covalent interactions.^[5] They are well known for their ability to form complementary H-bonds with their base pairs. The double helix of DNA is due to the canonical Watson and Crick base pairing (fig. 1.3), adenine forms a pair with thymine and guanosine with cytosine.

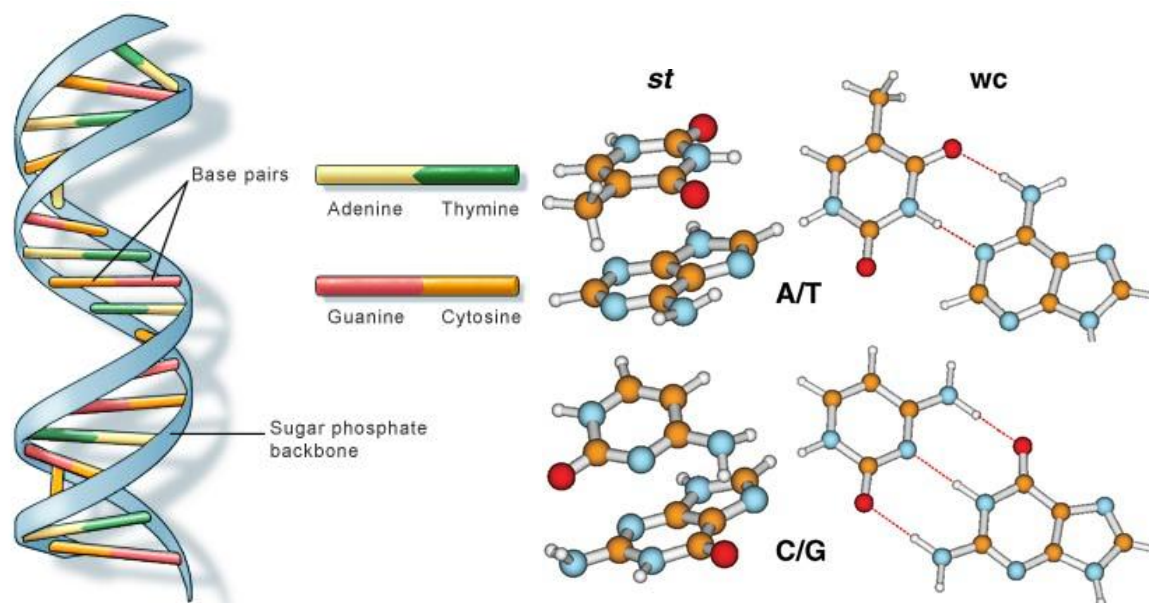


Figure 1.3

However alternative hydrogen bonding patterns, such as the Hoogsteen base pairing can occur giving rise to complex and functional tertiary structures. This one implies the N7 position (as a hydrogen bond acceptor) and C6 amino group (as a donor) of the purine base, which bind the Watson-Crick (N3–N4) edge of the pyrimidine base.

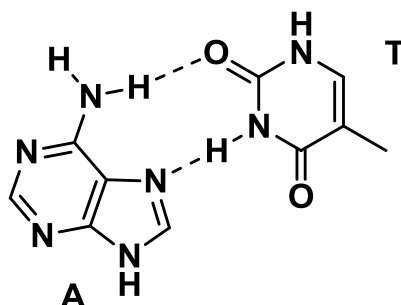


Figure 1.4: Hoogsteen base pair adenine-thymine

Among the other nucleobases, guanine is the most versatile indeed as it contains both a Watson-Crick edge and Hoogsteen edge.^[6] Moreover, the Watson-Crick edge has two hydrogen bond donors (N¹H, N²H) that can hydrogen bond with the two hydrogen bond acceptors (O⁶, N³ and N⁷) on the Hoogsteen edge. This leads guanine to form different supramolecular structures. Among these the most known is the so-called *G-quartet* which is a macrocyclic array of four guanines, hydrogen bonded through their self-complementary Watson-Crick (N¹H and N²H) and Hoogsteen (O⁶ and N⁷) edges.^[7] In addition, guanine can form two *ribbon-like* structures, characterized by different hydrogen-bonded patterns.

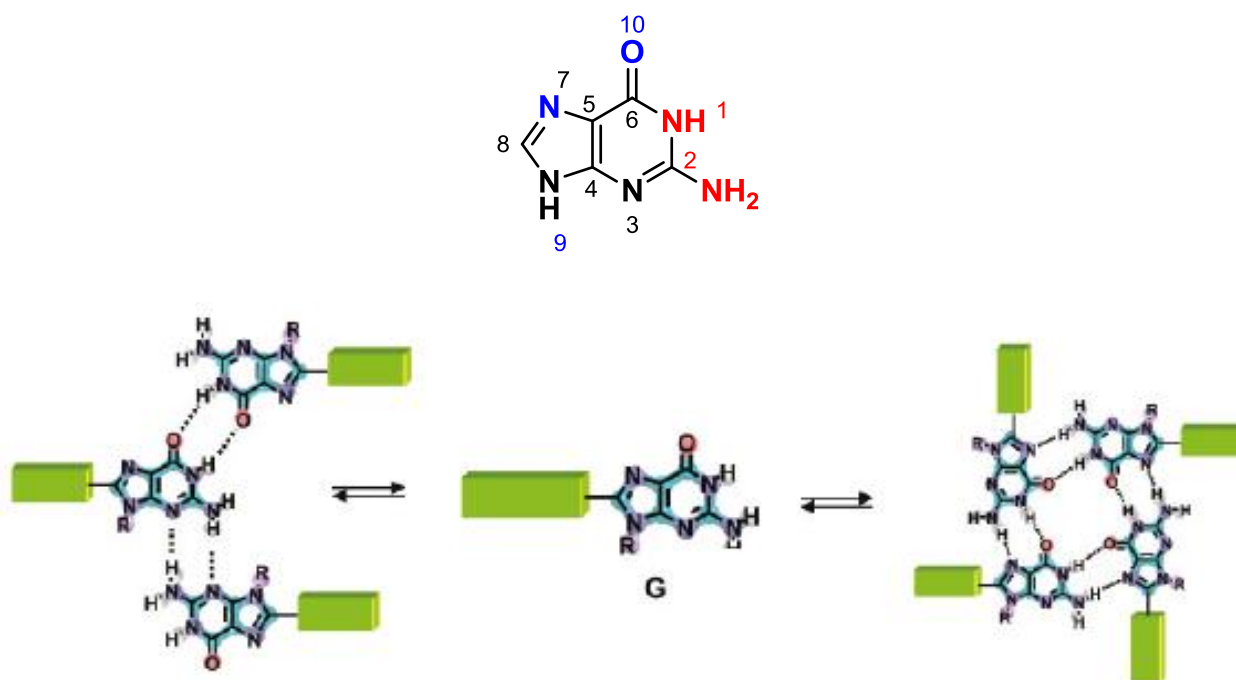


Figure 1.5 Guanine and supramolecular structure Schematic representation of the equilibrium between a ribbon (left) and a G-quartet structure (right). Figure ref [8]

1.5 DNA G-quadruplexes and their functions

The G-quartet was identified by Davies and coworkers in 1962 as the structural unit behind hydrogels formed by 5'-guanosine monophosphate (5'-GMP).^[9] But, only several years later did the possible biological relevance of DNA structures based on this moiety begin to be addressed.^[10] *G-quadruplexes*, have a core that is made up of guanine bases only, with four guanines arranged in a rotationally symmetric manner, and held together hydrogen bonds between N1–O6 and N2–N7 around the edges of the resulting square.^[11] These planar structures are called G-quartets, and are stabilized by monovalent cations, in particular K^+ and to a lesser extent NH_4^+ and Na^+ , which interact with the lone pairs on the O6 atoms surrounding the central core. They can form spontaneously at sufficiently high concentrations of guanine. These G-quartets have large π -surfaces, and hence tend to stack on each other. In particular, oligonucleotides with contiguous runs of guanine, such as d(TGGGT) can form stacked structures with the G-quartets linked by the sugar-phosphate backbone. These are called *G-quadruplexes* and can form from DNA or RNA strands.

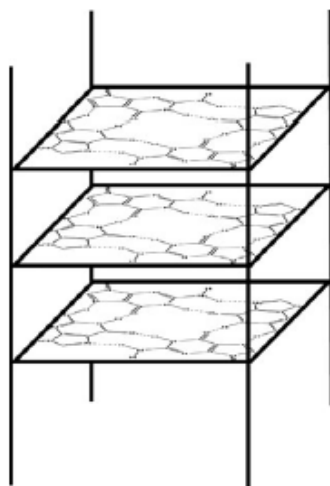


Figure. 1.6 Schematic representation of G-quadruplexes structure. Four G-quartet are held together from π -stacking and sugar backbones

These strands have a directionality described as from 5'-end to 3'-end and they can be parallel or antiparallel. At a molecular level, the different directionality of the strands relates to the conformational state of the glycosidic bond between the guanine base and the sugar. This may be either *syn* or *anti*, when all bases are in *anti* conformation the four strands are parallel, when the bases are in the *syn* all strands are antiparallel. This then affects the orientation of the backbone relative to the G-quartets, and hence results in grooves of different sizes.^[12] G-quadruplexes may be comprised of four separate strands, as in figure 1.7, forming tetramolecular G-quadruplexes, which are always found in the all-*anti* parallel form. Alternatively, they may be formed from two strands, each with two sets of contiguous guanines, or just from one strand, folding back on itself to form an intramolecular structure. In either of these cases, there will be loops that serve to connect the strands of the structure together.

Depending on which strands are connected, these loops may cross diagonally across the top of the structure, joining diagonally opposed antiparallel strands; go across a side, linking adjacent antiparallel strands; or may loop around the side of the structure linking parallel strands and forming a double-strand reversal loop.

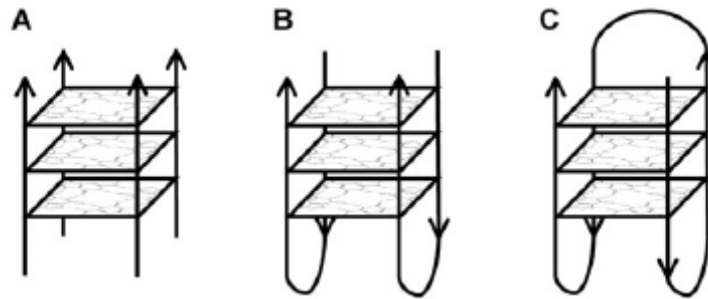


Figure 1.7 Different stoichiometries and folding patterns of G-quadruplexes. (A) Tetramolecular structure with all strands parallel; (B) bimolecular antiparallel structure with adjacent parallel strands; (C) unimolecular antiparallel structure with alternating parallel strands

1.5.1 Telomeres and telomerases

It is important for eukaryotic cells, which have linear chromosomes, to be able to distinguish between chromosome ends and unexpected breaks in the DNA.^[12] In order to facilitate this discrimination, they have repeated sequences at the ends, called telomeres^[13] Human cells' telomeres represent the chromosomal ends (preventing them from fusion events), ranging in length from 3000 to 15000 bases, composed of tandem repeats of the 5'-GGTTAG-3' sequence with a 3' overhang of the G-strand, which plays an important structural and functional role.^[14] Telomere length decreases with each cell division event, while reversion of this degradation by a specialized enzyme called telomerase increases cellular replicative capacity, leading to uncontrolled proliferation: in the majority of tumour cells (85–90%) this enzyme is over-expressed. Therefore there is a great deal of interest in developing approaches to reduce the activity of telomerase for therapeutic purposes.^[15-16]

The human telomeric sequence, $d(\text{GGGTTA})_n$ folds spontaneously into an intramolecular G-quadruplex form, with the GGG runs forming the G-quartet core, and TTA forming the loops of the structure^[14]. This structure is stable under physiological conditions, with a thermal melting temperature of around 65 °C. All telomeric sequences studied to date can also form G-quadruplex structures with comparable thermal stability. It has therefore been proposed that the physiologically relevant structure of the telomeric overhang has a series of G-quadruplexes, much like beads on a string. This telomeric repeat sequence has become an important target for drug development,^[15-16] as it has been shown that by binding to and stabilizing telomeric G-quadruplexes, it is possible to block telomerase

from acting and extending the telomeres, hence preventing the immortalisation of cancerous cells.

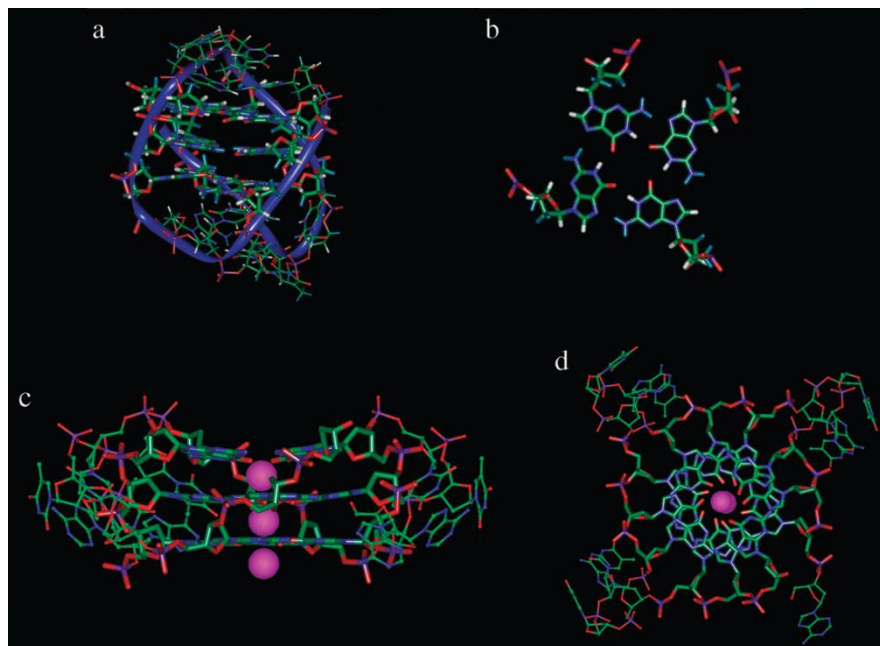


Figure 1.8 (a) Side view of the antiparallel human telomeric G-quadruplex structure solved by Wang and Patel using NMR spectroscopy, from PDB entry 143D. (b) Detailed view of the central G-quartet from PDB entry 143D. (c) Side view of the parallel human telomeric G-quadruplex structure solved by Parkinson, Lee and Neidle using X-ray crystallography, from PDB entry 1KF1. (d) Top view of the parallel structure from PDB entry 1KF1. In all cases, guanines are shown as cylinders, other bases as balls and sticks. Potassium ions are shown in magenta.

The structures formed by the telomeric repeat have been the subject of considerable study, and various structures have been solved for the telomeric repeat, using slightly different sequences and conditions. More recent studies have shown that the telomeric sequence can form a wide variety of different structures, which all seem to exist in equilibrium with each other.^[17]

1.5.2 Transcription regulation

One method that is used in some cases to regulate gene transcription, is based on the presence of G-quadruplexes located in the promoter region of a gene, broadly speaking the kilobase upstream of the transcription start site (TSS).^[16-18] This model was originally demonstrated by Hurley and co-workers for the oncogene *c-myc*,^[19] an important transcription factor involved in regulating around 15% of all human genes. As a result of this, overexpression of *c-myc* has been implicated in a wide range of cancers including colorectal cancer. This one controls the vast majority of the transcription of the gene, and studies in vitro of the sequence *d*(GGGGAGGGTGGGGAGGGTGGGGAAGG) show that it is capable of forming a family of polymorphic G-quadruplexes, using various combinations of the guanine runs underlined.^[20] It has further been shown that the G-quadruplex ligand TMPyP4 binds to this element leading to downregulation of *c-myc* expression.^[21] This clear proof of principle led to the proposal that this may be a general mechanism for gene regulation. The simplest form of the model (fig. 1.9) proposes that there is an equilibrium between two forms of the DNA.

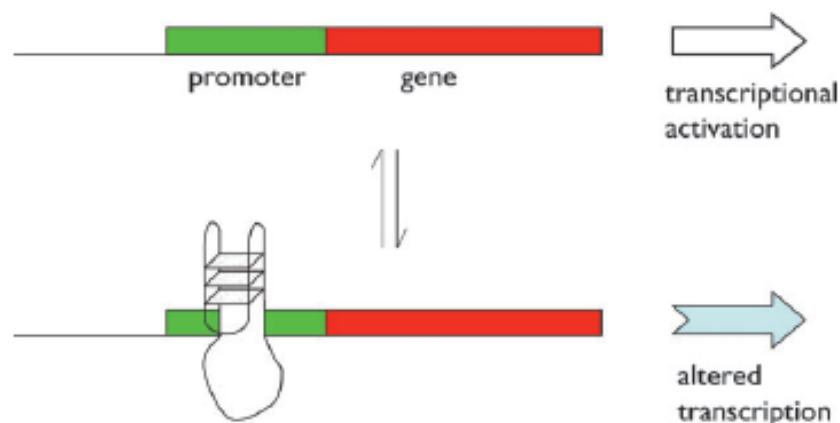


Figure 1.9 The formation of a G-quadruplex in a promoter can affect the level and nature of transcription from that gene. At the simplest level, it may act as a steric block to the transcription machinery.

On one side of the equilibrium is double helix DNA, and transcription occurs as normally; on the other side, one strand is separated, and has folded up into a G-quadruplex. This structure then acts as a steric block to transcription. Addition of a G-quadruplex ligand, whether a small molecule or a protein, will energetically favour the G-

quadruplex form, and hence move the equilibrium towards that side and reduce the transcriptional activity.

1.5.3 G-quadruplexes ligands^[12-13]

A range of G-quadruplex ligands have been shown to bind quadruplexes *in vitro*.^[22.] Some very interesting examples of compounds capable of stabilizing G-quadruplexes show a binding mode based on a loop and groove interaction, however the major part of ligands show the same chemical characteristics such as: an aromatic core which favours stacking interactions with G-tetrads and basic side-chains (positively charged under physiological conditions) which interact with the quadruple helix groove.^[23] These molecules recognize quadruplex DNA, adopting a terminal stacking mode as in figure 1.10: some of them have also been shown to induce telomere shortening or telomere instability, triggering apoptosis and/or senescence programs in various cell lines.^[24-25]

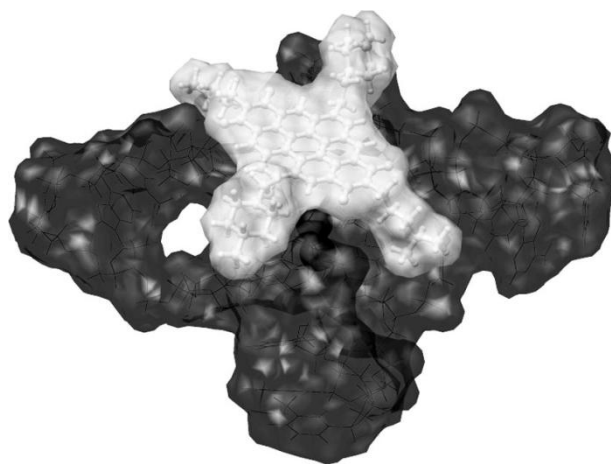


Figure 1.10 Representation of a complex between a coronene derivative (CORON3)^[26] as a ball and-stick model with a grey surface and a monomeric G-quadruplex (black surface).

It is worth noting that, as a result of their direct interaction with telomeres, G-quadruplex ligands have shown more rapid and specific effects than those that would be expected for simple telomerase inhibitors. Using the above principles, it is relatively easy to design compounds that will bind G-quadruplexes, although not necessarily with high affinities. Nonetheless, some good G-quadruplex binders have been developed, such as those depicted in figure 1.11. These include the cationic porphyrin 5,10,15,20-tetra(N-methyl-4-pyridyl) porphin, TMPyP4 (although widely used, this has only limited selectivity for

G-quadruplexes over duplexes) and a variety of acridine and acridone compounds, such as the 3,6,9-substituted acridine BRACO-19.

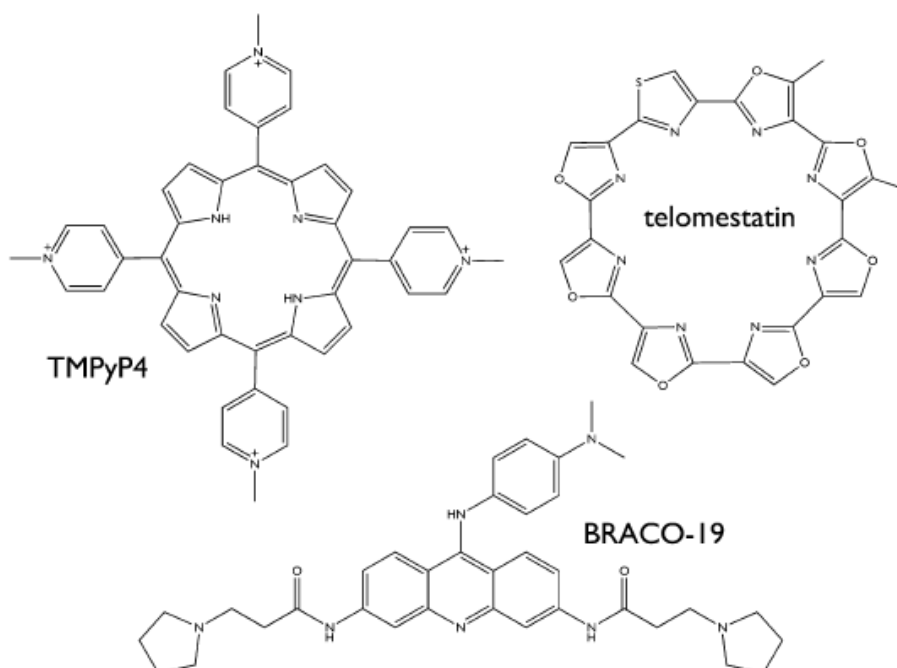


Figure 1.11

In order for ligand binding to be therapeutically effective, it is not enough for the ligand to bind to G-quadruplexes, or even to be very highly selective for them over duplex DNA. It must also be able to bind selectively to one G-quadruplex over another. This is a big challenge, since there are relatively few recognition points to discriminate different G-quadruplex structures. Various methods have been used to try to combine targeting of the loops and grooves of each structure with targeting of the G-quartet core, but to date this has only provided limited success.^[27]

1.5.4 Methods for studying G-quadruplexes

There are a number of different experimental techniques used to study G-quadruplex formation, each examining different aspects of the structures, and hence reporting on different aspects of their formation. The majority of these techniques are principally descriptive, and complete structure determination requires the use of either NMR structure determination or X-ray crystallography. NMR spectroscopy requires much less sample preparation than crystallography, but does require very pure and high-concentrated samples.

At the simplest level, it is possible to gain much information even from a 1-D ^1H NMR spectrum, as there are a relatively small number of protons in nucleic acids and the guanine NH1 imino protons have a characteristic shift when hydrogen bonded.

In addition, they exchange relatively slowly with the deuterated solvent when compared to non-hydrogen-bonded protons. This may therefore be used to show G-quadruplex formation. In order to provide more detailed analysis, multi-dimensional techniques are needed, which allow the complete assignment of resonances to the sequence being studied.^[12, 28]

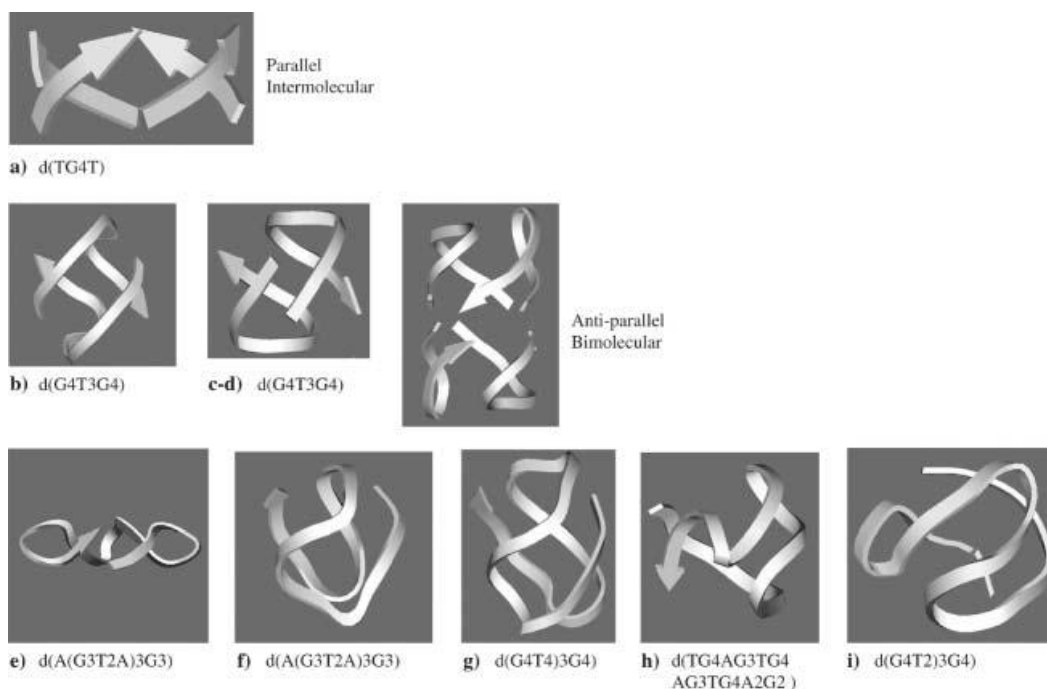


Figure 1.12 Typical folding topologies of G4-DNA forming sequences: a parallel intermolecular structure (a), bimolecular antiparallel structural motifs (b–d), intramolecular parallel (e) and antiparallel (f–i) monomolecular structures. Arrows represent backbones running from 5 to 3 end.

Circular dichroism (CD) is another common technique used to study G4-DNA.: it has been used to study 3D-structures, ligand binding and effect of cations. Although the topology of the folding of G4-DNA strands is very complex , only two basic types of CD spectra, which have been associated with the relative orientation of the strands parallel and antiparallel, are investigated (fig. 1.12).

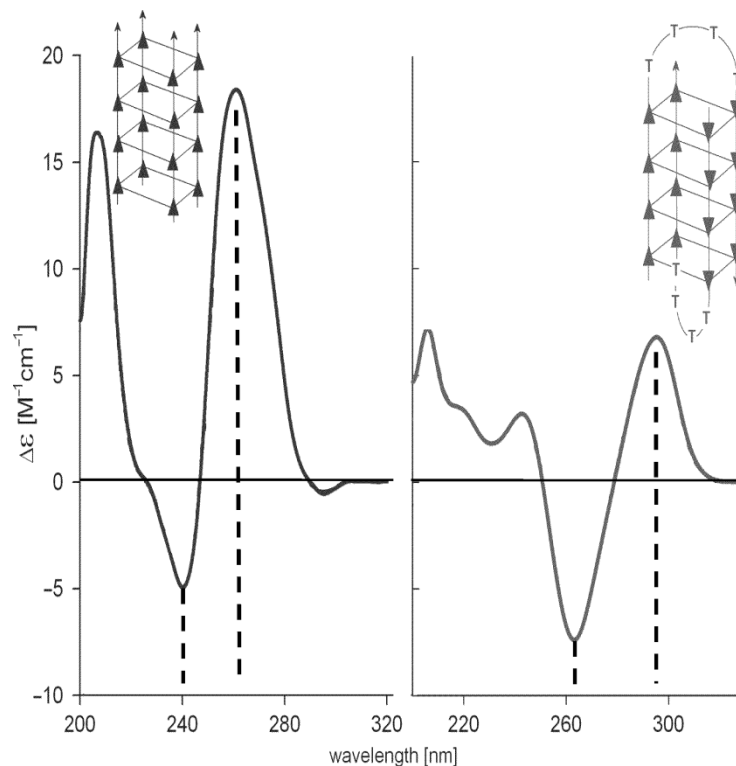


Figure 1.13 CD spectra of guanine quadruplexes. Left side: the parallel stranded quadruplex $[d(G4)]_4$ stabilized by 16 mM K^+ ; right side: Na^+ -induced antiparallel bimolecular quadruplex of $[d(G4T4G4)]_2$.

The spectra of parallel quadruplexes, in which four strands with all glycosidic bonds in *anti* have a dominant positive band at 260 nm, and a negative band at 240 nm while the spectra of antiparallel quadruplexes (where guanines alternate *syn* and *anti* glycosidic conformations along each strands) have a negative band at 260 nm and a positive band at 290 nm^[29-30] Although this empirical relationship for many case is the interpretation for most CD spectra of G4-DNA,^[11,29,31,32] it cannot be considered of general validity (fig. 1-13).

However starting from the chromophore it could be possible to explain how the different folding patterns origin different CD. In the case of G4-DNA the chromophore is represented by guanine, this one has two absorption band in 240-290 nm region connected to two $\pi-\pi$ transitions at 279nm and 248 nm. These transitions are short and long axis polarized respectively . In G4-DNA , G-quartets are stacked one on the top of

the other and they are rotated one with respect to the adjacent one: this rotation causes a chiral exciton coupling between transition dipole moments located in near-neighbour guanines.

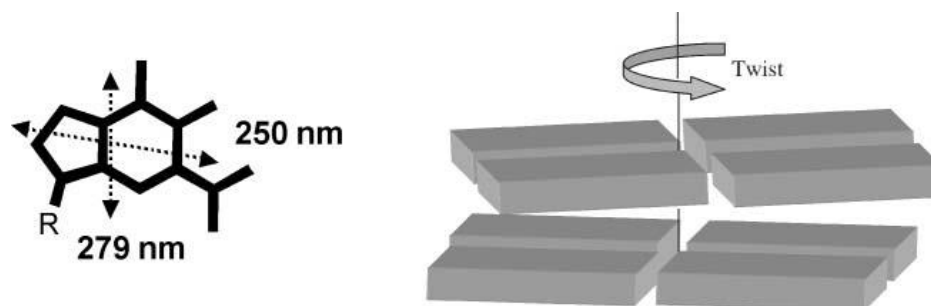


Figure 1.14 Orientation of the two most relevant electric transition moments (dotted double-head arrows) of the guanine chromophore (left) and a sketch of the chiral arrangement of two adjacent G-quartets (each parallelepiped represents a guanine base).

The first non empirical interpretation of CD of G4 DNA has been reported by Spada et al. by modeling the spectrum of polyguanilic acid, which shows the typical spectrum of “parallel G4-DNA and it has been reproduced by an exciton calculation considering only near-neighbour interactions between the guanine transitions of two stacked G-quartets.^[33-34] The two faces of G-quartet are diastereotopic so when the G-tetrads are piled, each quartet can stack onto the adjacent one through the same (head-to-head or tail-to tail) or the opposite (head to tail) face leading to a heteropolar or homopolar stacking.

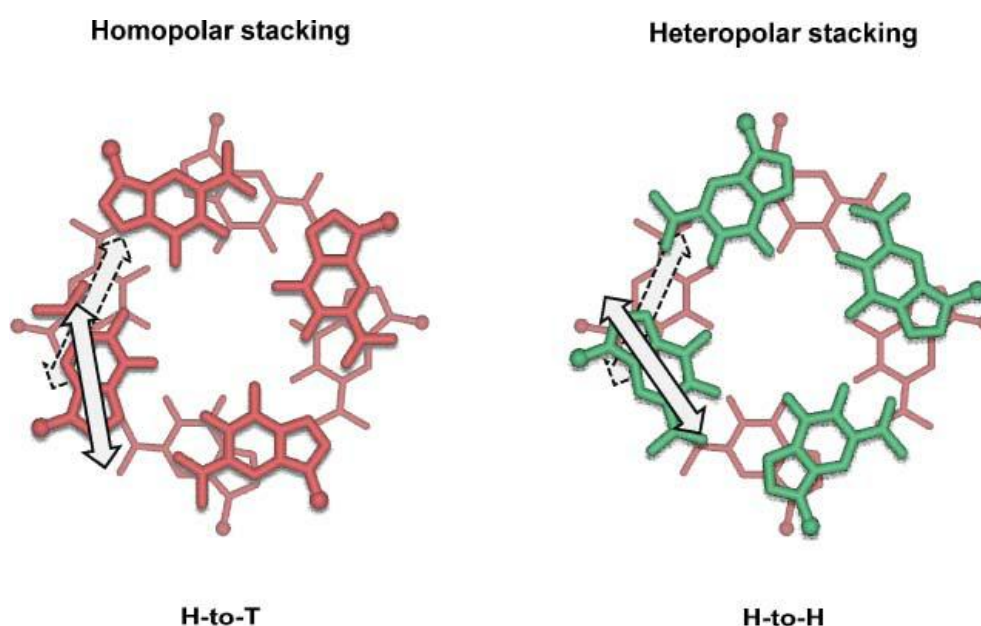


Figure 1.15 Top view of the heteropolar and homopolar stacking of two G-quartets: the “head” and the “tail” sides of the G-quartets are represented in red and green, respectively (the double-head arrows represent the transition moments corresponding to the absorption band at ca. 250 nm).

Considering the case of parallel G4-DNA, the disposition of two adjacent G-quartets in a H-to-T orientation is that reported in the figure 1.15 where the electric moments of a couple of near neighbour guanines have been proposed. Applying the simplified model of the exciton coupling it emerges that this chiral arrangement is expected to exhibit a positive exciton centered at 250 nm (see figure 1.16). When the glycosidic bonds of the guanines alternate in *syn* and *anti* conformations along each strand (antiparallel strands) the G-quartet polarity also alternates, while quadruplexes with parallel strands and all *anti* glycosidic bonds have a non-alternating G-quartet polarity. CD spectra in these two cases are expected to be different. Indeed in the heteropolar H-to-H stacking of two quartets, the relative orientation of the closest dipole moments is different from the case described above. Using the qualitative approach to exciton coupling, the chiral arrangement is expected to give a negative couplet centered at 250 nm (fig. 1.16)

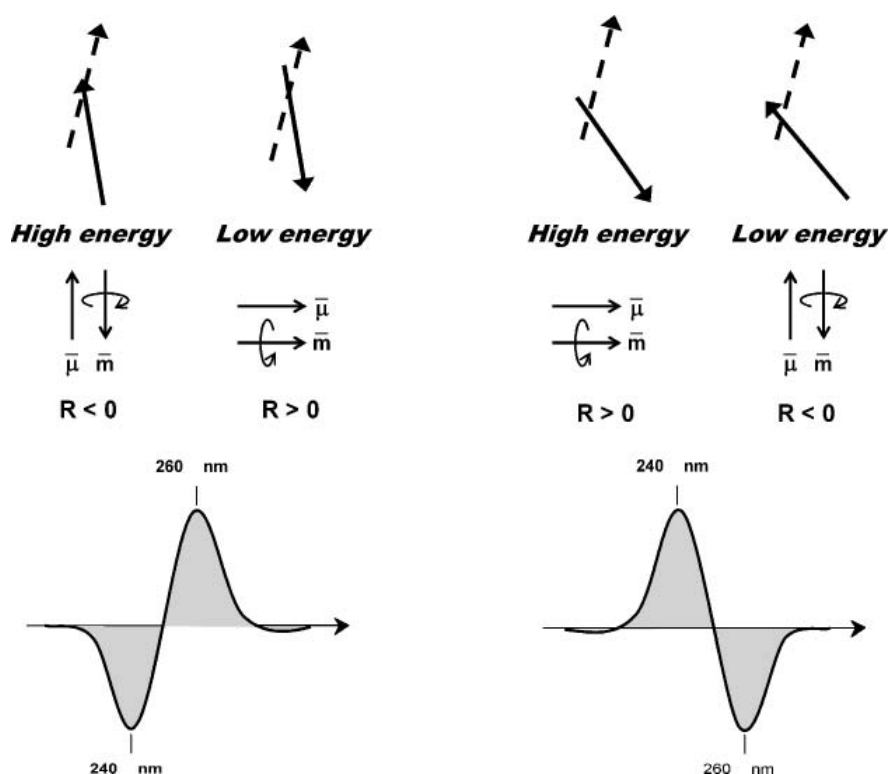


Figure 1.16 A simplified model for the origin of the positive (left side) and negative (right side) exciton couplets for the head-to-tail (H-to-T) and head-to-head (H-to-H) G-quartet stacking, respectively. Top: the arrangement of two 250 nm electric transition moments (full line: front vector; dashed line: rear vector) located in two closest guanines. Middle: the magnetic (\mathbf{m}) and electric (\mathbf{l}) moments generated by the coupling of the two guanine chromophore (more in details, in the high energy coupling of the left-side panel, the two electric transition moments—top—sum to a total electric vector pointing upward—middle—and generate a charge rotation with a resulting magnetic moments pointing downward, that is antiparallel). Bottom: the predicted CD spectra.

CD spectral calculations with the dipole approximation of the two G-quartet stacked with the same or the opposite polarity has been performed by Gray *et al.* (fig. 1.17)^[34] and their results confirm the late computations by Spada *et al.*^[33] on the homopolar stacked system and show how heteropolar stacking explains the emergence of a positive CD signals at 290 nm. The kind of CD spectrum is actually not directly related to the relative strands orientation: the stacking orientation of G tetrads obviously depends on the folding of the strands, however no direct relationship can be established between the two topological features.

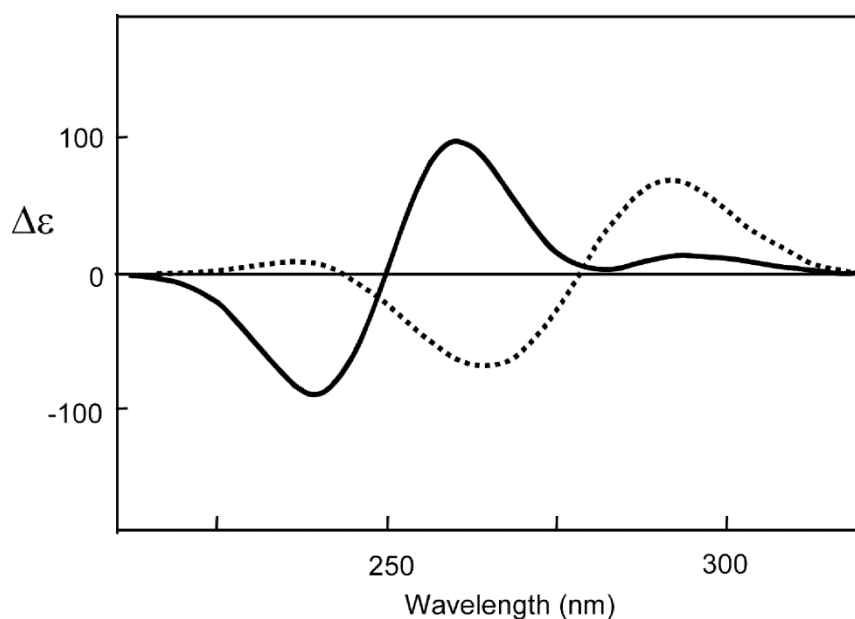


Figure 1.17 Superimposed calculated CD spectra of two G-quartets stacked in the H-to-T (solid line) or H-to-H (dashed line) orientation as shown in Fig. 1.15. The relative orientation of the G-quartets for the calculation were extracted from the solution structure of d(G3T4G3) that present mixed polarities of stacked G-quartets.

1.6 Conclusions

G-quadruplex structures are interesting on many levels. Structurally, they display a fascinating array of polymorphic structures, and we are unable as yet to predict their structure or stability theoretically. They seem to play a number of important biological roles, including regulating the critical processes of transcription and translation, and there is pharmaceutical interest in being able to manipulate these processes to develop novel therapeutics. They can also be used for a range of innovative nanotechnological applications—including all the ones no-one has yet envisaged. It is a rapidly growing field, with promise for chemists, biologists, physicists and computer scientists.

Bibliography

- 1 J. M. Lehn, *Proc. Natl. Acad. Sci USA*, **2002**, *99*, 4763-4768
- 2 K. Ariga, T. Kunitake, *Supramolecular chemistry: fundamentals and applications*, **2006**
- 3 Cram, D. J, *Angew. Chem., Int. Ed. Engl.* **1986**, *25*, 1039–1134.
- 4 N. Krasnogor, S. Gustafon, D. A. Pelta, J. L. Verdegay *Systems-self-assembly: multidisciplinary snapshots*
- 5 S. Sivakova, S. J. Rowan, *Chem. Soc. Rev.* **2005**, *34*, 9.
- 6 W Saenger, *Principles of Nucleic Acid Structure*, Springer-Verlag: New York, 1984.
- 7 G.P.Spada *et al.*, *Chem. Eur. J.* , **2009**, *15*, 7792-77806
- 8 D.Gonzales Rodriguez and A.P.H.J. Schenning, *Chem. Mater.* **2011**, *23*, 310-325
- 9 M. Gellert, M. N. Lipsett, D. R. Davies, *Proc. Natl. Acad. Sci.USA* **1962**, *48*, 2013–2018
- 10 D Rhodes, R. Giraldo, *Curr. Opin. Struct. Biol.*, **1995**, *5*, 311–322
- 11 S. Burge, G. N. Parkinson, P. Hazel, A. K. Todd and S. Neidle, *Nucleic Acids Res.*, **2006**, *34*, 5402
- 12 J. L. Huppert, *Chem. Soc. Rev.*, **2008**, *37*, 1375–1384
- 13 M. Franceschin, *Eur. J. Org. Chem.* **2009**, 2225–2238
- 14 S. Neidle, G. N. Parkinson, *Curr. Opin. Struct. Biol.* **2003**, *13*,275–283
- 15 J. L. Mergny, J. F. Riou, P. Mailliet, M. P. Teulade-Fichou, E.Gilson, *Nucleic Acids Res.* **2002**, *30*, 839–865
- 16 D. J. Patel, A. T. Phan and V. Kuryavyi, *Nucleic Acids Res.*, **2007**,*35*, 7429
- 17 J. Dai, C. PUNCHIHEWA, A. Ambrus, D. Chen, R. A. Jones and D. Yang, *Nucleic Acids Res.*, 2007, *35*, 2440.
- 18 . S. Dexheimer, M. Fry and L. H. Hurley, *DNA quadruplexes and gene regulation, in Quadruplex Nucleic Acids*, ed. S Neidle and S Balasubramanian, Royal Society of Chemistry Cambridge, UK, **2006**.
- 19 A. Siddiqui-Jain, C. L. Grand, D. J. Bearss and L. H. Hurley, *Proc. Natl. Acad. Sci. U.S.A.*, **2002**, *99*, 11593.

- 20 J. Seenisamy, E. M. Rezler, T. J. Powell, D. Tye, V. Gokhale, C. S. Joshi, A. Siddiqui-Jain and L. H. Hurley, *J. Am. Chem. Soc.*, **2004**, *126*, 8702.
- 21 . C. L. Grand, H. Han, R. M. Muñoz, S. Weitman, D. D. Von Hoff, L. H. Hurley and D. J. Bearss, *Mol. Cancer Ther.*, **2002**, *1*, 565.
- 22 C. M. Incles, C. M. Schultes, S. Neidle, *Curr. Opin. Investig. Drugs* **2003**, *4*, 675–685
- 23 a) S. M. Haider, G. N. Parkinson, S. Neidle, *J. Mol. Biol.* **2003**, *326*, 117–125; b) S. Neidle, R. J. Harrison, A. P. Reszka, M. A. Read, *Pharmacol. Ther.* **2000**, *85*, 133–139.
- 24 J. F. Riou, L. Guittat, P. Mailliet, A. Laoui, E. Renou, O. Petitgenet, F. Mégnin-Chanet, C. Hélène, J. L. Mergny, *Proc. Natl. Acad. Sci. USA* **2002**, *99*, 2672–2677
- 25 E. Salvati, C. Leonetti, A. Rizzo, M. Scarsella, M. Mottolese, R. Galati, I. Sperduti, M. F. Stevens, M. D’Incalci, M. Blasco, G. Chiorino, S. Bauwens, B. Horard, E. Gilson, A. Stoppacciaro, G. Zupi, A. Biroccio, *J. Clin. Invest.* **2007**, *117*, 3236–3247.
- 26 M. Franceschin, A. Alvino, V. Casagrande, C. Mauriello, E. Pascucci, M. Savino, G. Ortaggi, A. Bianco, *Bioorg. Med. Chem.*, **2007**, *15*, 1848–1858.
- 27 P. S. Shirude, E. R. Gillies, S. Ladame, F. Godde, K. Shin-Ya, I. Huc, S. Balasubramanian, *J. Am. Chem. Soc.*, **2007**, *129*, 11890–11891.
- 28 Stefano Masiero, Roberta Trotta, Silvia Pieraccini, Stefano De Tito, Rosaria Perone, Antonio Randazzo * and Gian Piero Spada *, *Org. Biomol. Chem.*, **2010**, *8*, 2683–2692
- 29 P. Balagurumoorthy, S. K. Brahmachari, D. Mohanty, M. Bansal and V. Sasisekharan, *Nucleic Acids Res.*, **1992**, *20*, 4061.
- 30 D. M. Gray and F. J. Bollum, *Biopolymers*, 1974, *13*, 2087; R. Jin, B. L. Gaffney, C. Wang, R. A. Jones and K. J. Breslauer, *Proc. Natl. Acad. Sci. U.S.A.*, **1992**, *89*, 8832.
- 31 M. Lu, Q. Guo and N. R. Kallenbach, *Biochemistry*, **1993**, *32*, 598.
- 32 F.W. Smith and J. Feigon, *Nature*, **1992**, *356*, 164; C. Kang, X. Zhang, R. Ratliff, R. Moyzis and A. Rich, *Nature*, **1992**, *356*, 126; J. R. Williamson, *Annu. Rev. Biophys. Biomol. Struct.*, **1994**, *23*, 703.

- 33 G. Gottarelli, P. Palmieri and G. P. Spada, *Gazz. Chim. It.*, **1990**, 120,101.
- 34 D. M. Gray, J.-D. Wen, C. W. Gray, R. Repges, C. Repges, G. Raabe and J. Fleischhauer, *Chirality*, **2008**, 20, 431

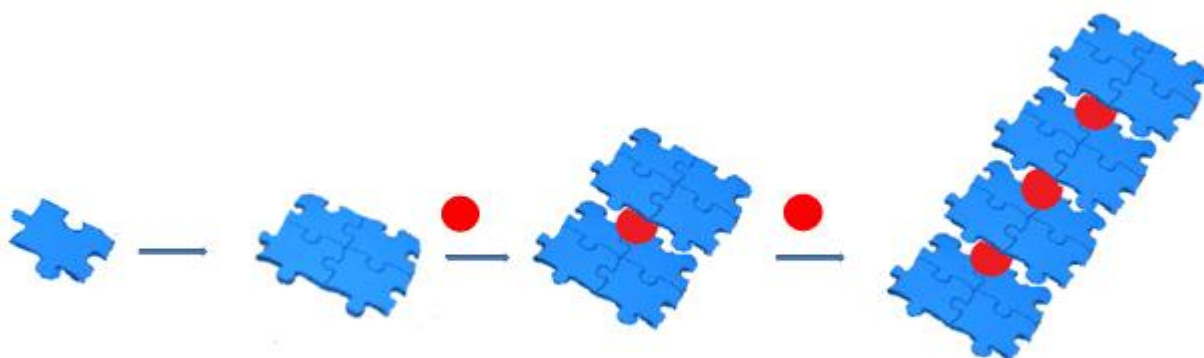
2 *Supramolecular organization of
guanosine derivatives*

2.1 Concepts

Although the large variety of supramolecular networks originated by guanosine derivatives has been investigated for a couple of decades, only in recent years research groups focused their attention on their application in supramolecular chemistry. Guanine moiety is a versatile hydrogen bonding building block. In particular, lipophilic guanosines or guanines can undergo different self-assembly pathways, originating different nanoarchitectures depending on environmental conditions, the two typical assemblies being ribbons and cyclic G-quartet systems. Furthermore the easy functionalisation of guanosine in the sugar hydroxyl groups or in the aromatic base makes it promising building block for the fabrications of complex architectures with functional units located in preprogrammed positions.^[1]

2.2 G-quartet based assemblies

Lipophilic guanosines (LipoG) can undergo in the presence of cation different self-assembly pathways depending on experimental conditions. In 1995^[2] our group showed that LipoG, in particular deoxyguanosine derivative dG(C10)₂ **1**, extracted K⁺ picrate from water into chlorinated solvent (CDCl₃) giving an octamer. The presence of cation was essential, for the formation of this lipophilic octamer. At the same time Davis et al^[3] demonstrated analogous behaviour for isoguanosine derivative.



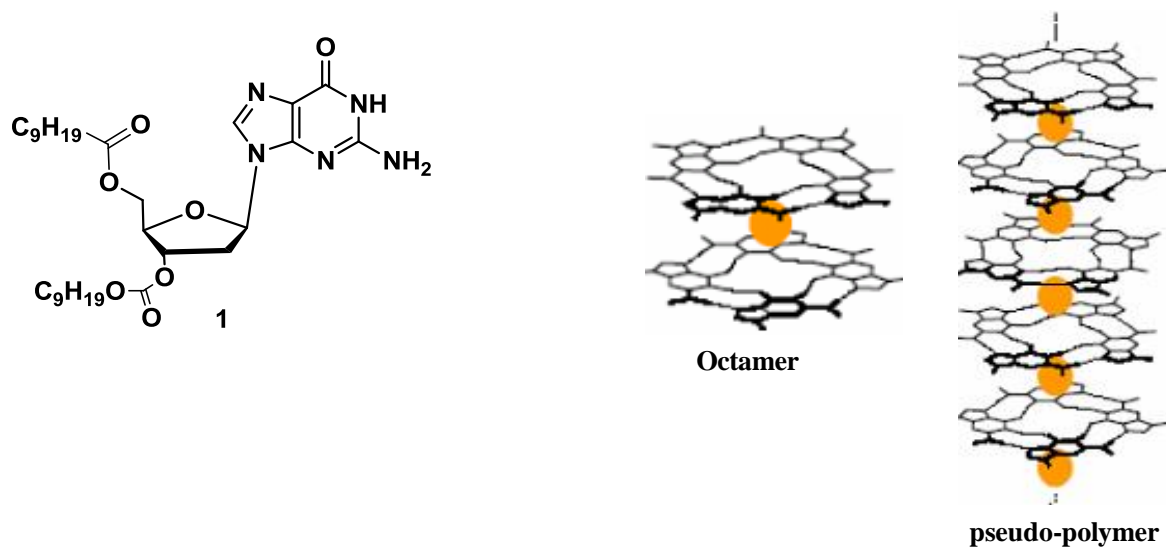


Figure 2.18: the cation-templated self-assembly of Lipo-G 1 from the unassembled molecule to an octameric species and finally to a pseudopolymeric aggregate (the spheres represent the cation).

For different Lipo-Gs,^[4] different, yet G-quartet based, different supramolecular assemblies have been characterized, depending on chemical modification of the guanosine and on the relative guanosine to metal ion ratio. In the last years, NMR spectroscopy has become a valuable tool for the characterization of these supramolecular systems. It provides informations on the structural size of complexes, the effect of the solvent, the role of the cation and anion. After reporting that **1** behaves as an ionophore and a solution of it in chloroform is able to extract potassium picrate (KPic) from water (or crystal state),^[5] two different supramolecular assemblies were proposed and later on solved (figure 2.19): depending on the relative amount of KPic (1:8 or 1:4 K⁺/G ratio) used in the extraction either a C₄-symmetric octamer or a pseudopolymeric-assembly can be obtained. In the 1:8 ratio case, the H NMR spectra,^[1] essentially temperature independent over more than 100°C, show two sets of signals in a 1:1 ratio corresponding each to nucleosides with different glycosydic conformation (*syn-like* and *anti-like*). It should be noted that there is another stereochemical consequence to the cation-templated self-assembly of guanosine derivatives.

As described in figure 1.54 the two faces of the G-quartets are diastereotopic and can be labelled head and tail (fig. 2.19).

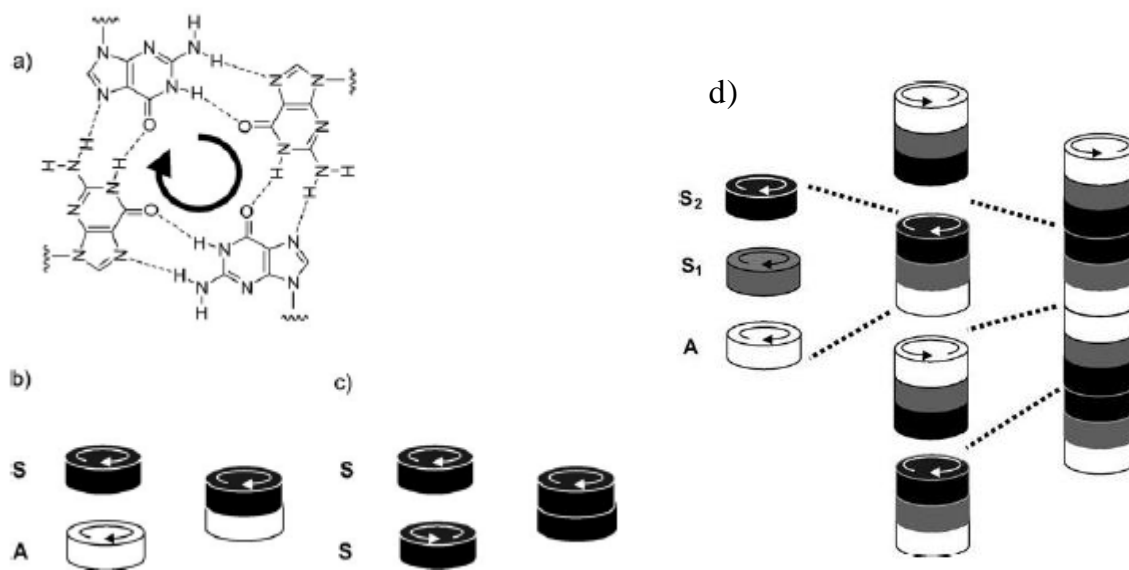


Figure 2.19. a) A G-quartet showing its head diastereotopic face. Schematic drawing of b) a C₄-symmetric and c) a D₄-symmetric octamer. In the C₄-symmetric octamer (obtained, e. g., from **2**), an all-syn G-quartet (S, black disk) with its tail-side (lower face) stacks on the head-side (upper face) of an all-anti (A, white disk) G-quartet. In the D₄-symmetric octamer (obtained, e.g., from **3**), two all-syn G-quartet stack facing their tail sides. Clockwise and counter-clockwise arrows refer to the head and tail faces, respectively. d) Cartoon of the assembly of the polymeric aggregate obtained from dG **1**. White, grey and black disks refer to all-*anti* (A), all-*syn*₁ (S₁) and all-*syn*₂ (S₂) quartets, respectively; clockwise and counter-clockwise arrows refer to the quartet head and tail faces, respectively.

In principle, the two quartets in the octamer can be arranged in three different orientations: head-to-tail (C₄ symmetry, fig. 2.19 b), head-to-head and tail-to-tail (D₄ symmetry; in figure 2.19 c the tail-to-tail arrangement is shown). Therefore, considering these two stereochemical aspects (*syn/anti* glycosidic conformation and relative G-quartets orientation) several diastereoisomers are possible for the octamer.

Remarkably, the NMR data indicated that this octamer was a single diastereomer of C₄ symmetry. In one G-quartet, all monomers had a *syn* conformation, while the other tetramer had an “*all-anti*” conformation. NOE interactions indicated a relative orientation with the head-side of the “*all-anti*” G-quartet facing the tail-side of the “*all-syn*” G-quartet (Figure 2.19 b). While derivative **1** forms the K⁺-templated C₄-symmetric octamer structure or pseudo-polymeric assembly in solution, other lipo-G derivatives (especially those with ribose, in place of deoxyribose, including 2',3'-di-O-isopropylidene-guanosine derivative **2** can give a different stereoregular octamer with a D₄ symmetry.^[6-7]

While in the case of **1** two sets of signals are observed in the ¹H NMR spectrum (the two G-quartets are diastereotopic), in the latter case only a single set of signals is observed for

the two homotopic G-quartets. Furthermore circular dichroism is diagnostic of the stacking polarity of two contiguous G-quartets.^[8]

The tetramers do not stack in register, but are rotated with respect to each other to give, in the 230–300 nm region characteristic of the π - π^* transitions of guanine chromophore, a double-signed exciton-like CD signal. This couplet, the sign of which allows the assignment of the stacking helicity (handedness), exhibits opposite signed bands at about 260 and 240 nm for the head-to-tail (*C4*-symmetric) stacking in compound **1**, while both bands are blue-shifted by 20–30 nm in the case of *D4*-symmetric stacking (compound **2**).

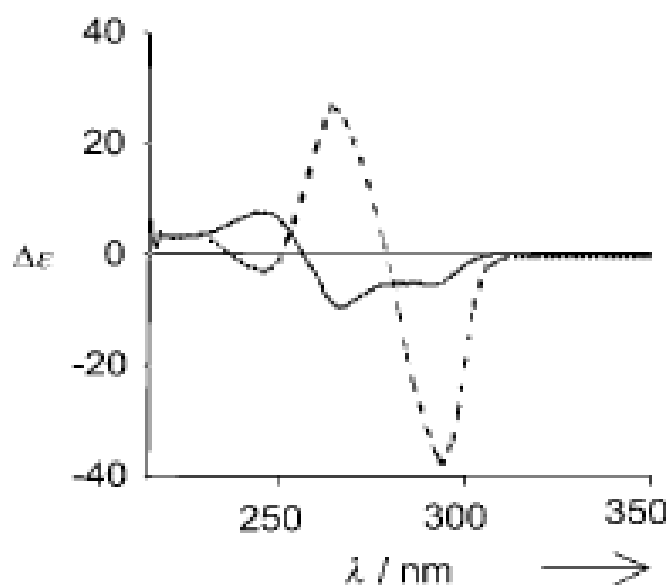
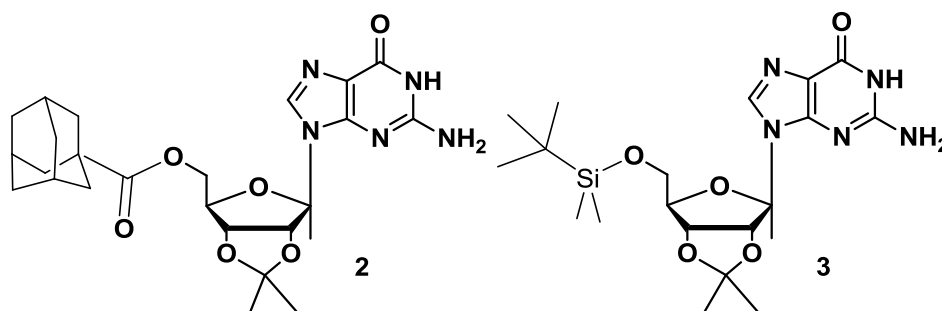


Figure 2.20 Comparison between CD spectra of *C4*- (solid line) and *D4*-symmetric (dashed line) octamers G8·M⁺ obtained from **1** and **2**, respectively (Data from references [2-9]).

Another different metal ion templated supramolecular structure was observed for the compound **3**. In the presence of KPic^[6] NMR experiments (including DOSY NMR data)^[10] indicated that a *D4*-symmetric hexadecamer composed of four stacked G-quartets is the major species in solution (figure 2.21). H NMR spectra show two sets of signals,

present in a 1:1 ratio, assigned to the distinct “outer” and “inner” quartets. X-ray crystallography confirmed that derivative **3** forms an ordered hexadecamer.^[11] This assembly, with empirical formula $G_{16} \cdot 3K^+ / Cs^+ \cdot 4 Pic^-$, is stabilised by four co-axial cations and by four picrate anions. It can be described as a pair of head-to-tail C_4 -symmetric octamers $G_8 \cdot M^+$, with each octamer using its eight carbonyl oxygen atoms to coordinate a K^+ ion, while a third K^+ ion holds the two $G_8 \cdot M^+$ octamers together in a head-to-head orientation: this leads to a D_4 -symmetric assembly. Finally, a Cs^+ ion loosely bound, in solution caps the structure. In addition to stabilization by cations, four picrate anions form hydrogen bonds to N2 amino groups that extend from the two “inner” G-quartets. The lipophilic G-quadruplex looks like a cation channel with an anionic belt wrapped around its middle. Similar solid-state structures for $G_{16} \cdot M_2^{2+} \cdot 4 Pic^-_4$ were obtained with the divalent cations Ba^{2+} and Sr^{2+} .^[12]

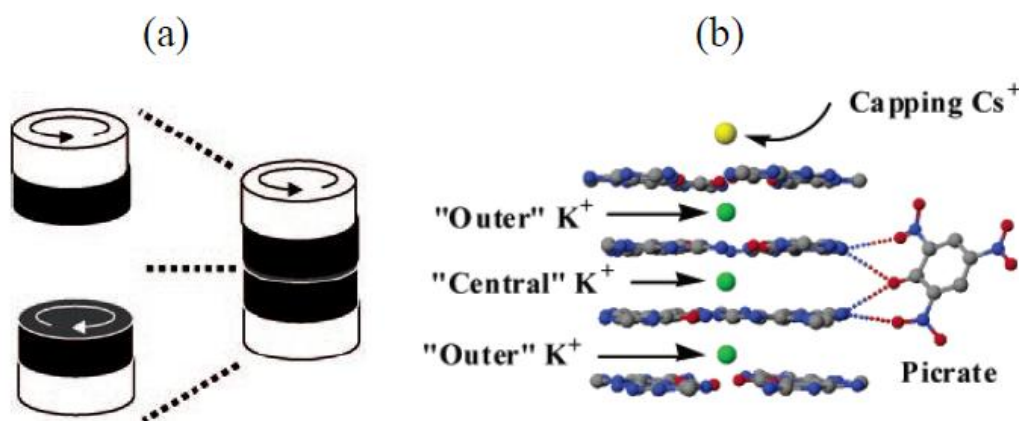


Figure 2.21 a) Schematic cartoon of the quartet assemblies in the D_4 -symmetric hexadecamer (black and white refer to inner and outer quartets, respectively; clockwise and counter-clockwise arrows refer to the head and tail faces, respectively); b) a schematic showing the nucleobase–picrate hydrogen bonds in the hexadecamer $G_{16} \cdot 3K^+ / Cs^+ \cdot 4Pic^-$. (Figure 2.21b adapted from reference [11])

Recent studies have already underlined the subtle role of specific anions in this self-assembly process. For instance, in the presence of dinitrophenolate (DNP) salts, two octamers are linked to produce a D_4 -symmetric hexadecamer, owing to the formation of bifurcated hydrogen bonds between the DNP anion and the amino protons of the inner G-quartets.^[13-11] Other studies provide a more general qualitative analysis of the role of the anion, or, more concretely, of the Coulombic interactions between the dissociated ion pairs, in the thermodynamics of G-quadruplex self-assembly. Because the cation is complexed inside the G-quartet cavity, the energy of such interactions can be modulated within a certain range by tuning the stability of the dissociated anion in solution as a

function of three factors: solvent polarity, the nature of the anion and the cation-anion distance (modified by steric effects around the complexes). They demonstrate that the role of the ion-pair separation energy, although it can usually be neglected in aqueous solutions, is important in G-quadruplex self-assembly and becomes a critical factor in less polar solvents.^[14] This Coulombic contribution alone obviously does not explain the rich polymorphism observed in G-quadruplex self-assembly, but it has been underlined how it can be adjusted within a certain range to regulate, in a precise manner, the growth of G-quadruplex stacks, to form quantitatively assemblies of 8, 12, 16 or 24 guanosine molecules. The last of these species, in particular, comprising 5 cations, 5 anions, and 24 hydrogen-bonded molecules self-assembled in a single object, represents a record in the supramolecular synthesis of discrete, well-defined nanostructures.

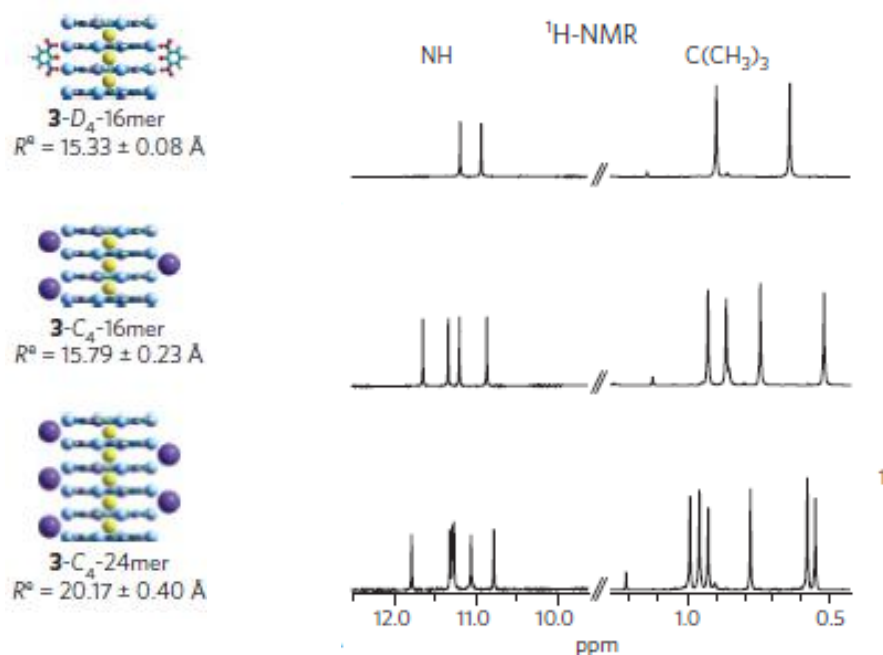


Figure 2.22 Model of the complex formed, experimental hydrodynamic radii R_h , amide and t-butyl regions of the ¹H-NMR spectra (0.02 M; 298 K) of **3** in THF-_d8 (+0.25 equivalents KMeDNP); THF-_d8 (+0.25 equivalents KPF₆); and acetone-_d6 (+0.25 equivalents KPF₆)^[14]

2.3 Linear ribbons from guanosine

In the absence of metal ions, **1** has been shown to self-assemble into ribbon-like structures in organic solvents.^[15] The same AADD homocoupling at the basis of the G-quartet formation may indeed drive to the formation of a different supramolecular motif

(fig. 2.23): in fact, when a couple of guanines exposes to the observer their opposite sides, an infinite H-bonded motif is obtained (“ribbon A”). Furthermore, a different homocoupling (ADDA) in which different H-bonding sites of the guanine are involved, leads to the formation of a further kind of H-bonded ribbon (“ribbon B”). The transformation over time from “ribbon A” (non centrosymmetric) to “ribbon B” (centrosymmetric) has been observed in CDCl_3 by solution-state NMR.^[16]

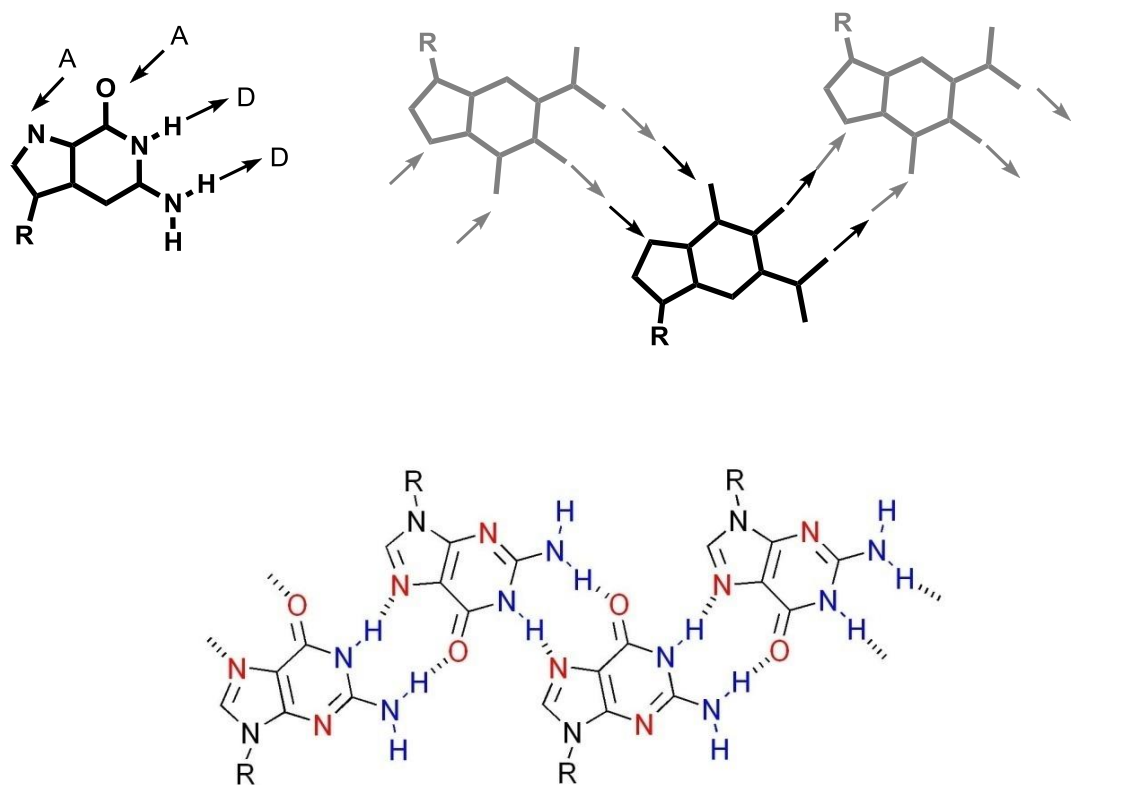
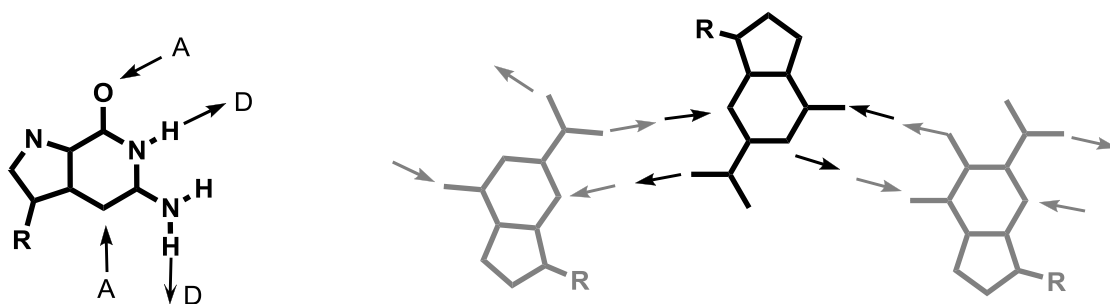


Figura 2.23 The non-centrosymmetric ribbon supramolecular structure by guanine, characterized by $\text{N2-H}\dots\text{O6}$, as composed by AADD homocoupling of guanines (“ribbon A”).



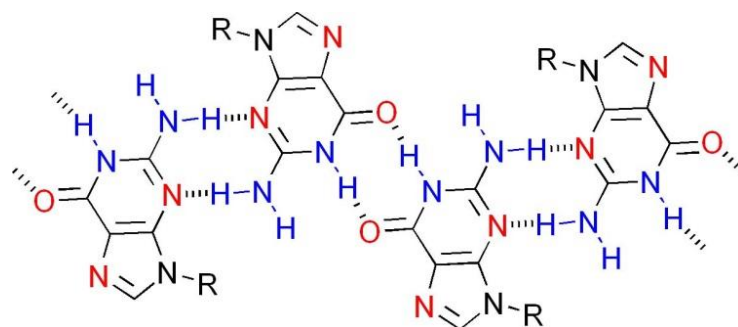


Figure 2.24 The centrosymmetric ribbon supramolecular structures by guanine, characterized by N1–H O6, as composed by ADDA homocoupling of guanines (“ribbon B”).

These long anisometric supramolecular ribbons may form in organic solvents liquid-crystalline phases.^[17] For example derivative **1** in hexadecane above a critical concentrations, gives a viscous birefringent liquid-crystalline phase. A texture of this phase is reported in figure 2.25.

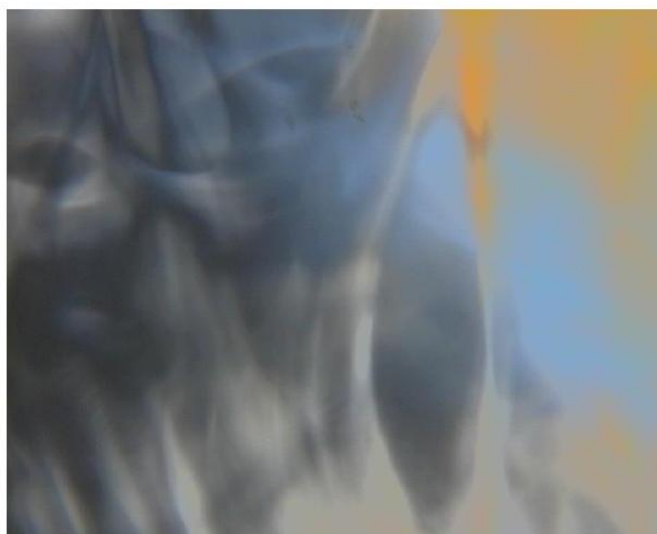


Figure 2.25 Optical texture of derivative **1** in a solution in hexadecane (C=9% w/w)

While it has not been possible to obtain a diffraction structure for the longer-chain derivative **1**, an X-ray single-crystal diffraction structure for the three-carbon atom tail derivative dG(C3)₂ reveals the “ribbon A” type self-assembly^[18]

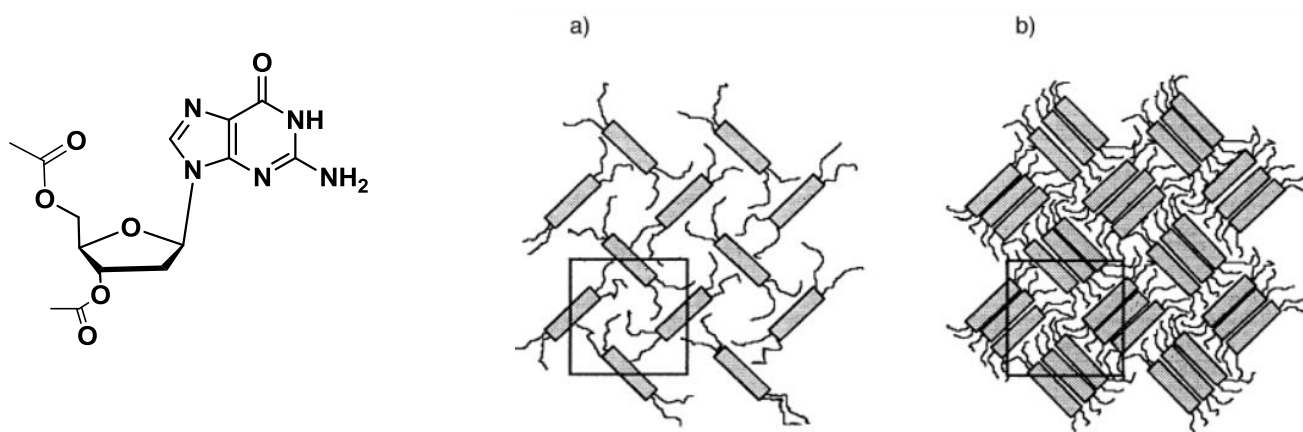


Figure 2.26 Model for gel like phases in hydrocarbon solvent (a) and in chloroform (b) of dG(C3)₂ derivative

Similar ribbon-like self-assembly is observed in crystal structures presented by Araki and co-workers for a guanosine derivative with three Me₂t-BuSi- substituents^[19] and deoxyguanosine derivatives with two Ph₂t-BuSi- or two i-Pri₃Si substituents^[20], while longer-chain alkylsilyl derivatives have been shown to self assemble into supramolecular films^[21] or supramolecular vesicles composed of two-dimensional hydrogen-bonded sheets.^[22] Guanosine ribbon-like and G-quartet self assemblies have been observed on surfaces by SFM and STM.^{[16],[23],[24],[25]} Nikan and Sherman have shown that guanosine-linked cavitands also exhibit guanosine quartets in the absence of metal ions.^[26] LipoG **1** has been used to fill the gap between nanocontacts obtained by electron beam lithography, so as to produce devices with interesting electrical properties, namely, photoconductive devices^[27], and, when the gap between the contacts is smaller than 100 nm, they act as rectifiers.^{[28],[29]}

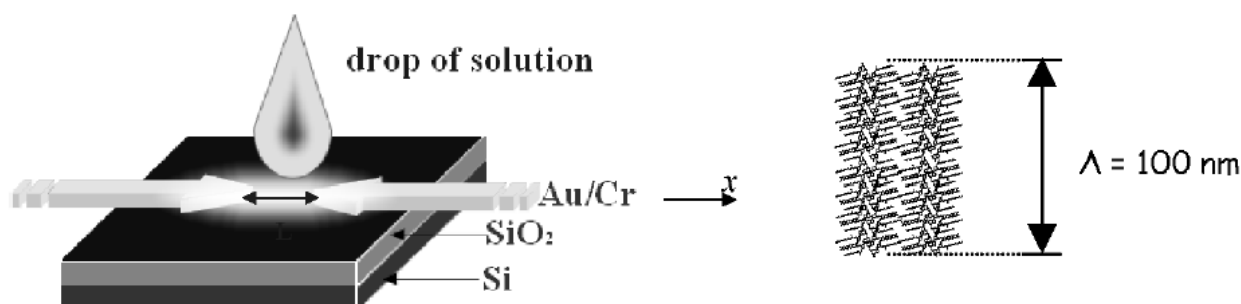


Figure 2.27 Schematic preparation of a G-based electronic nanodevice

Derivative **1** has also been used for biophotonic applications^[30] and to produce a molecular electronic device with rectifying properties when conjugated to a wide band gap GaN semiconductor.^[31]

2.4 Switching between supramolecular assemblies of Lipo-Gs

The control of molecular assembly into well-defined structures on the nanoscale is a key step to improve the performances of materials ^{[32]-[33]} to be used, for example, as components in electronic nanodevices, such as solar cells, light-emitting diodes (LEDs), and field effect transistors (FETs). This control has enormous potential for materials science due to the possibility of bridging the gap between the molecular scale and the macroscopic one in terms of structural order, when precise control of such self-assembly processes is achieved. Among weak interactions, π -stacking has been the first to be employed to drive the self-assembly of conjugated (macro)-molecular systems into well-defined nanoscale assemblies that feature a high degree of order at the supramolecular level.^{[34]-[35]} Further control of nanoarchitectures might be possible by incorporating more specific noncovalent interaction sites in the building blocks.^{[36]-[37]} Among the various non-covalent interactions, multiple hydrogen bonds have been widely adopted because of their directionality and selectivity.^[38] Many examples of bottom-up nanostructurization of π -conjugated oligomers assisted by multiple hydrogen-bonding interactions have been reported.^[36]

Guanine moiety is a versatile hydrogen bonding building block. In particular, lipophilic guanosines can undergo different self-assembly pathways originating diverse nanoarchitectures, and two typical assemblies are the ribbons and the cyclic-quartet system previously described. The equilibrium between the different nanoarchitectures can be controlled and accordingly some physical properties, possibly relevant for molecular electronics, organic photovoltaics, photonics and spintronics, can be tuned.

Three types of stimuli will be considered:

- chemical stimulus (namely, addition or removal of cations)
- variation of solvent polarity
- light (UV-vis).

2.4.1 Addition/removal of cations

Considering that the supramolecular motifs obtained in the presence or in the absence of cations are different, an obvious chemical stimulus is represented by the addition and removal of potassium ions to/from a solution of a LipoG, e.g. **1**.

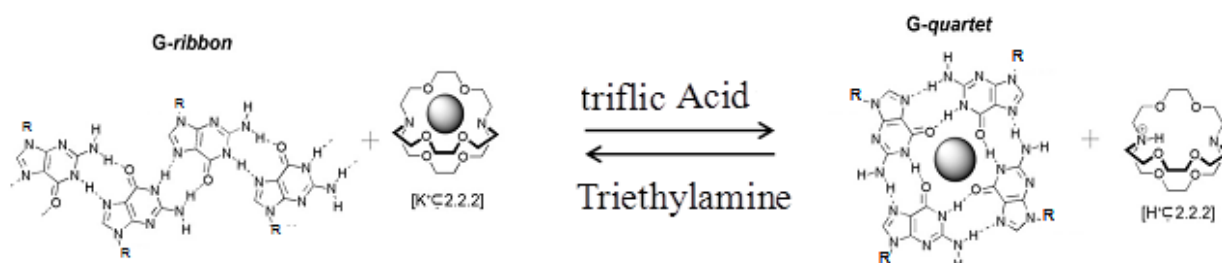


Figure 2.28 The acid/base controlled interconversion between G-ribbons and G-quartet base structures.

We could control the addition/removal of K⁺ ions by means of cryptand [2.2.2].^[39] In fact this cryptand has a high affinity for K⁺ and allows its removal from the system. However, the ability of [2.2.2] to capture the K⁺ ion is pH-dependent and in its protonated form this macrocycle is no longer active as cryptand. This fact can be exploited to switch reversibly from one supramolecular motif to the other by successive addition of acid and base.^[38] More in detail, the addition of potassium picrate to a chloroform solution of **1** transforms the supramolecular ribbon into the octameric complex based on the G-quartet motif. Upon subsequent addition to the quadruplex solution of the [2.2.2] cryptand, potassium is captured by the cryptand (hence the cryptate is formed) and the system reverts to the original G-ribbon. At this point upon addition of an acid (namely, triflic acid), K⁺ is released from the cryptate and the G-quartet based system is regenerated. Finally, adding thereafter a base (namely triethylamine) the protonated cryptand deprotonates, the free cryptand recaptures K⁺ and the G-ribbon is formed again. The acid/base addition steps can be repeated several times. ¹H-NMR and Circular Dichroism (CD) can be both exploited to monitor the ribbon-quadruplex interconversion. Without entering into details, NMR spectra of octamer and ribbon are definitely different: for example, the former has a double set of signals (a few selected signals are marked with triangles in fig. 2.29) arising from its C₄-symmetry, while the latter shows a single set (marked with a star in fig.2.29).

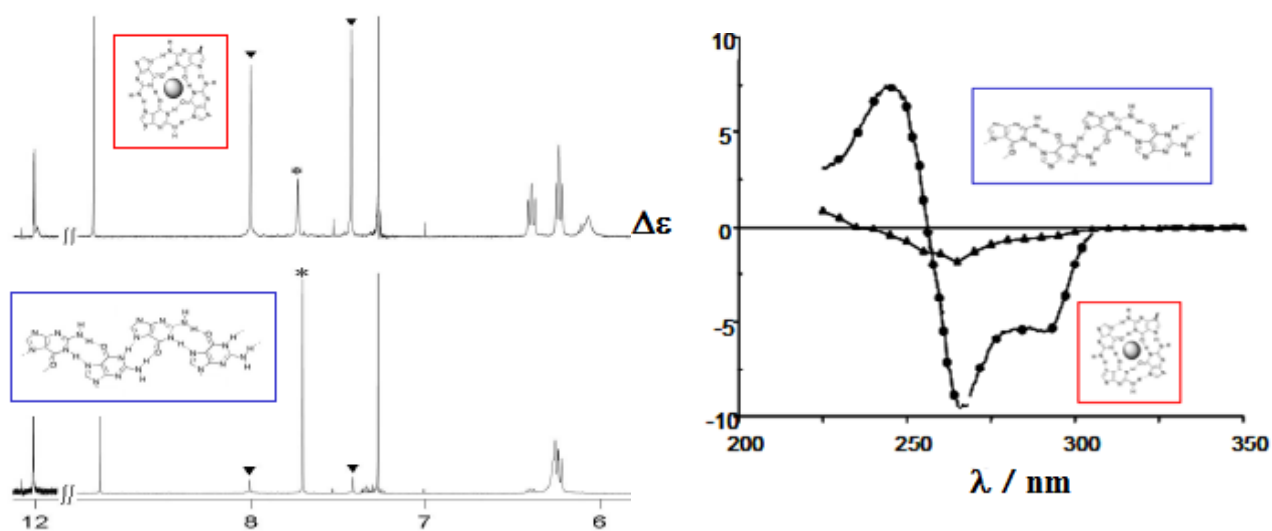


Figure 2.29 ¹H-NMR (left) and Circular Dichroism (right) spectral variation upon reversible quartet-to-ribbon transformation upon acid/base addition.

This same chemical-stimulus-controlled self-assembly has been exploited with guanosine derivatives armed with one or two persistent paramagnetic units, 4-carbonyl-2,2,6,6-tetramethylpiperidine-1-oxyl (TEMPO).^{[41],[42]} As shown in the ESR spectra, in the absence of metal cations the spectrum of LipoG **4** (fig. 2.30, trace a) is characterised by three equally spaced lines (with a broadening between them indicating that intramolecular spin exchange is occurring). In sharp contrast, the ESR spectrum recorded after solid-liquid extraction of potassium picrate shows mainly one very broad signal whose integrated intensity corresponds to the initial amount of radicals (fig 2.30, trace b). The broadening of the signal is independent of concentration and temperature, and thus inter-assembly interactions and motional broadening can be discounted. This spectrum is reminiscent of those obtained from very concentrated nitroxide solutions (>0.05 M).^[43] Since the spectrum was obtained at 0.5 mM concentration, the signal broadening is ascribed to the proximity of spin centers of LipoG **4** within the framework of the octamer.

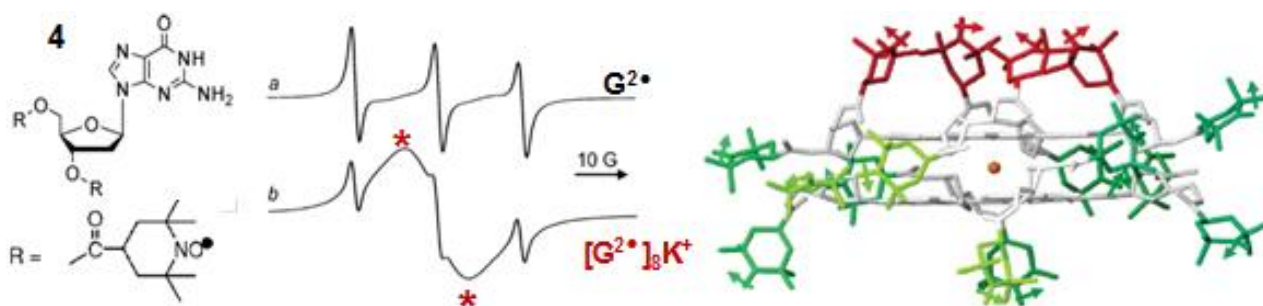


Figure 2.30 The EPR spectrum of LipoG **4** before and after K^+ -directed formation of an octameric G-quartet based species. Stars mark the signals due to intermolecular spin-spin exchange. Molecular model of the assembled species..

The octameric assembly allows the confinement of 16 paramagnetic units in a small volume giving rise to a drastic change of magnetic properties. Since the relative geometry of the radical units is the outcome of K^+ -directed self-assembly, the spin-spin interaction is suppressed by removing the alkaline ion by means of the cryptand/acid-base system described above.

2.4.2 Variation of solvent polarity

In favourable conditions also a variation of solvent properties may control the type of supramolecular organisation of LipoGs.^[44]

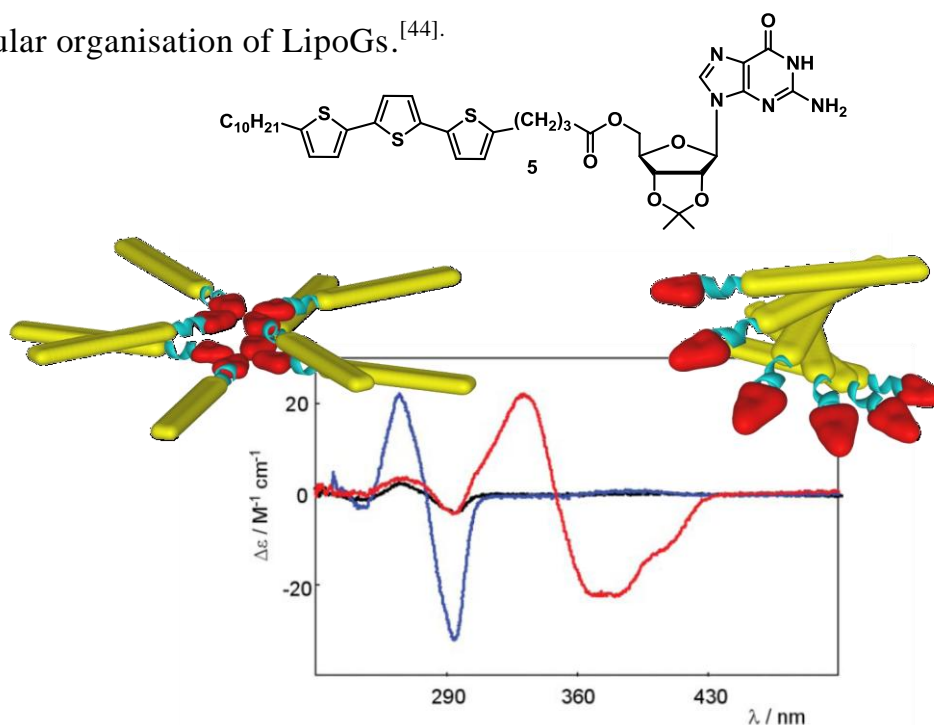


Figure 2.31 CD spectra of **5-KPic** in $CHCl_3$ (blue line) and in $CH_3CN/CHCl_3$ 9/1 (red line). The idealised models represent the supramolecular structures in the two solvent conditions (in red the guanine, in light blue the sugar and in yellow the terthienyl moiety)

An interesting case is represented by LipoG **5**, armed with a terthiophene unit, that can form in THF either a ribbon-like motif or a G-quartet based columnar structure in the absence or presence of alkali metal ions, respectively^[45], thus allowing the control of the inter-oligothiophene interactions. Interestingly, LipoG **5** undergoes a pronounced variation of its supramolecular organisation by changing the polarity of the solvent.^[46] In chloroform the guanosine derivative, templated by alkali metal ions, assembles via H-bonding in G-quartet based D_4 -symmetric octamers; the polar guanine bases are located into the inner part of the assembly and act as a scaffold for the terthienyl pendants. On the other hand, in the more polar (and H-bond competing) acetonitrile (CH_3CN) different aggregates are observed, where the terthiophene chains are π - π stacked in a helicoidal (left-handed) arrangement in the central core and the guanine bases, free from hydrogen bonding, are located at the periphery and exposed to the solvent. The system can be switched from one state (guanine-directed) to the other (thiophene-directed) by subsequent addition of chloroform and acetonitrile. The solvent-induced switching can be easily followed by Circular Dichroism spectroscopy (fig. 2.31): the CD exciton-couplet in the guanine chromophore absorption region observed in chloroform disappears after addition of acetonitrile, indicating the disassembly of the G-quartet based octameric structure, while an intense quasi-conservative exciton splitting in the 300-450 nm spectral region becomes predominant in the CD spectrum. This latter strong bisignate optical activity can be ascribed to the helical packing of conjugated terthiophene moieties stabilised by π - π interactions. NMR spectra and photophysical investigations confirm the structures of the guanine-directed and thiophene-directed assemblies in chloroform and acetonitrile, respectively.

2.4.3 UV-VIS IRRADIATION

In the following it was described the photocontrolled self-assembly of a modified guanosine nucleobase. We investigated the behaviour of LipoG *E-6*,^[47] whose photoresponsive structure was inspired by previous work of Ogasawara and coworkers on oligonucleotides containing a modified guanosine.^{[48],[49]}

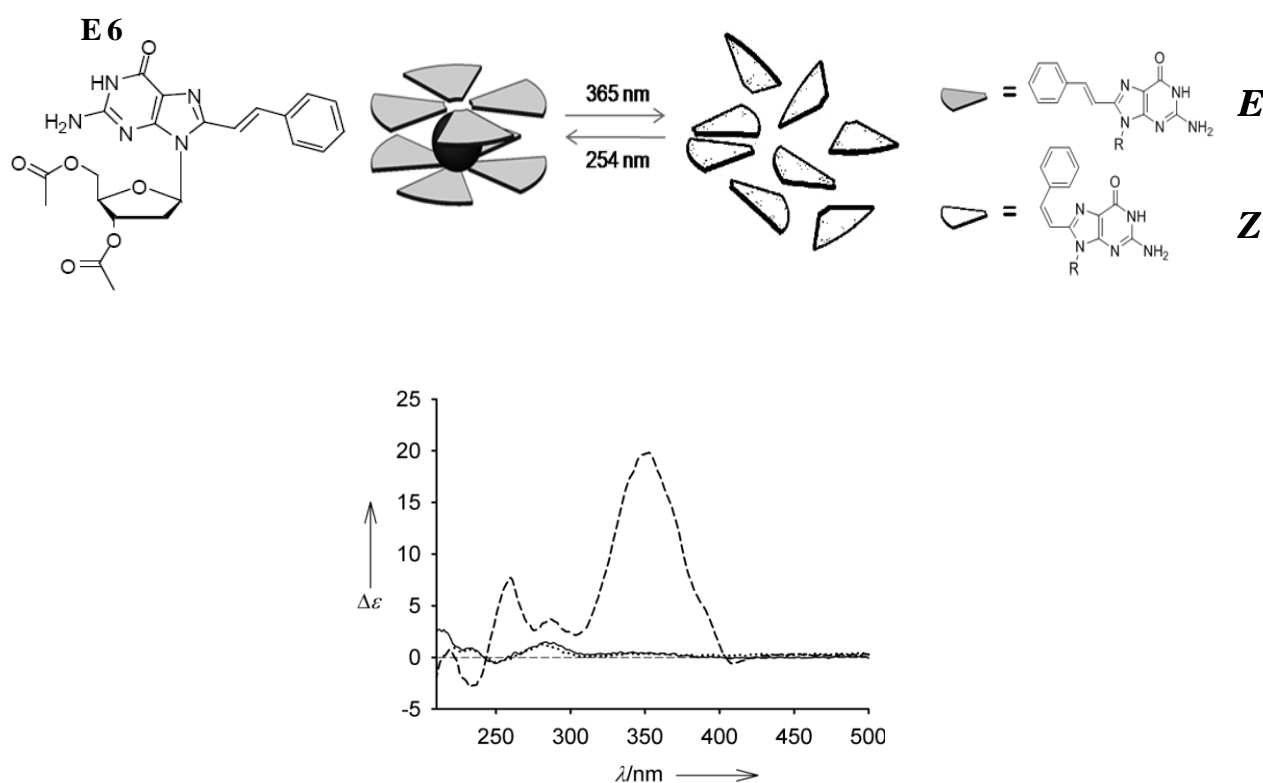


Figure 2.32 Top: Cartoon of the photo-triggering of self-assembly of **6**. Bottom: CD spectra of a solution of *E*-**6**/KI (dashed line), of **6**/KI at the Z-PSS (dotted line) and **6** at the Z-PSS (solid line) in acetonitrile.

When a weighted amount of KI is added to an acetonitrile solution of *E*-**6**, $^1\text{H-NMR}$ and CD spectra are indicative of the formation of stacked G-quartets templated by the cation. In particular, an octameric species composed of two stacked G-quartets arranged in a *D4*-symmetry is formed. Although no detailed information on the electronic transitions are available so far for 8-styrylguanine chromophore, the CD spectral changes observed upon addition of potassium ion closely resemble those reported for analogous modified lipophilic guanosines.^{[1],[50]} The strong increase of the CD signal associated with the formation of the *E*-**6**/ K^+ aggregate can analogously be attributed to interchromophore couplings taking place in the stacked complex (fig. 2.32, dashed line in the CD spectra). When samples of the *E*-**6**/ K^+ octameric complex are irradiated at 365 nm, photoconversion to the *Z* isomer takes place and the Z-PSS is reached. The photoisomerization has a dramatic effect on the assembled species. The CD spectrum of the solution of **6**/KI recorded at the Z-PSS shows very weak signals (fig. 2.32, dotted line in the CD spectra): this spectrum is practically

superimposable to the CD spectrum of *Z-6* prior to KI addition (fig. 2.32, solid line in the CD spectra) and it is similar to that of uncomplexed *E-6*. The disappearance of the strong CD bands at 255 and 350 nm is an evidence of the complex decomposition: stacked G-quartets no longer exist in solution. The absence of G-quartets in the case of *Z-6* is likely due to the fact that in the *Z* form the phenyl group of the styryl unit is twisted with respect to the G-quartet plane. The consequent steric hindrance could force quartets away from van der Waals contact or it could produce a conformational change around the glycosidic bond, which, in turn, would hamper the stacking. Additionally, in the *Z* form the N7 is probably shielded by the styryl unit and is no longer available for H-bonding. The *Z* form can be converted back to the *E* form either photochemically, by irradiating at 254 nm, or thermally. Retroisomerization to the *E* isomer determines, at the supramolecular level, the recreation of the octameric complex: the CD spectrum of the solution at this point perfectly overlaps to the starting (*E-6*)K⁺ trace. Thus, the G-quartet based complex can be cyclically assembled and disassembled by light.

2.5 Conclusions

The combination of a variety of effects, such as π - π stacking, van der Waals interactions, H-bonding, amphiphilicity, may allow fine tuning of the self-aggregating behaviour. These findings extend the comprehension of the experimental tools available for controlling the supramolecular organization of multifunctional derivatives. Any stimulus acting on one (or more) of the above mentioned effects, will, in principle, affect the self-aggregation behaviour and hence the properties of the system.

Bibliography

1. S. Lena, S. Masiero, S. Pieraccini and G. P. Spada *Chem. Eur. J.* **2009**, *15*, 7792 – 7806
2. G. Gottarelli, S. Masiero, G. P. Spada, *J. Chem. Soc.-Chem. Commun.* **1995**, 2555.
3. J. T. Davis, S. Tirumala, J.R. Jenssen, E. Radler, D. J. Fabris, *Org. Chem.* **1995**, *60*, 4167
4. S. Masiero, L. Gramigna, P. Neviani, Rosaria C. Perone, Silvia Pieraccini, and Gian Piero Spada *IRE.B.I.C.* **2011**, *2*, 87-95
5. G. Gottarelli, S. Masiero, G. P. Spada, *J. Chem. Soc. Chem. Commun.*, **1995**, 2555.
6. M. S. Kaucher, Y.-F. Lam, S. Pieraccini, G. Gottarelli, J. T. Davis, *Chem. Eur. J.* **2005**, *11*, 164.
7. G. P. Spada, S. Lena, S. Masiero, S. Pieraccini, M. Surin, P. Samorì, *Adv. Mater.* **2008**, *20*, 2433.
8. a) D. M. Gray, J.-D. Wen, C. W. Gray, R. Repges, C. Repges, G. Raabe, J. Fleishhauer, *Chirality* **2008**, *20*, 431; b) G. Gottarelli, S. Masiero, G. P. Spada, *Enantiomer* **1998**, *3*, 429; c) G. Gottarelli, S. Lena, S. Masiero, S. Pieraccini, G. P. Spada, *Chirality* **2008**, *20*, 471
9. C. Graziano, S. Pieraccini, S. Masiero, M. Lucarini, G. P. Spada, *Org. Lett.* **2008**, *10*, 1739.
10. X. D. Shi, K. M. Mullaugh, J. C. Fettinger, Y. Jiang, S. A. Hofstadler, J. T. Davis, *J. Am. Chem. Soc.* **2003**, *125*, 10830.
11. S. L. Forman, J. C. Fettinger, S. Pieraccini, G. Gottarelli, J. T. Davis, *J. Am. Chem. Soc.* **2000**, *122*, 4060.
12. a) X. D. Shi, J. C. Fettinger, J. T. Davis, *J. Am. Chem. Soc.* **2001**, *123*, 6738; b) X. Shi, J. C. Fettinger, J. T. Davis, *Angew. Chem.* **2001**, *113*, 2909; *Angew. Chem. Int. Ed.* **2001**, *40*, 2827.
13. Shi, X. et al. *J. Am. Chem. Soc.* **2003**. *125*, 1083
14. D. G. Rodriguez, J. L. J. van Dongen, M. Lutz, A.L. Spek, A.P. H. J. Schenning and E. W. Meijer *Nature*, **2009**, *1*, 151
15. G. Gottarelli, S. Masiero, E. Mezzina, G. P. Spada, P. Mariani, M. Recanatini, *Helv. Chim. Acta* **1998**, *81*, 2078.
16. G. Gottarelli, S. Masiero, E. Mezzina, S. Pieraccini, J. P.; Rabe, P. Samori, G. P. Spada, *Chem.-Eur. J.* **2000**, *6*, 3242.
17. G. Gottarelli, S. Masiero, E. Mezzina, S. Pieraccini, G. P. Spada, P. Mariani, *Liq. Cryst.* **1999**, *26*, 965.

18. T. Giorgi, F. Grepioni, I. Manet, P. Mariani, S. Masiero, E. Mezzina, S. Pieraccini, L. Saturni, G. P Spada, G. Gottarelli *Chem.-Eur. J.* **2002**, *8*, 2143
19. K. Araki, R. Takasawa, I. Yoshikawa, *Chem. Commun.* 2001, 1826.
20. T. Sato, M. Seko, R. Takasawa, I. Yoshikawa, K. Araki, *J. Mater. Chem.* **2001**, *11*, 3018.
21. I. Yoshikawa, J. Li, Y. Sakata, K. Araki, *Angew. Chem, Int. Ed. Engl.* **2004**, *43*, 100
22. I. Yoshikawa, J. Sawayama, K. Araki, *Angew. Chem, Int. Ed. Engl.* **2008**, *47*, 1038.
23. T. Giorgi, S. Lena, P. Mariani, M. A. Cremonini, S. Masiero, S. Pieraccini, J. P. Rabe, P. Samori, G. P. Spada, G. Gottarelli, *J. Am. Chem. Soc.* **2003**, *125*, 14741
24. S. Lena, G. Brancolini, G. Gottarelli, P. Mariani, S. Masiero, A. Venturini, V. Palermo, O. Pandoli, S. Pieraccini, P. Samori, G. P Spada, *Chem.-Eur. J.* **2007**, *13*, 3757.
25. A. M. S. Kumar, J. D. Fox, L. E.; Buerkle, R. E Marchant., S. J. Rowan, *Langmuir* **2009**, *25*, 653.
26. M. Nikan, J. C. Sherman, *Angew. Chem, Int. Ed. Engl.* **2008**, *47*, 4900.
27. R. Rinaldi, E. Branca, R. Cingolani, S. Masiero, G. P. Spada, G. Gottarelli, *Appl. Phys. Lett.* **2001**, *78*, 3541.
28. G. Maruccio, P. Visconti, V. Arima, S. D'Amico, A. Blasco, E. D'Amone, R. Cingolani, R. Rinaldi, S. Masiero, T. Giorgi, G. Gottarelli, *Nano Lett.* **2003**, *3*, 479.
29. R. Rinaldi, G. Maruccio, A. Biasco, V. Arima, R. Cingolani, T. Giorgi, S. Masiero, G. P. Spada, G. Gottarelli, *Nanotechnology* **2002**, *13*, 398.
30. A. Neogi, J. Li, P. B. Neogi, A. Sarkar, H. Moroc, *Elec. Lett.* **2004**, *40*, 1605.
31. H. Liddar, J. Li, A. Neogi, P. B. Neogi, A. Sarkar, S. Cho, H. Morkoc, *Appl. Phys. Lett.* **2008**, *92*.
32. A. C. Grimsdale, K Müllen, *Angew. Chem. Int. Ed.* **2005**, *44*, 5592;
33. V. Palermo, P. Samorì, *Angew. Chem. Int. Ed.* **2007**, *46*, 4428.
34. P. Samorì, V. Francke, K. Müllen, J. P. Rabe, *Chem. Eur. J.* **1999**, *5*, 2312
35. A. P. H. J. Schenning, A. F. M. Kilbinger, F. Biscarini, M. Cavallini, H. J. Cooper, P. J. Derrick, Feast, W. J.; R. Lazzaroni, Leclère, L. A. McDonell, E. W. Meijer, J. S. C. Meskers, *J. Am. Chem. Soc.* **2002**, *124*, 1269.
36. A. P. H. J. Schenning, E. W. Meijer, *Chem. Commun.* **2005**, 3245;
37. V. Palermo, P. Samorì, *Angew. Chem. Int. Ed.* **2007**, *46*, 4428.
38. J.-M. Lehn, *Supramolecular Chemistry, Concepts and Perspectives*, **1995**. VCH, Weinheim.

39. J. M. Lehn, J. P. Sauvage, *J. Am. Chem. Soc.* **1975**, *97*, 6700
40. S. Pieraccini, S. Masiero, O. Pandoli, P. Samorì, Spada, G. P. *Org. Lett.* **2006**, *8*, 3125.
41. C. Graziano, S. Pieraccini, S. Masiero, M. Lucarini, G. P. Spada, *Org. Lett.* **2008**, *10*, 1739
- .
42. P. Neviani, E. Mileo, S. Masiero, S. Pieraccini, M. Lucarini, Spada, G. P. *Org. Lett.* **2009**, *11*, 3004.
43. J. E. Wertz, J. R. Bolton, *Electron Spin Resonance*, **1986** Chapman and Hall, New York
44. J. E. Betancourt, M. Martin-Hidalgo, V. Gubala, J. M. Rivera, *J. Am. Chem. Soc.* **2009**, *131*, 3186.
45. G. P. Spada, S. Lena, S. Masiero, S. Pieraccini, M. Surin, P. Samorì, *Adv. Mater.* **2008**, *20*, 2433.
46. S. Pieraccini, S. Bonacchi, S. Lena, S. Masiero, M. Montalti, N. Zaccheroni, G. P. Spada, *Org. Biomol. Chem.* **2010**, *8*, 774.
47. S. Lena, P. Neviani, S. Masiero, S. Pieraccini, G. P. Spada, *Angew. Chem. Int. Ed.* **2010**, *49*, 3657.
48. S. Ogasawara, M. Maeda, *Angew. Chem. Int. Ed.* **2008**, *47*, 8839.
49. S. Ogasawara, M. Maeda, *Angew. Chem. Int. Ed.* **2009**, *48*, 6671.
50. J. T. Davis, G. P. Spada, *Chem. Soc. Rev.* **2007**, *36*, 296.

3 *N*⁹-alkyl-guanines

3.1 Concepts

N⁹-alkyl-guanine, such as benzyl-guanine, have demonstrated outstanding potential in a wide range of biological system. For example these derivatives demonstrated potent activity as purine nucleoside phosphorylase inhibitors, HIV integrase inhibitors, antitumor agents and antiviral agents.^[1-6] In addition to the diverse biological activities lipophilic guanine derivatives have served as important model compounds to investigate guanine oxidation mechanism and as precursors for model ion channel formation and G-quadruplexes structures^[7-11] In our group have been studied self-assembling properties of lipophilic-guanosines, as described in chapter 2. The ultimate aim of this work is the synthesis and supramolecular characterization of new lipophilic guanine derivatives which could be used to obtain new functional nanopatterned materials, that is, materials in which macroscopic properties depend on order and organisation at *nano-level* of appropriate functional units.

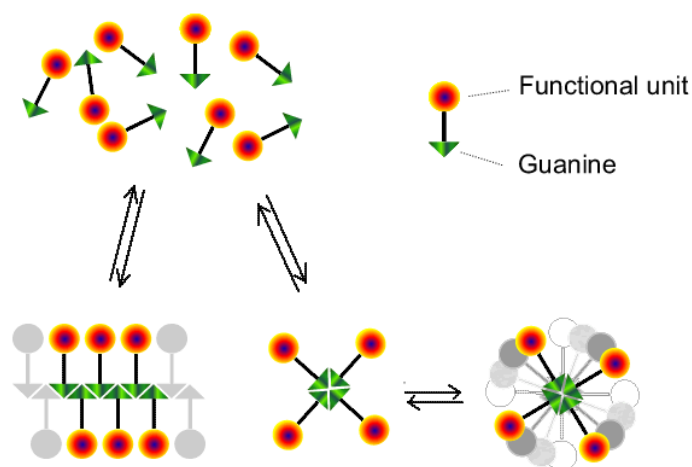


Figure 3.33: the different spatial distribution of the functional units in interconvertible different assemblies leads to different properties

Functionalization of guanine base at N⁹ position preserves all hydrogen bond donor (N¹-H-N²-H) and acceptor (N⁷-O⁶) groups required to the formation of supramolecular aggregates analyzed in the precedent sections. Therefore we studied if the absence of the sugar can induce some changes in the aggregation of octamers, ribbons or pseudo-polymers. In guanosine derivatives sugar (ribose or deoxyribose) has two possible conformations with respect to glycosidic bond (*syn* or *anti* fig.3.34) and the introduction of a bulky substituent in 8 position forces the base to have a *syn* conformation. Sessler

has shown^[12] that attaching a sterically demanding group to the C(8)-position (derivative **7**), enables the molecules to self-associate into isolated G-quartets, both in the solid state and in solution, even in the absence of templating metal cations. Only the *syn* stereochemistry was observed for the G-quartets formed from **7**.

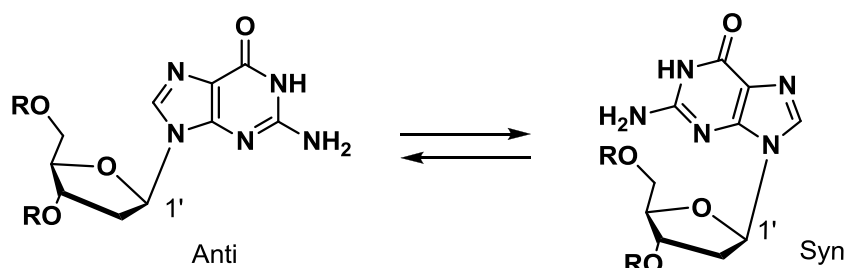
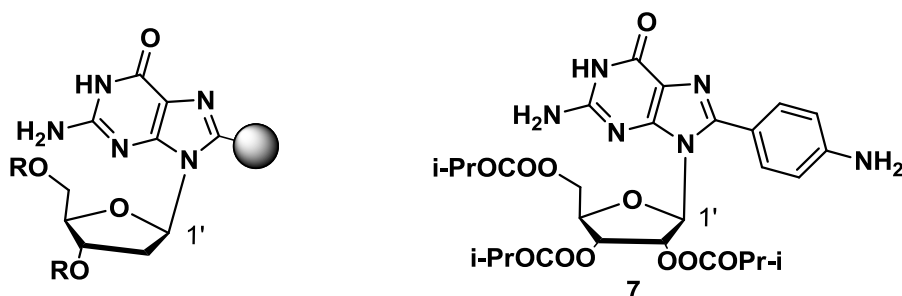


Figure 3.34 *Anti* and *syn* conformation of guanosine



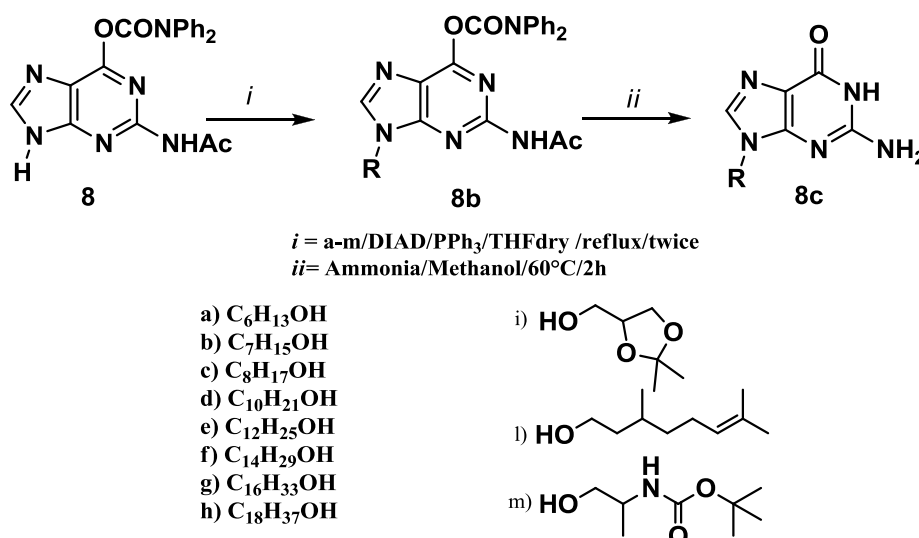
An N^9 -substituted guanine are expected to have a greater conformational freedom (even in presence of bulky groups in C8). Trough different synthetic approaches, lipophilic chains of different nature have been introduced in N^9 -position and they allowed to modulate lipophilic and chiral characteristics of these new derivatives. Depending on experimental conditions (presence or absence of cations) we studied different aggregates and the possible additional interactions involving the introduced lipophilic chains.

3.2 Synthetic approaches

Synthesis of N^9 -guanine derivatives has been realized by using different synthetic ways. In literature many approaches are reported but they do not work efficiently with electron-rich purines such as guanine due to side reactions.^[13] Three methods have been reported for the synthesis of nucleoside analogues regarding the formation of the carbon-base

bond: (a) palladium-catalyzed displacement of an allylic ester or carbonate; (b) direct nucleophilic displacement of halides or activated alcohols; and (c) Mitsunobu coupling.

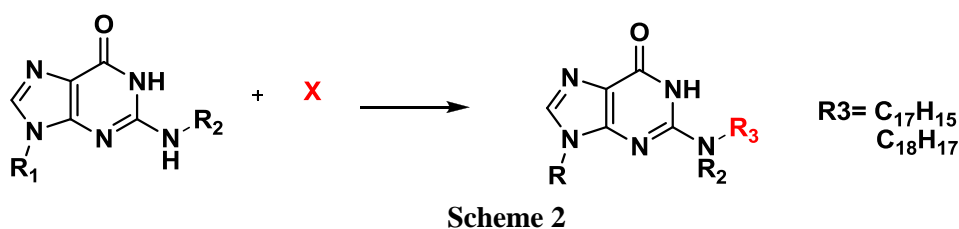
The first two strategies often suffer from considerable competition between N-9 and N-7 positions of the purine base^[14] and the reactions give modest yields (usually lower than 60%).^[15] The well-studied Mitsunobu reaction involves two sequential steps: the activation of primary or secondary alcohols by dialkylazodicarboxylate (DIAD) followed by nucleophilic substitution.^[16] It was believed that acidic nucleophiles are necessary, since the dialkylazodicarboxylate must be protonated during the course of the reaction. Therefore, this reaction was usually applied to the synthesis of esters, phenyl ethers, thioethers, and amines (from the nucleophilic addition of phthalimide or hydrogenazide).^[17] We have used an efficient and practical synthesis of non-sugar nucleoside using optimized Mitsunobu coupling of guanine and different alcohols described in literature^[18] (Scheme 1). Guanine is first converted into O⁶-carbamate-N²-acetate protected guanine in two steps (see experimental part), as these turned out to be the best protecting groups producing the desired coupling product. The protected guanine was used in the subsequent Mitsunobu coupling. While it is known that alcohol can be activated by DIAD even at low temperature, both guanine and protected guanine have poor solubility in non polar organic solvents such as THF: thus, to increase the purine base solubility, the reaction is carried out at 70°C. We noticed that the addition of one or more equivalents of activated alcohol after 6 hours increases the yield, as it apparently minimizes side reactions.

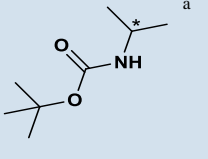
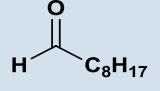
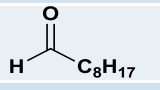
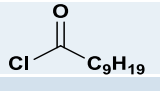
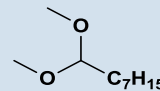


Scheme 1

Compounds **8b** can be readily converted to the desired N⁹-alkylguanines by treatment with a 1:1 mixture of ammonia and methanol solution at 60° C in high yields.^[19]

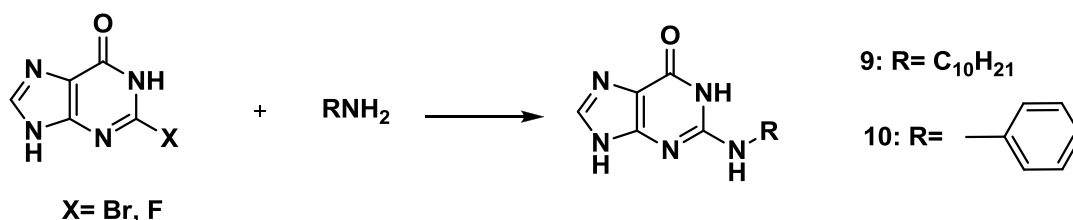
Most of derivatives **7c** show a poor solubility in apolar organic solvents, to improve solubility, several approaches were tried to introduce a lipophilic alkyl or aromatic chain on the exocyclic amino-group (N²). In scheme 2 (tab.1) are reported the different synthetic procedures carried out to obtain N2-alkyl guanine derivatives. Starting materials were commercial guanine, N⁹-alkylguanine or N²-N⁹ diacetyl-protected guanine and the classical procedure was a reductive amination carried out with aldehydes (heptanal-octanal) and NaBH₃CN.^[20-21] This method is based on the thermal condensation of the aldehyde with the exocyclic amino group in the guanine ring and subsequent reduction of the resulting imino-group by a moderately active reducing agent.



R1	R2	X	SOLVENT	REDUCING AGENT	TEMP C°	YIELD %
	H		CH ₃ OH	NaBH ₃ CN	50	10
H	H		CH ₃ OH	NaBH ₃ CN	50	10
ACETYL GROUP	ACETYL GROUP		THF	LiAlH ₄	room temp.	
H	H		1) DMF 2) THF	LiAlH ₄	room temp.	15
H	H		1) DMF 2) THF	NaBH ₃ CN	90	10

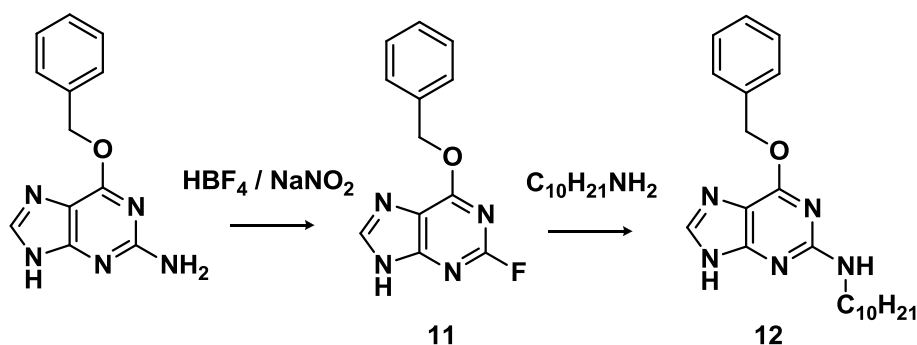
Tab.1: ^aMethod: a mixture of guanine or N9-alkyl guanine(0.30 mmol) and an excess of X (4 eq.) was heated at 50 °C for one week in dry methanol containing NaBH₃CN(6 eq.).Pure compound was obtained with a chromatographic column (dichloromethane /acetone 9:1) and a recrystallization from ethanol ^bMethod: to a solution of guanine (1,6 mmol) in dry DMF it was added X (2 eq.) Pure dialkyl substituted compound was isolated and it was carried out a reduction using two different reducing agents. ^cMethod:to a solution of LiAlH₄ (2.5 eq.) in dry THF at 0°C was added slowly a solution of diacetylguanine (0.85 mmol) in dry THF and was stirred for 2 h at room temperature.

All methods described above gave low yields due to the very low solubility of pure or substituted nucleobase in the reported solvents. For this reason it was developed an alternative synthetic approach (Scheme 3) currently still under investigation



Scheme 3

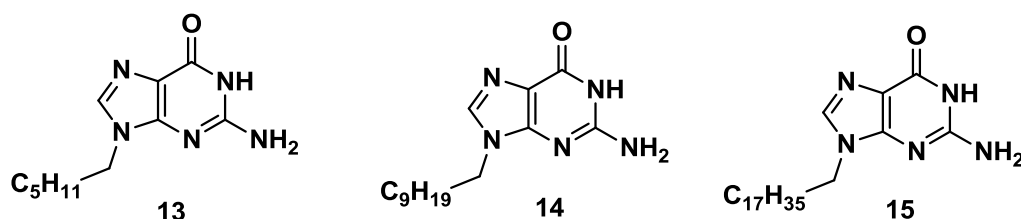
According to the literature ^[22] synthesis of **9** and **10** was carried out by reacting commercial 2-bromohipoxanthine with the appropriate ammine in refluxing 2-methoxyethanol in high yields. The reaction yield doesn't change if 2-fluorohipoxathine is used as starting material. Synthesis of this one can be carried out using as starting material O₆-benzylguanine (Scheme 4), through diazotization followed by addition of HBF₄ 48% that converts amimo NH₂ group connected to protected guanine to a fluorine.^[23-24] (see experimental part)



Scheme 4

3.3 Supramolecular studies in solution

N⁹-alkyl guanine derivatives with linear or chiral chain were studied in organic solvents to observe if in the absence of sugar they formed the typical supramolecular assemblies of lipophilic guanosine derivatives. In particular it is known Lipo-G are able to transfer alkaline picrates ($M^+ Pic^-$)^[25] from the aqueous to the organic phase, via G-quartet formation. On the other hand, in the absence of cations they are able to form other linear supramolecular aggregates. Three techniques were employed to study the self-assembly of *N⁹-alkyl* guanine derivatives, NMR (monodimensional and bidimensional experiments) and CD (circular dichroism). This latter can be used only for derivatives with chiral substituents. Due to solubility problems among all derivatives substituted with a linear alkyl chain only **12**, **13** and **14** were studied in the presence and in the absence of cations.



The solution self-assembly of these three derivatives was followed by NMR at different temperatures. ¹HNMR spectra of these compounds in a solvent as DMSO show non-aggregated molecules, but when solutions 6mM were prepared in tetrachloroethane, a non-competing solvent for hydrogen-bond, a change in the spectra (Tab.2) due to the formation of supramolecular aggregates in the range of 30°-90°C was observed. For all of the three compounds deshielding of both -NH1 and -NH2 signals was observed by lowering temperature, indicating their progressive involvement in

hydrogen bonding. The same behavior was observed for Lipo-G and is suggestive of ribbon-like architecture stabilization via an extended network of hydrogen bonds ^[26]

13-14-15	δ ppm in DMSO-d ₆	δ ppm in C ₂ D ₂ Cl ₄
NH-(1)	10.5(brs)	11.9 (brs)
NH-(2)	6.5 (brs)	5.8 (brs)
H8	7.6 (s)	7.6 (brs)
N9- α CH2	3.9 (t)	4(t)

Tab. 2

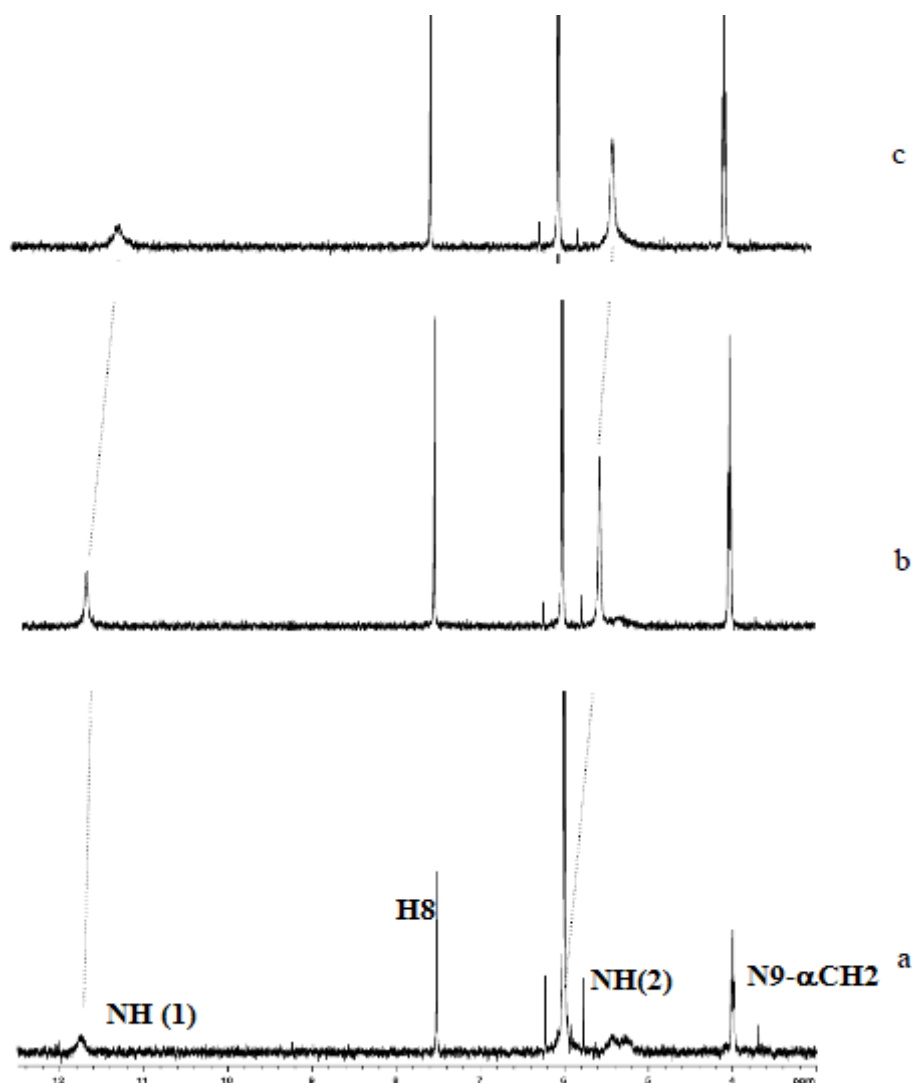


Figure 3.35 ¹H NMR spectra (400 MHz) recorded in C₂D₂Cl₄ (6 mM) at variable temperature 30 (a)-60 (b)-90 (c) C°

Compounds **13-14-15** show a similar behaviour at the same concentration in the same solvent.^[27] This establishes that the absence of sugar doesn't hinder the ability of N⁹-

alkyl guanine derivatives to form ordered supramolecular aggregates (ribbons) in solution as Lipo-G. 9-Octadecylguanine^[28] (**15**) was studied in the presence of cations: to a solution of 6 mM **15** in C₂D₂Cl₄ a weighted (1/8 mol/mol) amount of potassium iodide (KI) was added. The characteristic features of an octameric aggregate consisting of two stacked G-quartets can be recognized. The NH₂ signal shifts down to 6.7 ppm. Upon cooling to -20°C this signal first disappears (at 0°C) then reappears as two broad signals at 4.8 and 9.4 ppm (see ref. [29]). The H8 signal doubles, but other weaker lines are clearly visible. The NH region shows several signals as well (see ref. [30]), indicating the presence, beside the octamer, of higher order stacked aggregates in solution.

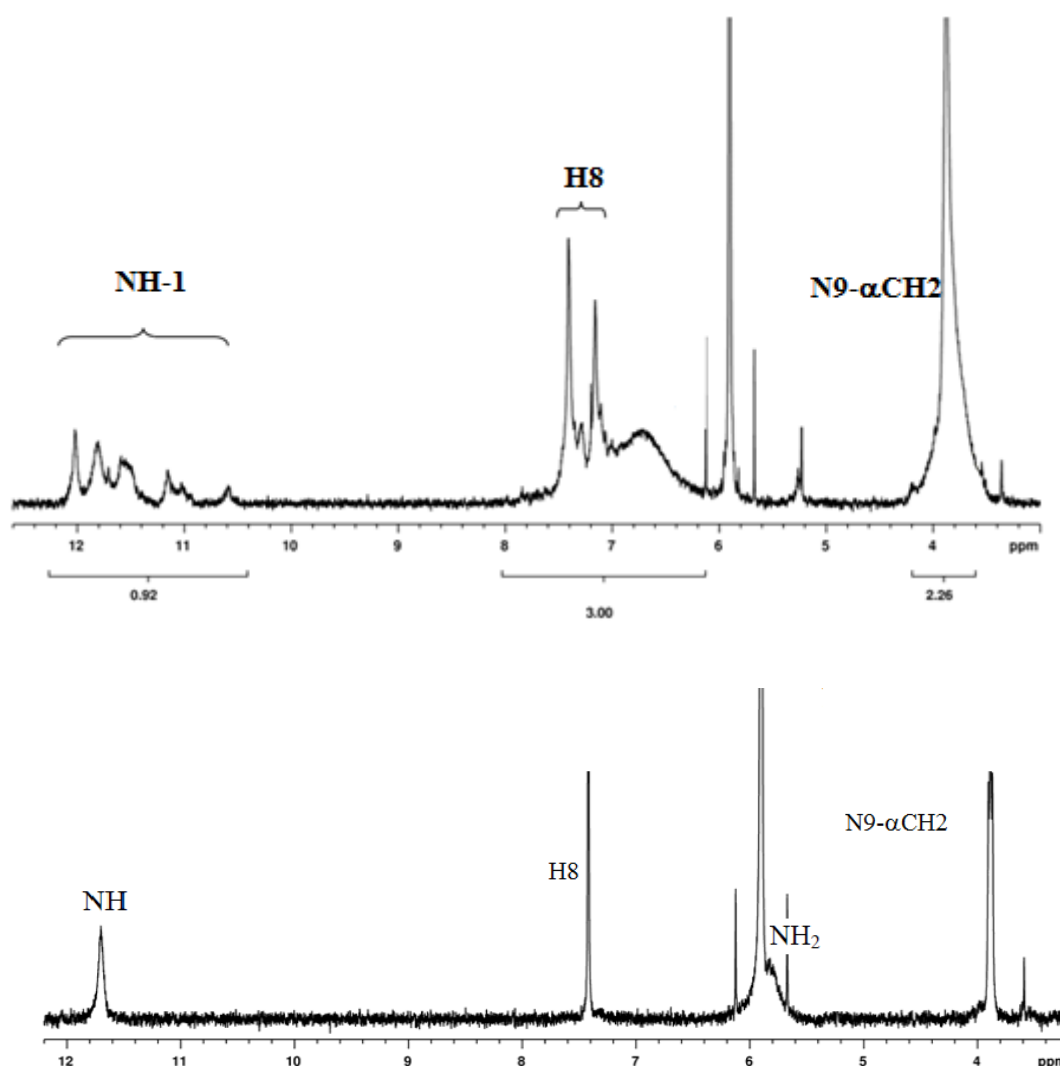
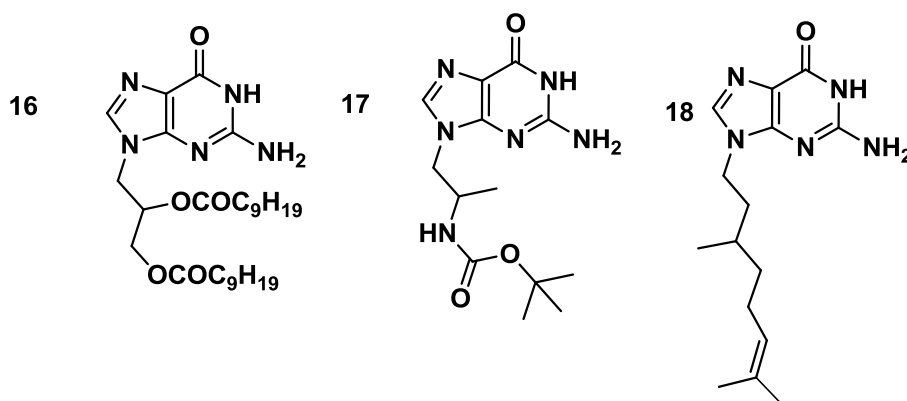


Figure 3.36: room temperature ¹H NMR spectra of **15** (400 MHz) before addition of KI (bottom), after addition of a weighted (1/8 mol/mol) amount of KI in C₂D₂Cl₄ (top)

In guanine derivatives substituted with linear alkyl chains at N9 position it's not possible to follow the supramolecular assembly in solution with circular dichroism due to the lack of a chiral substituent in the nucleobase. As we mentioned in section 1.5, in the case of

guanosine derivatives circular dichroism is diagnostic of both the formation of G-quartet based assemblies^[31] and the stacking polarity of two contiguous G-quartets. In fact, the tetramers do not stack in register, but are rotated with respect to each other to give, in the 230-300 nm region, characteristic of the π - π^* transition of guanine chromophore, a double signed exciton-like CD signal. This couplet, whose sign allows the assignment of the stacking helicity (handedness), exhibits opposite signed bands at ca. 260 and 240 nm for the head to tail (*C4*-symmetric) stacking while both bands are blue-shifted by 20-30 nm in the *D4*-symmetric stacking.^[32] In order to obtain a more detailed picture of *N*⁹-alkyl guanine derivatives self-assembly in the presence of alkali metal ions three guanine derivatives (**16**, **17**, **18**) with chiral substituents in *N*⁹-position were synthesized.



Self-assembly derivatives of **16-17-18** were studied by NMR and circular dichroism in organic solvents both in the presence and in the absence of cations. Derivative **16** in chloroform, analogously to the achiral compounds described above, forms ribbon aggregates stabilized by hydrogen bonds. ¹H-NMR spectra show in a solution 10 mM of CDCl₃ deshielding of NH-1 due to its involvement in the formation of hydrogen bonds. Moreover, the spectrum shows broad signals for H8-NH1-NH2 protons caused by the formation of these oligomeric aggregates. Also **17** and **18** compounds form in this solvent the same hydrogen bonding networks.

Derivatives **16** and **18** behave as ionophores; they are able to extract in organic solution cations via G-quartet formation. Solid-liquid extraction of **16** with a weighted 1/8 amount of strontium picrate in chloroform leads to the formation of an octameric aggregate. The ¹H-NMR spectrum shows a double set of signals. Integration of the picrate and H8 protons supports a 8:1 stoichiometry for the complex. The observation of signal doubling is thus consistent with a *C4*-symmetric octamer. (fig. 2.19). At room temperature amino protons are baseline broadened, but become clearly visible as two

different sets of signals centered at 5.6 ppm and to 9.6 ppm on decreasing temperature down to 0°C. The first set arises from amino protons not involved in the formation of hydrogen bonds while the downfield set belongs to the amino proton involved in the formation of G-quartets.

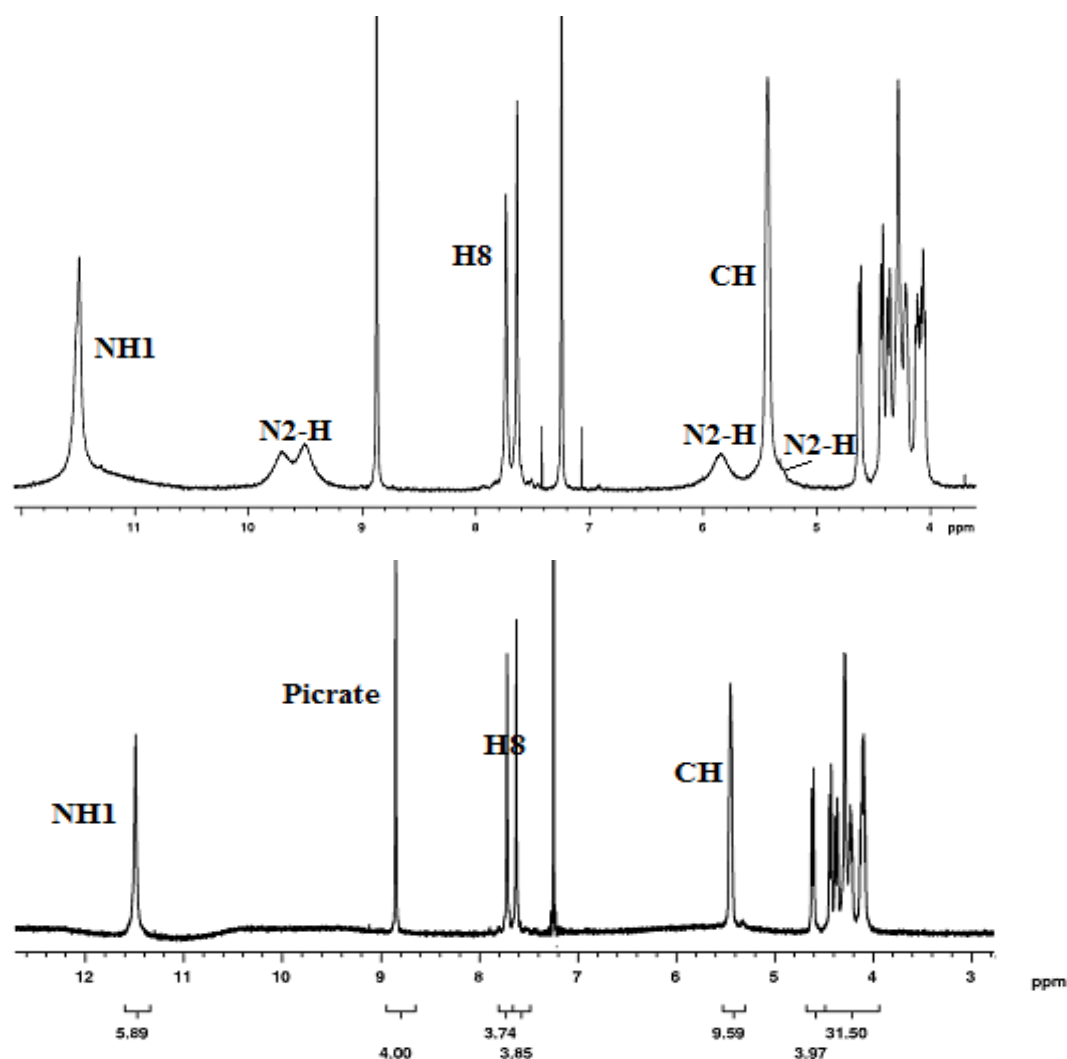


Figure 3.37: ¹H NMR spectra (600 MHz) of **16** after the addition of a weighted (1/8 mol/mol) amount of strontium picrate in CDCl₃ at 0°C (top) and room temperature (bottom).

Also solid-liquid extraction of **18** with a weighted 1/8 amount of either strontium picrate or potassium picrate in chloroform leads to the formation of an octameric aggregate or a pseudopolymeric aggregate. (fig. 3.38). CD spectra of chiral guanine derivatives confirms the presence of supramolecular aggregates in solution. CD spectrum of **18** in tetrachloroethane shows an intense exciton couplet centered to 260-290 nm, while spectrum of **16** exhibits a different bands and it was also characterized by CD induced

signal on picrate. The picrate anion feels chirality of supramolecular aggregate due to the aggregation induced by strontium ions.

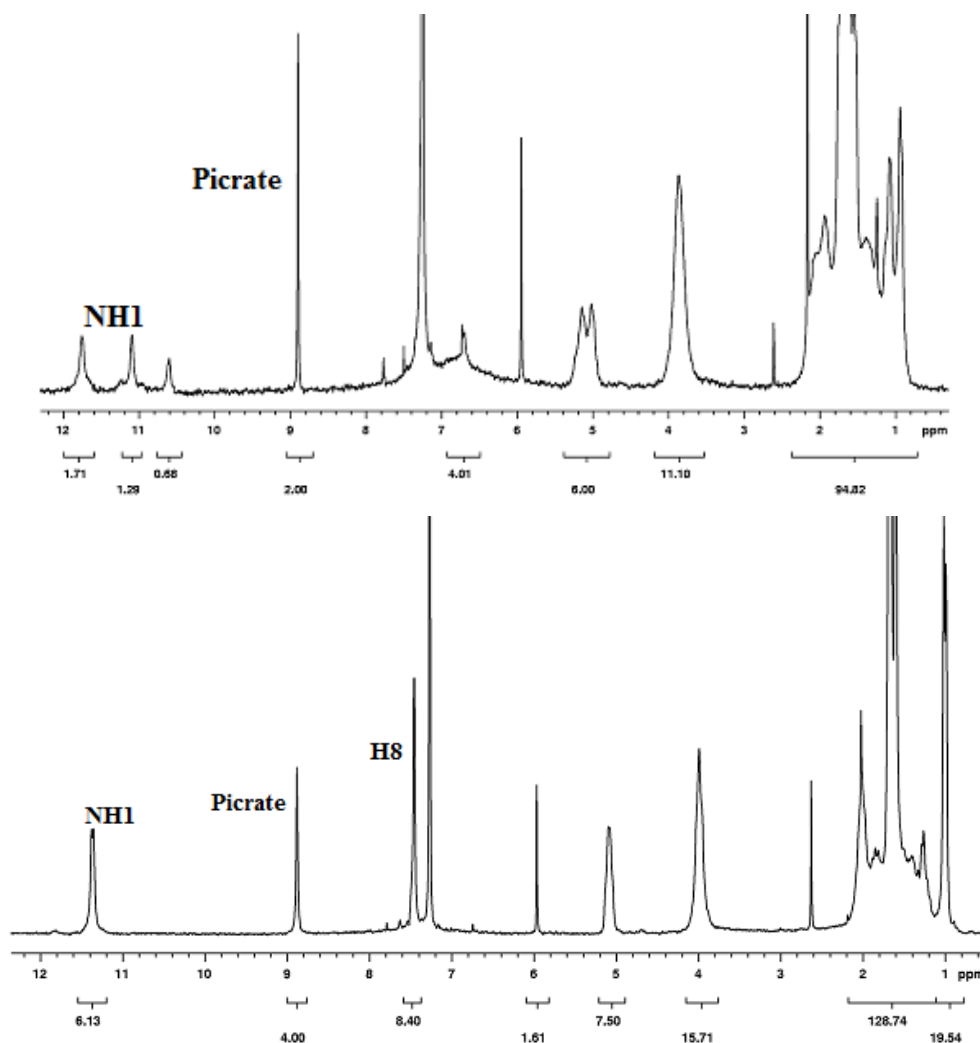


Figure 3.38: ¹H-NMR spectra (200 MHz) in CDCl₃ of **19** after the addition of a weighted (1/8 mol/mol) amount of strontium picrate (bottom) and potassium picrate (top).

CD spectra of chiral guanine derivatives confirm the presence of supramolecular aggregates in solution. The CD spectrum of **19** in tetrachloroethane shows an intense exciton couplet centered to 260-290 nm, while spectrum of **16 c** exhibits another band and it was also characterized by CD induced signal on picrate. The picrate anion feels chirality of supramolecular aggregate due to the aggregation induced by strontium ion

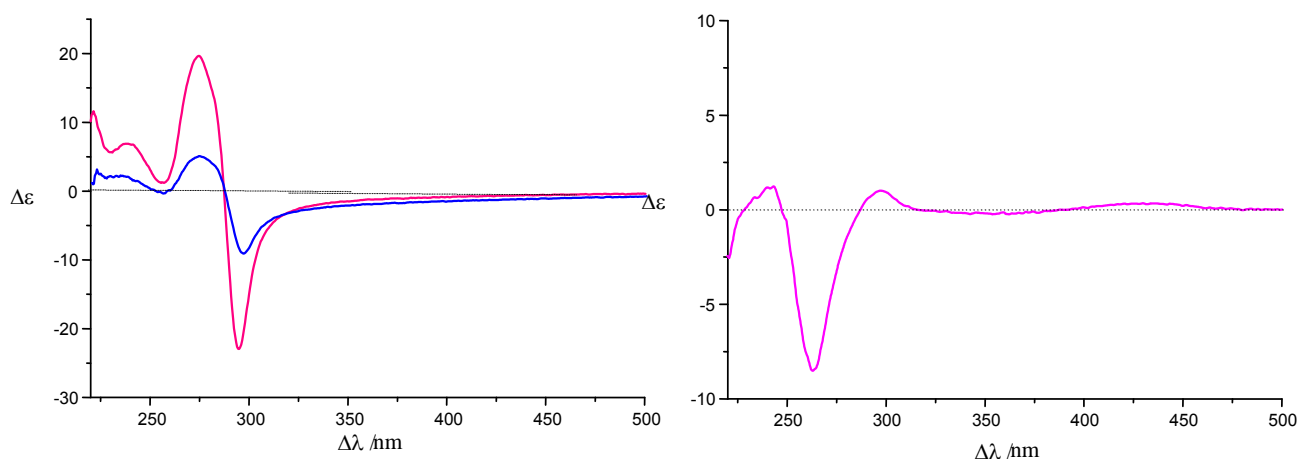


Figure 3.39: (left) CD spectrum of **19** in $C_2H_2Cl_4$ 10 mM after extraction with potassium picrate (8:1 pink line) and strontium picrate (8:1 blue line); (right) **16** in CH_3Cl 10 mM (pink line), after extraction with strontium picrate (8:1)

Studies in solutions show that all studied derivatives form, in analogy with lipophilic guanosine derivatives, either ribbon-like aggregates or cation-templated Gquartet based columnar structures. Therefore N^9 -substituted guanine can be used for the formation of supramolecular aggregates and derivatization with α -electro-active moieties could lead to organic optoelectronic devices such as OLED or OPV.

3.4 N^9 -alkylated guanines: STM study^[27]

3.4.1 Introduction

STM study of the self-assembly at the solid–liquid interface of substituted guanines carrying in the N^9 -position alkyl side chains with different lengths revealed the formation of distinct crystalline nanopatterns. The self-assembly of small molecular modules into non-covalently linked polymeric nanostructures is a subject of continuous interest.^[29,33] In particular, supramolecular structures with a high degree of order can be obtained through the self-association of organic molecules on flat solid surfaces. Such structures can be used as scaffolds to position electrically/optically active groups in pre-determined locations in 2D.^[34] Thereby paving the way towards a wide range of applications, e.g. in electronic and optical devices.^[35] For guanosine derivatives physisorbed at surfaces the thermodynamically stable ribbons were found to be characterized by cyclic $NH(2)–O(6)$ and $NH(1)–N(7)$ hydrogen bonds. In the solid state, the ribbons, by bridging gold electrodes, were found to be photoconductive.^[36] More interestingly, these ribbons also exhibit rectifying properties. A field-effect transistor

based on these supramolecular structures was described.^[37] Hitherto guanine based H-bonded supramolecular architectures were self-assembled on surfaces into highly ordered motifs and studied with scanning tunneling microscopy (STM) under ultra-high vacuum (UHV).^[38] Conversely at the solid–liquid interface our effort was mainly addressed towards the study of lipophilic guanosine monolayers.^[26,39] In collaboration with Prof. Paolo Samorì was decided to extend our studies at the solid–liquid interface to physisorbed monolayers of N⁹-alkylguanines because the absence of the sugar when compared to the previously studied guanosines and the presence of an aliphatic side-group can be foreseen to favor the molecular adsorption on graphite.^[29] In general, the formation of ordered motifs stabilized by hydrogen bonds on a solid surface requires the fine tuning of the interplay between the interactions among adjacent molecules and the adsorbate– substrate interactions.^[40] To achieve a full understanding of the self-assembly of guanine at the solid–liquid interface, it was performed a sub-molecularly resolved STM study of physisorbed monolayers on graphite of a series of N9-alkylguanines with linear alkyl side-chains. STM studies reported in this chapter have been performed by Dott. Arthur Ciesielski, in the group of Prof. Paolo Samorì from Strasbourg (France). The principle of the STM is straightforward. It consists essentially in scanning a metal tip over the surface at constant tunnel current as shown in figure 3.39. The displacements of the metal tip given by the voltages applied to the piezodrives then yield a topographic picture of the surface. The very high resolution of the STM rests on the strong dependence of the tunnel current on the distance between the two tunnel electrodes, i.e., the metal tip and the scanned surface. The tunnel current through a planar tunnel barrier of average height ψ and width s is given by^[41]

$$J_T \propto \exp(-A \psi^{1/2} s), \quad (1)$$

where $A = (4\pi/h) 2m)^{1/2} = 1.025 \text{ \AA}^{-1} \text{ eV}^{-1/2}$ with m the free-electron mass, appropriate for a vacuum tunnel barrier. With barrier heights (work functions) of a few electronvolts, a change of the tunnel barrier width by a single atomic step (2-5 Å) changes the tunnel current up to three orders of magnitude. Using only the distance dependence as given by Eq. (1), and a spherical tip of radius R , one estimates a lateral spread δ of a surface step as $\delta \approx 3r_0 = 3(2R/A \psi^{1/2})$. Thus, a lateral resolution considerably below 100 Å requires tip radii of the order of 100 Å. Such tips are standard in field emission microscopy.

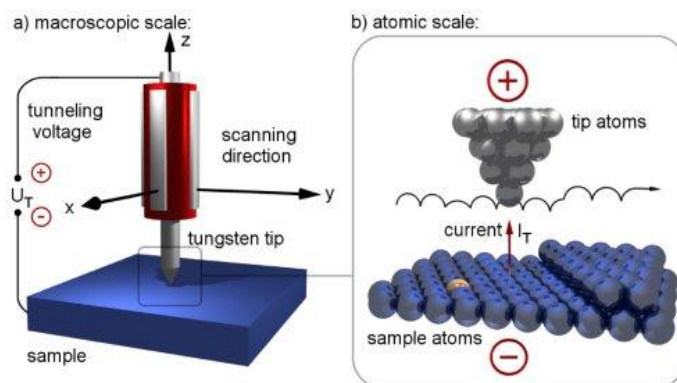


Figure 3.39: Principle of scanning tunneling microscopy: Applying a negative sample voltage yields electron tunneling from occupied states at the surface into unoccupied states of the tip. Keeping the tunneling current constant while scanning the tip over the surface, the tip height follows a contour of constant local density of states

Compared to (UHV) conditions, solid-liquid interface has many advantages: a simple experimental approach which doesn't require an expensive infrastructure, the dynamic exchange of molecules adsorbed on the surface and the one on liquid phase promotes self-healing of defects in the self-assembled layers,^[42] solid-liquid interface provides an excellent environment for *in-situ* chemical modifications of adsorbed molecules.

HOPG is widely used as a model substrate for exploring molecular self-assembly at a solid-liquid interface.^[43] It has a layered structure as do mica and MoS₂. In each layer, the carbon atoms adopt sp² hybridization. The remaining p orbitals are perpendicular to the plane and parallel to each other. Thus, all atoms in one layer form an infinite superconjugated π -bond network at the macroscopic scale of the sample size (fig. 3.40 a). This provides a good substrate for investigating how the molecule-substrate interaction influences formation of the self-assembled structures of various molecules. Two adjacent layers with a large separation of 3.35 Å are weakly linked by van der Waals forces, which make it easy to prepare a fresh surface by simply peeling off the outer layers. As shown in fig. 3.40 b, the lattice of two adjacent layers (A and B) is offset from each other. Each atomic layer of graphite packs in an ABABAB pattern. Thus, the upper layer has one-half of the atoms overlapping with its adjacent lower layer. This overlap makes one-half of the atoms of the upper layer identifiable in a STM image. The graphite surface has three-fold symmetry, and the carbon atoms along the direction of any C3 axis display the same zigzag extension as the zigzag skeleton of the carbon backbone of an all-trans alkyl chain (fig. 3.40 c). The distance 2.46 Å between two interval carbon atoms along any C3 axis is very close to the separation of two interval carbon atoms of the all-trans alkyl chain, 2.52 Å. This coincidence makes the all-trans alkyl chain match

very well with the underlying zigzag lattice of the graphite surface when it self-assembles on graphite, maximizing the molecule-substrate interaction. This lattice match for self-assembly of all-trans long-chain organic molecules on HOPG has been confirmed widely.^[44] This comparative study was carried out by applying a drop of 1 ± 0.1 mM solutions of *N⁹-alkyl-guanine* with a linear side chains (see fig. 3.41) in 1,2,4-trichlorobenzene (TCB) on freshly cleaved highly oriented pyrolytic graphite (HOPG). (see experimental part).

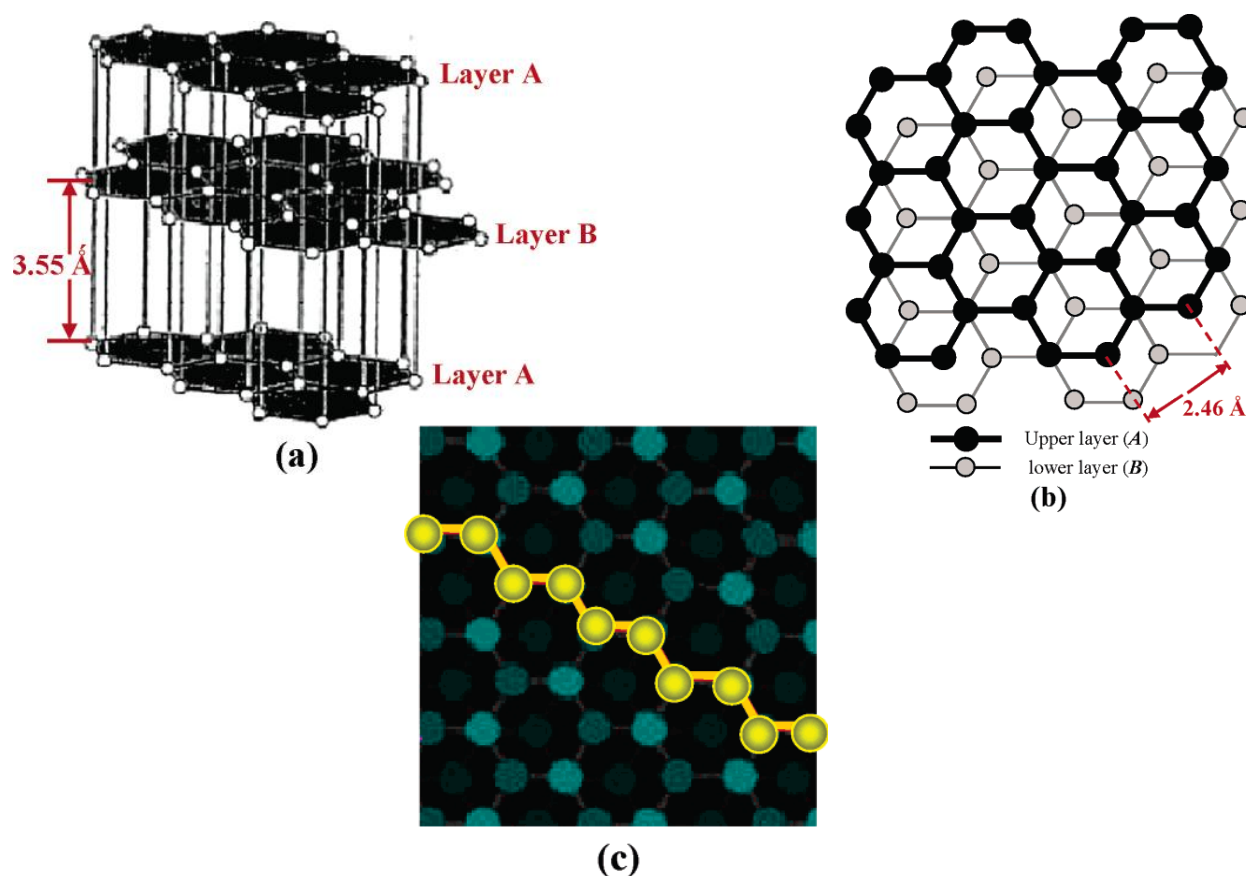


Figure 3.40: (a) Positional relationship between two adjacent graphite layers *A* and *B*. (b) Graphite structure can be described as an alternate succession of these planes ...*ABABAB*.... (c) Structural match between the carbon skeleton of all-trans long-chain organic molecules and the zigzag lattice of the graphite surface. The superimposed zigzag chain represents the carbon skeleton of an all-trans alkyl chain.

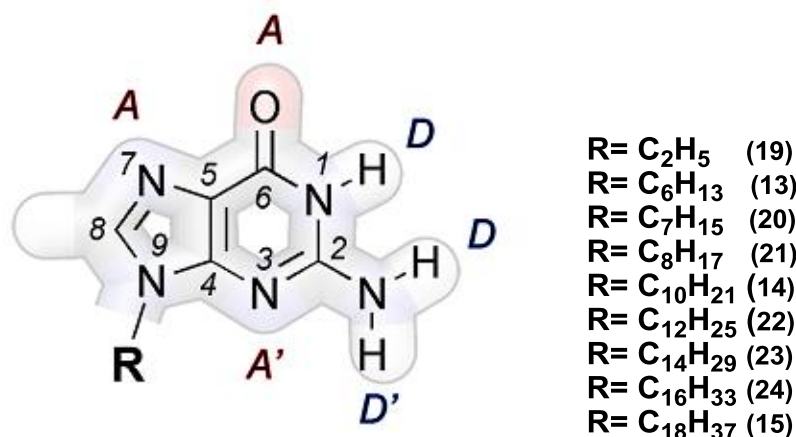


Figure 3.41 Chemical formula of investigated guanine

3.4.2 Results and discussions

Derivative **19** was commercially available, the others compounds have been synthesized following the procedure described in the experimental part. For the crystalline pattern obtained from each guanine self-assembled on HOPG the unit cell parameters, i.e. length of vectors a and b , α (angle between the vectors), unit cell area (A), number of molecules in the unit cell (N_{mol}), area occupied by a single molecule in the unit cell (A_{mol} , with $A_{mol}=A/N_{mol}$) and estimated projection of the molecular van der Waals volume onto surface (A_{vdw}) are given in Table 3. All proposed packing motifs for molecules described above have been compared with theoretical models. Fig. 3.42 a shows an STM image of the monolayer obtained from molecule **19** it reveals a crystalline ribbon-like architecture. In this 2D crystal the ethyl side chains are most likely physisorbed flat on the surface, although due to their high conformational dynamics they could not be resolved. The area occupied by a single molecule **19** corresponds to $0.75 \pm 0.1 \text{ nm}^2$, being in good agreement with the van der Waals area of **19**. The supramolecular motif can be well described by the formation of a one-dimensional H-bonded ribbon involving the following pairing: $NH(2)-O(6)$ and $NH(1)-N(7)$ (model in Fig. 2.23), in good accordance with previous observations on N9-octadecylguanine **15**^[29] and guanosine derivatives.^[26]

Table 3 Unit cell parameters of all guanine derivatives at the solid and liquid interface

N ⁹ -Guanine	Side chain	Unit cell parameters ^a						
		<i>a</i> /nm	<i>b</i> /nm	∠	<i>A</i> /nm ²	<i>N</i> /mol	<i>A</i> _{mol} /nm ²	<i>A</i> _{vdw} /nm ²
19	C ₂ H ₅	1.00 ± 0.2	1.51 ± 0.2	(92 ± 3)°	1.51 ± 0.21	2	0.75 ± 0.1	0.55 ± 0.02
13	C ₆ H ₁₃	0.98 ± 0.2	1.63 ± 0.2	(84 ± 3)°	1.58 ± 0.20	1	1.58 ± 0.2	0.75 ± 0.02
20	C ₇ H ₁₅	0.97 ± 0.2	1.85 ± 0.2	(81 ± 3)°	1.77 ± 0.19	2	0.88 ± 0.1	0.80 ± 0.02
21	C ₈ H ₁₇	1.27 ± 0.2	2.01 ± 0.2	(58 ± 3)°	2.15 ± 0.22	2	1.07 ± 0.1	0.85 ± 0.02
14	C ₁₀ H ₂₁	1.19 ± 0.2	1.46 ± 0.2	(96 ± 3)°	1.72 ± 0.21	1	1.72 ± 0.2	0.90 ± 0.02
22	C ₁₂ H ₂₅	1.00 ± 0.2	4.19 ± 0.2	(68 ± 3)°	3.76 ± 0.21	4	0.94 ± 0.1	1.00 ± 0.02
23	C ₁₄ H ₂₉	1.00 ± 0.2	4.73 ± 0.2	(68 ± 3)°	4.25 ± 0.21	4	1.06 ± 0.1	1.10 ± 0.02
24	C ₁₆ H ₂₃	1.00 ± 0.2	5.27 ± 0.2	(68 ± 3)°	4.73 ± 0.21	4	1.18 ± 0.1	1.20 ± 0.02
15	C ₁₈ H ₃₇	1.00 ± 0.2	5.81 ± 0.2	(68 ± 3)°	5.22 ± 0.21	4	1.31 ± 0.1	1.30 ± 0.02

^a *a* and *b* are the vector lengths and μ the angle between those vectors; *A* is the unit cell area, *N*_{mol}, the number of molecules in the unit cell and *A*_{mol} (= *A*/*N*_{mol}) is the area occupied by single molecule within the unit cell; *A*_{vdw} is the estimated van der Waals area

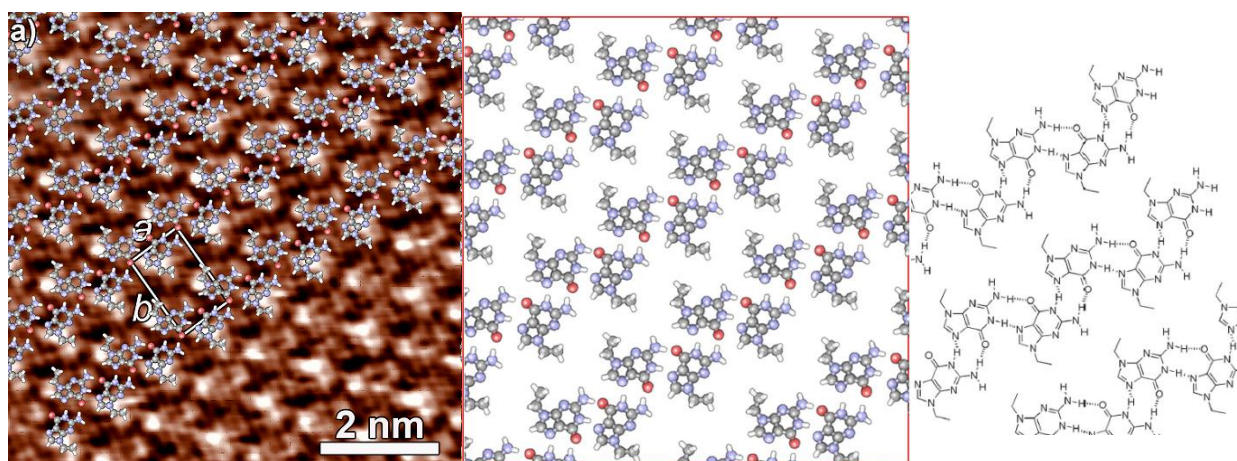


Figure 3.42a: STM image of a monolayer of ribbon-like structure of **19**. Tunneling parameters: average tunneling current (*I*_t) = 15 pA, bias voltage (*V*_t) = 350 mV. Comparison of the proposed molecular packing with the theoretical model

Self-assembled structures of molecule **13** exhibit a 2D crystal with the hexyl side-chains physisorbed flat on the surface (fig. 3.43b). Differently from the monolayer of **19** self assembly of **13** is not dictated by the formation of H-bonding between adjacent molecules, but rather unspecific van der Waals interactions between molecules and the substrate rule the generation of an ordered monolayer.

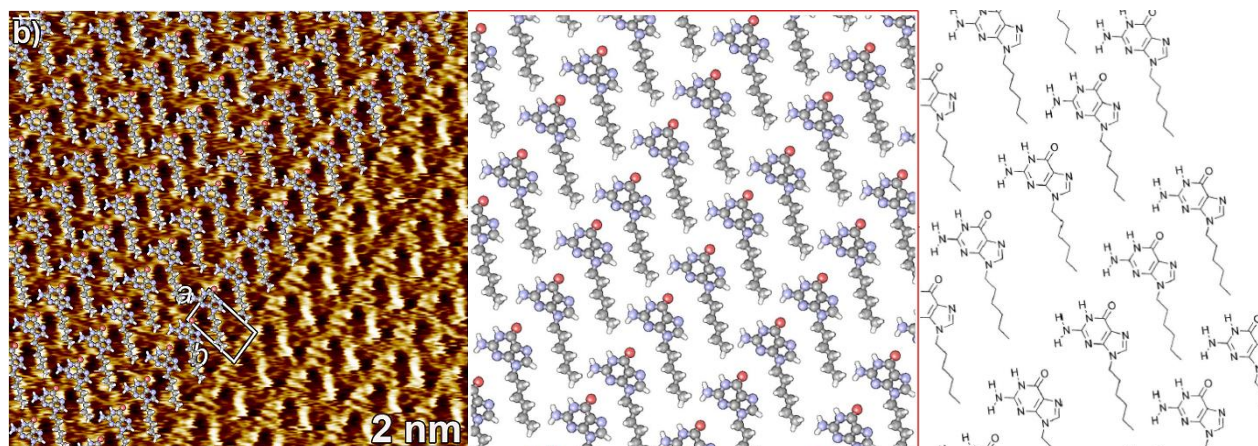


Figure 3.43b: STM image of a monolayer of **13**. Tunneling parameters: average tunneling current (I_t) = 15 pA, bias voltage (V_t) = 350 mV. Comparison of the proposed molecular packing with the theoretical model

A similar motif was observed in a monolayer of **14** (fig. 3.44). The packing is very loose as proved by the large discrepancy between A_{mol} and A_{vdW} . Despite such large voids which could host a second ad-molecule, we observed only one molecule per unit cell as probably ruled by the registry with the substrate.

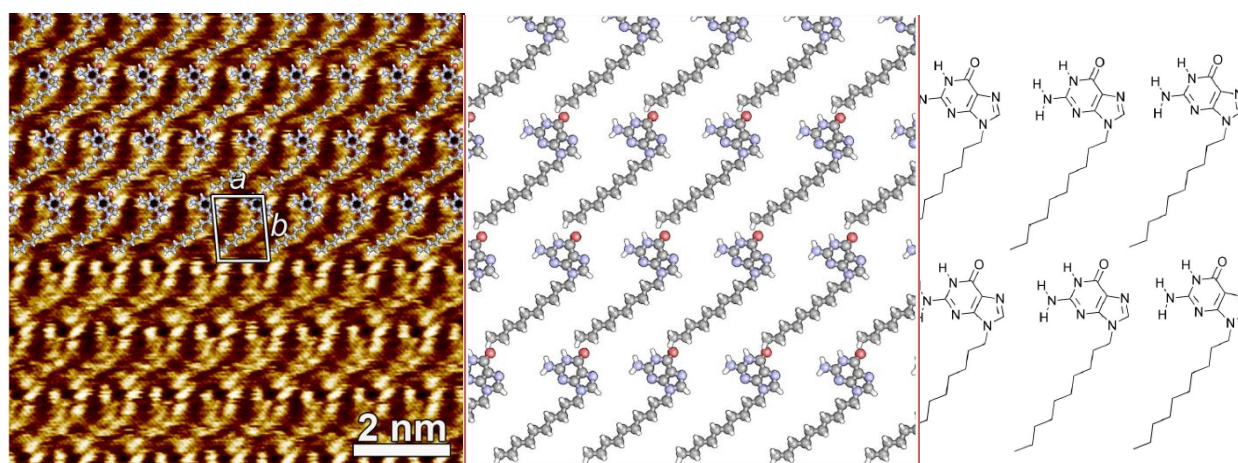


Figure 3.44: STM image of a monolayer of **14**. Tunneling parameters: average tunneling current (I_t) = 15 pA, bias voltage (V_t) = 350 mV. Comparison of the proposed molecular packing with the theoretical model

Fig 3.45 portrays the STM image recorded for a monolayer of molecule **20**. It reveals large ordered lamellae featuring a dimer packing motif involving the following pairing: NH(2)–N(7) and NH(1)–O(6). The comparison of the area occupied by a single molecule, i.e. $0.88 \pm 0.1 \text{ nm}^2$, with the van der Waals molecule's size of $0.80 \pm 0.02 \text{ nm}^2$ suggests that the heptyl side chains are physisorbed at the surface, though due to their high conformational dynamics they could not be resolved.

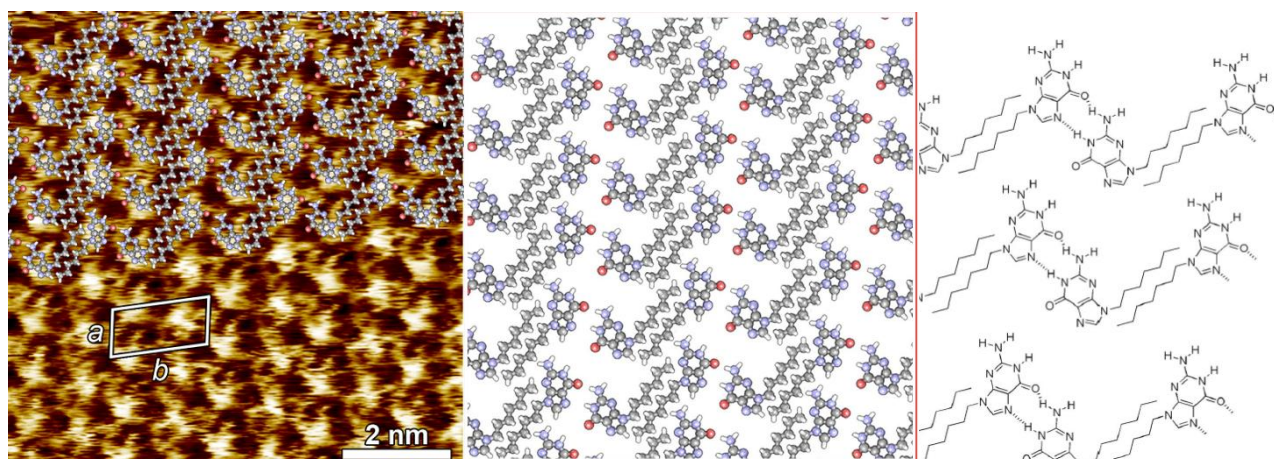


Figure 3.45: STM image of a monolayer of **20**. Tunneling parameters: average tunneling current (I_t) = 15 pA, bias voltage (V_t) = 350 mV. Comparison of the proposed molecular packing with the theoretical model

Fig. 3.46 shows a monolayer of **21** at the HOPG–solution interface. As in the case of **20**, the packing can be described by the formation of a dimer involving the pairing NH(2)–(7) and NH(1)–O(6). The octyl side chains are supposedly physisorbed on the graphite surface. However, differently from the case of the pattern formed through self-assembly of **20**, within the dimers only one alkyl chain is physisorbed on the HOPG surface.

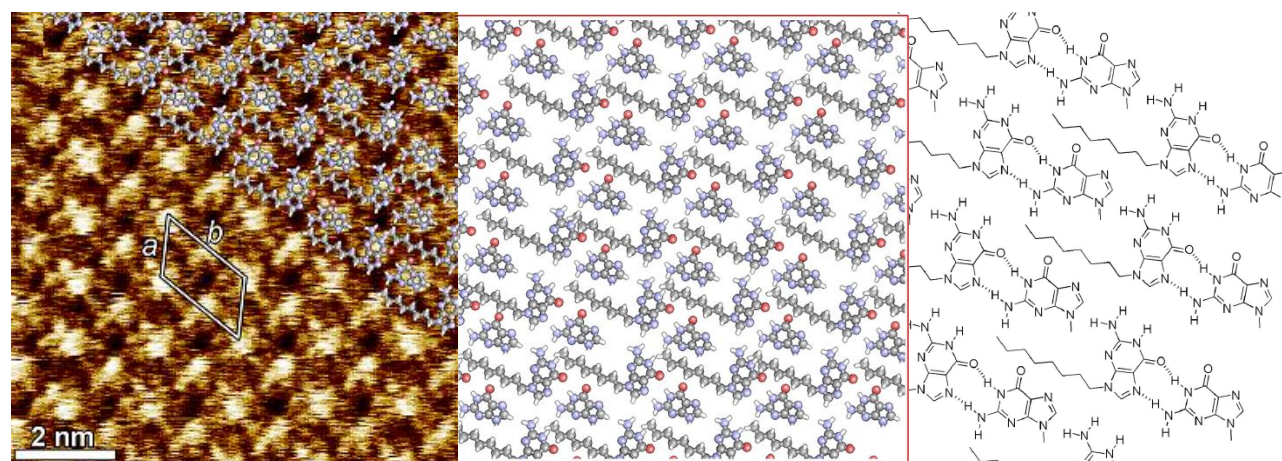


Figure 3.46: STM image of a monolayer of **21**. Tunneling parameters: average tunneling current (I_t) = 15 pA, bias voltage (V_t) = 350 mV. Comparison of the proposed molecular packing with the theoretical mode

Subsequently, we have focused our attention on the self-assembly of guanines exposing longer alkyl side chains. Interestingly, regardless of the length of the side chain ($C_{12}H_{25}$ for **22**, $C_{14}H_{29}$ for **23**, $C_{16}H_{33}$ for **24** and $C_{18}H_{37}$ for **15**) the observed monolayers exhibit a similar motif consisting of H-bonded ribbons, involving the pairing NH(2)–O(6) and NH(1)–N(7) (fig. 3.47). In the 2D crystals the long side chains are clearly visible:

they are physisorbed flat on the surface and are interdigitated between adjacent supramolecular ribbons, thereby stabilizing the entire monolayer. Further, the comparison of the unit cell parameters of monolayers of **22–24**, **15** self-assembled at the HOPG–solution interface (Table 3) reveals that the only difference between those structures is the value of the b vector, thus affecting also the area occupied by a single guanine molecule (A_{mol}). Interestingly, the difference between $A_{\text{mol}}\mathbf{22}$ and $A_{\text{mol}}\mathbf{23}$ matches the difference between $A_{\text{mol}}\mathbf{23}$ and $A_{\text{mol}}\mathbf{24}$, i.e. 0.11 nm^2 , being in good agreement with the area occupied by an ethylene group, i.e. $0.12 \pm 0.01 \text{ nm}^2$. The difference between $A_{\text{mol}}\mathbf{24}$ and $A_{\text{mol}}\mathbf{15}$ amounts to $0.13 \pm 0.01 \text{ nm}^2$. For monolayers of **22–24**, **15** the packing is extremely tight as revealed by the very similar values of A_{mol} and A_{vdW} for each system. The thermodynamic characteristics of guanine association, obtained from the gas phase experiments^[45] revealed that the energy of supramolecular polymerization in motifs like those visualized by STM amounts to $32\text{--}36 \text{ kcal mol}^{-1}$ per molecule. In comparison the adsorption energy of alkyl chains on the HOPG surface, determined by temperature-programmed desorption experiments,^[46] increases linearly with the chain.

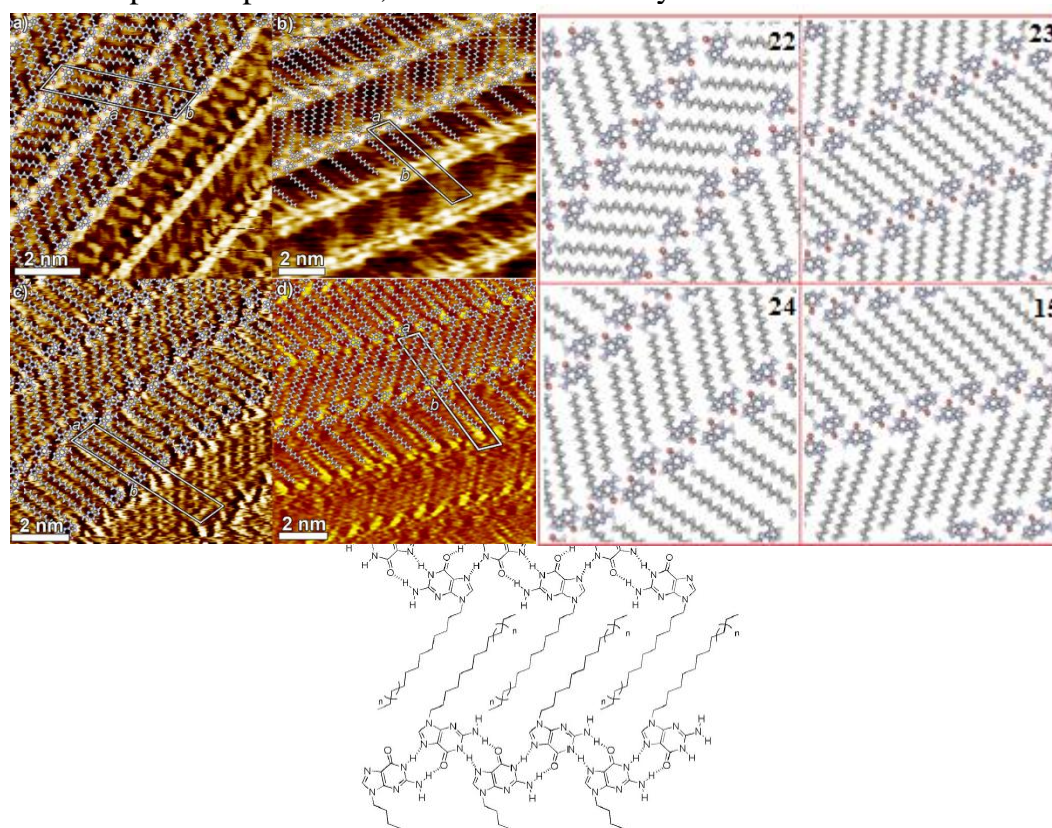


Figure 3.47: STM image of hydrogen bond ribbons formed by **22(a)**, **23(b)**, **24(c)**-**15(d)**. Tunneling parameters: average tunneling current (I_t) = 15 pA, bias voltage (V_t) = 350 mV. Comparison of the proposed molecular packing with the theoretical mode.

N ⁹ -Guanine	Side chain	Adsorption energy in Kcal/mol*
19	C ₂ H ₅	5.2
13	C ₆ H ₁₃	15.6
20	C ₇ H ₁₅	18.2
21	C ₈ H ₁₇	20.8
14	C ₁₀ H ₂₁	26
22	C ₁₂ H ₂₅	31.2
23	C ₁₄ H ₂₉	36.4
24	C ₁₆ H ₃₃	41.6
15	C ₁₈ H ₃₇	46.8

Table 3: * The adsorption energy of alkyl chains on the HOPG surface

3.4.3 Conclusions

In summary, it was performed a comparative STM study on the self-assembly at the HOPG–solution interface of substituted guanines exposing in the N⁹-position alkyl side chains with different length. Molecules **13–15, 19–24** were found to form monomorphic 2D crystals, which are stable on the several tens of min time scale and exceed various hundreds of nm². Subtle changes in the length of the alkyl side-chains dramatically influenced the 2D patterns on graphite. Derivatives with alkyl tails longer than C₁₂ (**22–24, 15**) self-assembled into linear H-bonded ribbons through the NH(2)–O(6) and NH(1)–N(7) pairing with 4 molecules in the unit cell. The same H-bonding pattern was observed for N⁹-ethylguanine **19**, but the packing shows only 2 molecules in the unit cell (the adjacent H-bonded noncentrosymmetric ribbons run indeed in a parallel way while for **22–24, 15** they are antiparallel). For derivatives with tails of intermediate length (from C₆ to C₁₀) no H-bonded supramolecular polymers were formed at the surface: ordered monolayers of single (non-H-bonded) molecules (**13** and **14**) or H-bonded dimers (**20** and **21**) were observed. In light of the dynamic self-assembly characteristics of guanines, our results may be of interest for the generation of responsive nanopatterned surfaces featuring pre-programmed structural motifs at the supramolecular level.

3.5 Reversible Assembly/Reassembly Process

The metal templated reversible assembly/re-assembly into quartets and ribbons has been described also at the solid-liquid interface by means sub-molecularly resolved STM.^[28] The molecule used in this study was a N⁹-alkylguanine, **15**, and the substrate used also in case was a highly oriented pyrolytic graphite (HOPG) surface. The presence of a long aliphatic side-chain and the absence of the sugar are expected to promote the molecular physisorption on HOPG. The self-assembly on HOPG has been studied for neat **15** and upon sub-sequent addition of [2.2.2] cryptand, potassium picrate and trifluoromethanesulfonic acid to trigger the reversible interconversion between two different highly ordered supramolecular motifs.

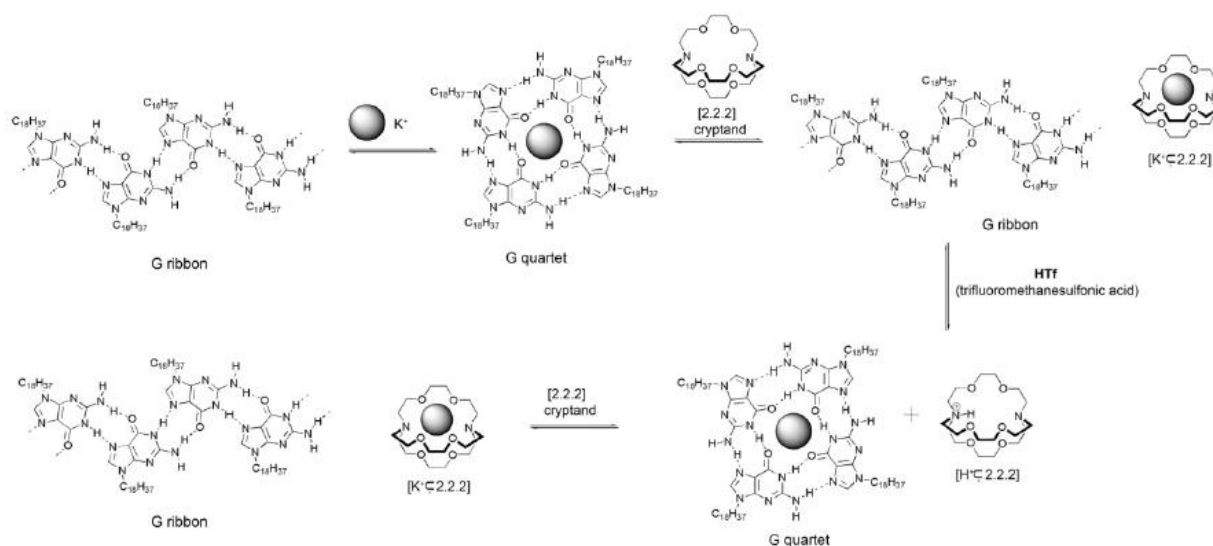


Figure 3.48: the stepwise reversible interconversion between G-ribbon and G-quartet.

Initially the self-assembly of **15** was investigated by applying a drop of a solution in 1,2,4-trichlorobenzene (TCB) on the graphite surface. STM image of the obtained monolayer showed a crystalline structure consisting of ribbon-like architectures (fig. 3.49 a)^[29-47]. In this 2D crystal the octadecyl side chains are physisorbed flat on the surface and are interdigitated between adjacent supramolecular ribbons (fig. 3.49 c). The supramolecular motif can be well described by the formation of a one dimensional H-bonded ribbon involving the following pairing: NH(2)-O(6) and NH(1)-N(7) (fig. 2.23, “ribbon A”). The STM study of a monolayer of guanine solution containing potassium

picrate revealed the formation of a G-quartet based architecture at surface (fig. 3.49b). Figure 3.49.d shows the proposed G-quartet based molecular packing motif. The circular feature exhibiting a high contrast in figure 3.49b can be ascribed to the potassium ions, located in the center of G-quartet structure. With respect to the solution case, we observe here the formation of NH(2)-N(7) hydrogen bonds between adjacent G-quartets, stabilizing the entire supramolecular arrangement (the alkyl chains of **15** are back-folded into the supernatant solution).

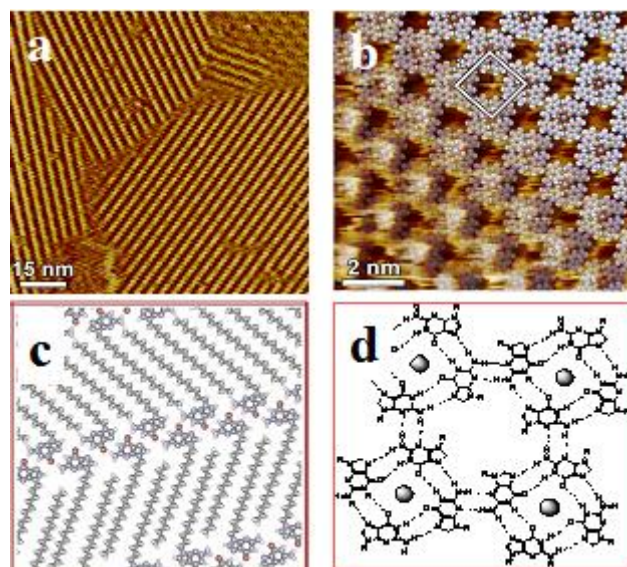


Figure 3.49: STM images of monolayers of supramolecular architectures of **15** at the solid-liquid interface self-assembled from TCB solution; a) ribbon-like structure and c) G-quartet based architecture. The model of their packing motif are shown in c) and d), respectively

To gain deeper insight into the two structures, and into their interconversion, *in-situ* successive assembly/re-assembly cycles from ribbon to G-quartet based architectures were accomplished [29]. To the initial ribbon-like motif (fig. 3.50a), upon *in-situ* addition of potassium picrate solution in TCB, the G-quartet supramolecular motif was obtained (fig. 3.50b). To sequester the ions from the G-quartet, we opted again to use the cryptand [2.2.2] to yield the cryptate $[K^+ \subset 2.2.2]$ [48]. Upon subsequent *in-situ* addition of [2.2.2] cryptand solution to the G-quartet supramolecular architectures, the guanine re-assembled on HOPG into the original ribbon (fig. 3.50c). By adding a solution of trifluoromethanesulfonic acid (HTf), the potassium ions were released from the cryptate and the G-quartet assembly was re-generated (fig. 3.50d). Upon further addition of a [2.2.2] cryptand solution, the ribbon structure was created again (fig. 3.50e).

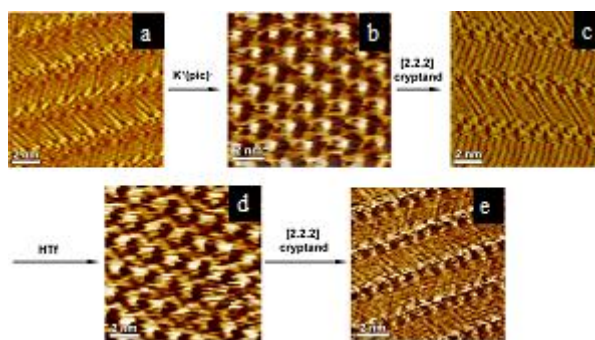
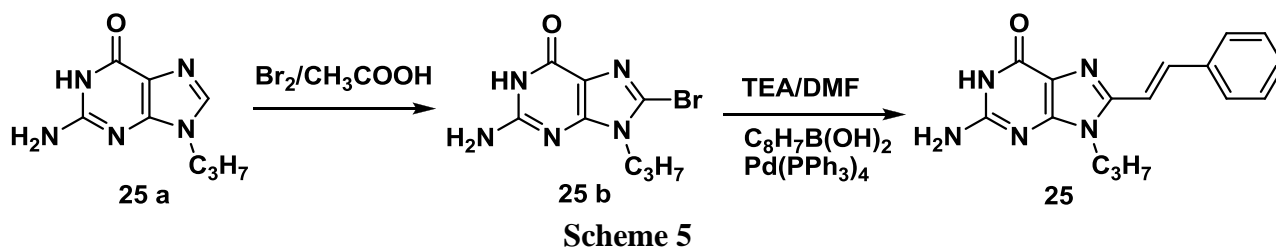


Figure 3.49: Consecutive STM images showing the structural evolution of a monolayer of **3**. a), c) and e) show ribbon-like structure, whereas b) and d) exhibit G-quartet based architectures

Clearly, inspired by results in solution described in chapter 2.4.3 of LipoG *E-6* [49] our next challenge is to control this reversible assembly/re-assembly process at the solid-liquid interface by photons. To this aim in Scheme 5 it is shown the synthetic pathway for photochromic derivative **25**, due to the low solubility it's not possible to study this compound in solution. Previously it has been synthesized another similar compound with a longer alkyl chain (octadecylguanines) than **25**, but its solubility was probably too high to form any self assembled nanopattern on the HOPG surface, study of this system in in different solvents i.e. TCB, 1-phenyloctane, and heptanoic acid did not produced any meaningful results. Only disordered structures were observed with STM. Thereby it was investigated the derivative **25** where the octadecanoic alkyl chain has been substituted by a shorter propyl chain. After trying different solvents as a result of the poor stability of the self-assembled nanopattern, a drop of a $100 \pm 1 \mu\text{M}$ solution in heptanoic acid was applied to the graphite surface. Figure 3.50 shows STM height images of the obtained physisorbed monolayer featuring a polycrystalline structure, which consists of hundreds of square nanometers large crystalline domains that are stable over several minutes. These domains exhibit a unit cell: $a = (2.02 \pm 0.2) \text{ nm}$, $b = (1.02 \pm 0.2) \text{ nm}$, $\alpha = (80 \pm 3)^\circ$ leading to an area $A = (2.03 \pm 0.44) \text{ nm}^2$, where each unit cell contains one molecule (Fig. 3.51b).



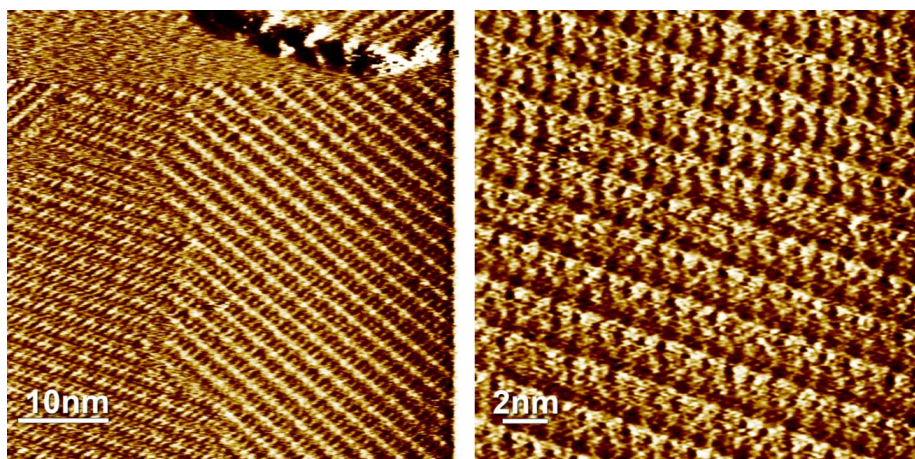


Figure 3.50. a) and b) STM height images of a **25** monolayers at the liquid-graphite interface self-assembled from solution in heptanoic acid forming the 2D nanopattern

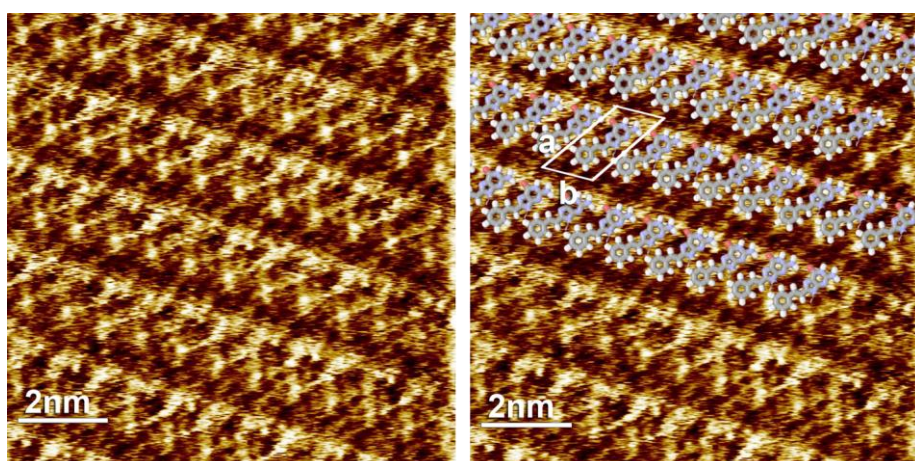


Figure 3.5 a) Small scale STM height image of **25** at the solid-liquid interface; b) Proposed CPK model of the **25**. Tunneling parameters: Average tunneling current (I_t) = 20pA, tip bias voltage (V_t) = 300 mV

25 was formed the assembled structures on the surface, however photoisomerisation nor the expected consequent dynamic rearrangement under UV irradiation (fig.3.52) (365nm) were observed in all the experiment performed.

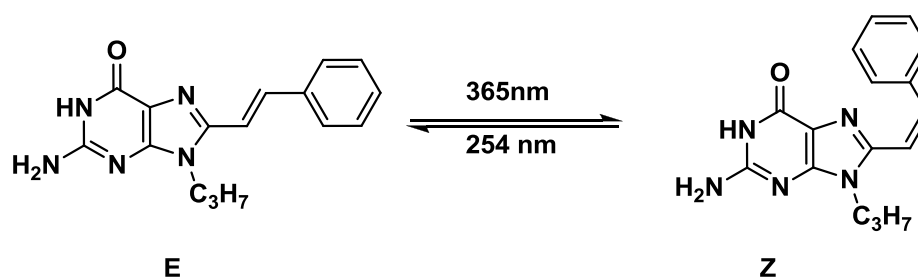


Figure 3.52: expected photoisomerisation

Bibliography

- 1 M. S. Casthilo, M. P. Postigo, C. B. V. de Paula, C. A. Montanari, G. Oliva, A. D. Andricopulo, *Bioorg. Med. Chem.* **2006**, *14*, 516.
- 2 D. Murthy, M. Brakta, L. O. Ellis, *Med. Chem. Res.* **2003**, *12*, 13.
- 3 V. Nair, V. Uchil, N. Neamati, *Bioorg. Med. Chem. Lett.* **2006**, *16*, 1920.
- 4 J. W. Chern, D. S. Wise, D. S. Shewach, P. E. Daddona, L. B. Townsend, *Eur. J. Med. Chem.* **1994**, *29*, 3.
- 5 S. R. Kasibhatla, K. Hong, M. A. Biamonte, D. J. Busch, P. L. Karjian, J. L. Sensintaffar, A. Kamal, R. E. Lough, J. Brekken, K. Lundgren, R. Grecko, G. A. Timony, Y. Ran, R. Mansfield, L. C. Fritz, E. Ulm, F. J. Burrows, M. F. Boehm, *J. Med. Chem.* **2007**, *50*, 2767.
- 6 L. Chen, N. Kode, D. Murthy, S. Phadtare, *Med. Chem. Res.* **2005**, *14*, 445.
- 7 J. E. B. McCallum, C. Y. Kuniyoshi, C. S. Foote, *J. Am. Chem. Soc.* **2004**, *126*, 16777.
- 8 C. Sheu, P. Kang, S. Khan, C. S. Foote, *J. Am. Chem. Soc.* **2002**, *124*, 3905.
- 9 C. Sheu, C. S. Foote, *J. Am. Chem. Soc.* **1995**, *117*, 474.
- 10 C. Sheu, C. S. Foote, *J. Am. Chem. Soc.* **1995**, *117*, 6439.
- 11 J. T. Davis, G. P. Spada, *Chem. Soc. Rev.* **2007**, *36*, 296.
- 12 J. L. Sessler, M. Sathiosatham, K. Doerr, V. Lynch, K. H. Abboud, *Angew. Chem., Int. Ed.* **2000**, *39*, 1300.
- 13 D. L. Hughes, *The Mitsunobu reaction. In Organic Reactions*; Oxford: New York, **1992**; Vol. 42, 335-656.
- 14 (a) H. Chen, S. J. Li, *Phys. Chem.* **2006**, *110*, 12360-12362. (b) M. J. Robins, M. J. Zhong, *Org. Chem.* **2006**, *71*, 8901-8906. (c) Garner, P.; Yoo, J. U.; Sarabu, R. *Tetrahedron* **1992**, *48*, 4259-4270.
- 15 W. Chen, M. T. Flavin, R. Filler, Z. Xu, *Nucleosides Nucleotides*, **1996**, *15*, 1771-1778.
- 16 L. Kurti, B. Czako, *Strategic Applications of Named Reactions in Organic Synthesis*; Elsevier: Boston, MA, **2005**; 294-295.
- 17 a) Mitsunobu, O. *Synthesis* **1981**, *1*, 1-28. (b) D. L. Hughes, *Organic Reactions*; Wiley: New York, **1992**; Vol. 42, 335-656.
- 18 W. Lu, S. Sengupta, J. L. Petersen, N. G. Akhmedov, X. Shi. *J. Org. Chem.* **2007**, *72*, 5012-5013

- 19 R. Zou, M. J. Robbins, *Can. J. Chem.* 1987, **65**, 1436. (b) H. Choo, Y. Chong, C. K. Chu, *Org. Lett.* **2001**, **3**, 1471-1473
- 20 M. Sako,* H. Kawada, and K. Hirota *J. Org. Chem.*, **1999**, **24**, 5721.
- 21 J. A. Haines, C. B. Reese, L. J. Todd, *Chem. Soc.* **1962**, 5281-5288. J. W. Jones, R. K. Robins, *J. Am. Chem. Soc.* **1963**, **85**, 193-201. A. D. Broom, L. B. Townsend, J. W. Jones, R. K. Robins, *Biochemistry* **1964**, **3**, 494-500.
- 22 E. Wright, L. W. Dudycz, *J. Med. Chem.* **1984**, **27**, 175-181
- 23 J. W. Beach, Kim, O. Hea, Lak. S. Jeong, S. Nampalli, Islam, Qamrul et al. *J. Org. Chem.* **1992**, **54**, 3887-3894
- 24** W02008/101514 A1, *NANODREAM S.R.L. UNIPERSONAL*, **2008**
- 25 G. Gottarelli, S. Masiero, G. P. Spada *J. Chem. Soc. Chem. Commun.* **1995**, 2555
- 26 G. Gottarelli, S. Masiero, E. Mezzina, S. Pieraccini, J. P. Rabe, P. Samorì, G. P. Spada, *Chem. Eur. J.* **2000**, **6**, 3242.
- 27 A. Ciesielski, R. Perone, S. Pieraccini, G. P. Spada, P. Samorì, *Chem. Commun.* **2010**, 46, 4493.
- 28** A. Ciesielski, S. Lena, S. Masiero, G. P. Spada and P. Samorì, *Angew. Chem., Int. Ed.*, **2010**, **49**, **1963**.
- 29 A. Marlow, E. Mezzina, S. Masiero, G. P. Spada, J. T. Davis, G. Gottarelli *J. Org. Chem.*, **1999**, **64**, 5116
- 30 E. Mezzina, P. Mariani, R. Itri, S. Masiero, S. Pieraccini, G. P. Spada, F. Spinozzi, J. T. Davis, G. Gottarelli *Chem. Eur. J.*, **2001**, **7**, 388
- 31 S. Paramasivan, I. Rujan, P. H. Bolton, *Methods* **2007**, **43**, 324-331; G. Gottarelli, G. P. Spada, A. Garbesi, In *Comprehensive Supramolecular Chemistry*; J.-P. Sauvage, M. W. Hosseini Eds.; Pergamon: Oxford, **1996**; Vol. 9, 483-506.
- 32 a) D. M. Gray, J.-D. Wen, C. W. Gray, R. Repges, C. Repges, G. Raabe, J. Fleishhauer, *Chirality* **2008**, **20**, 431; b) G. Gottarelli, S. Masiero, G. P. Spada, *Enantiomer* **1998**, **3**, 429; c) G. Gottarelli, S. Lena, S. Masiero, S. Pieraccini, G. P. Spada, *Chirality* **2008**, **20**, 471
- 33 (a) J. M. Lehn, *Science*, **2002**, **295**, 2400; (b) T. F. A. de Greef and E. W. Meijer, *Nature*, **2008**, **453**, 171; (c) O. Ivasenko, J. M. MacLeod, K. Y. Chernichenko, E. S. Balenkova, R. V. Shpanchenko, V. G. Nenajdenko, F. Rosei and D. F. Perepichka, *Chem. Commun.*, **2009**, 1192; (d) A. Ciesielski, S. Lena, S. Masiero, G. P. Spada and P. Samorì, *Angew. Chem., Int. Ed.*, **2010**, **49**, 1963.

- 34 (a) G. P. Spada, S. Lena, S. Masiero, S. Pieraccini, M. Surin and P. Samorì, *Adv. Mater.*, **2008**, *20*, 2433; (b) A. Ciesielski, L. Piot, P. Samorì, A. Jouaiti and M. W. Hosseini, *Adv. Mater.*, **2009**, *21*, 1131
- 35 A. P. H. J. Schenning and E. W. Meijer, *Chem. Commun.*, **2005**, 3245
- 36 R. Rinaldi, E. Branca, R. Cingolani, S. Masiero, G. P. Spada and G. Gottarelli, *Appl. Phys. Lett.*, **2001**, *78*, 3541.
- 37 R. Rinaldi, G. Maruccio, A. Biasco, V. Arima, R. Cingolani, T. Giorgi, S. Masiero, G. P. Spada and G. Gottarelli, *Nanotechnology*, **2002**, *13*, 398
- 38 R. Otero, M. Schock, L. M. Molina, E. Laegsgaard, I. Stensgaard, B. Hammer and F. Besenbacher, *Angew. Chem., Int. Ed.*, **2005**, *44*, 2270
- 39 (a) T. Giorgi, S. Lena, P. Mariani, M. A. Cremonini, S. Masiero, S. Pieraccini, J. P. Rabe, P. Samorì, G. P. Spada and G. Gottarelli, *J. Am. Chem. Soc.*, **2003**, *125*, 14741; (b) S. Lena, G. Brancolini, G. Gottarelli, P. Mariani, S. Masiero, A. Venturini, V. Palermo, O. Pandoli, S. Pieraccini, P. Samorì and G. P. Spada, *Chem. Eur. J.*, **2007**, *13*, 3757.
- 40 S. De Feyter and F. C. De Schryver, *Chem. Soc. Rev.*, **2003**, *32*, 139
- 41 R. H. Fowler and L. Nordheim, *Proc. Roy. Soc. London, Ser. A*, **1928**, *119*, 173 J. Frenkel, *Phys. Rev.* **1930**, *36*, 1604.
- 42 S. Burattini, H. M. Colquhoun, B. M. Greenland, W. Hayes, *Faraday Discuss* **2009**, *143*, 251- L.C. Giancarlo, G. W. Flynn, *Annu. Rev. Phys. Chem.* **1998**, *49*, 297
- 43 V. T. Shalamov, *Graphite*; Norton: New York, 1981-Rowntree, P. A.; Ph.D. Thesis, Princeton University, **1990**
- 44 D. M. Cyr, B. Venkataraman, G. W. Flynn, *Chem. Mater.* **1996**, *8*, 1600 Y. G. Cai, S. L. Bernasek, *J. Phys. Chem. B* **2005**, *109*, 4514
- 45 J. Sponer, J. Leszczynski and P. Hobza, *J. Phys. Chem.*, **1996**, *100*, 1965
- 46 (a) K. Paserba and A. J. Gellman, *Phys. Rev. Lett.*, **2001**, *86*, 4338; (b) A. J. Gellman and K. P. Paserba, *J. Phys. Chem. B*, **2002**, *106*, 13231; (c) T. Muller, G. W. Flynn, A. T. Mathauser and A. Teplyakov, *Langmuir*, **2003**, *19*, 2812.
- 47 S. Pieraccini, S. Bonacchi, S. Lena, S. Masiero, M. Montalti, N. Zaccheroni, G. P. Spada, *Org. Biomol. Chem.* **2010**, *8*, 774]
- 48 J. M. Lehn, J. P. Sauvage *J. Am. Chem. Soc.* **1975**, *97*, 6700
- 49 S. Lena, P. Neviani, S. Masiero, S. Pieraccini, G. P. Spada, *Angew. Chem. Int. Ed.* **2010**, *49*, 3657.

*Synthesis of a guanosine derivative
functionalized as PTM derivative*

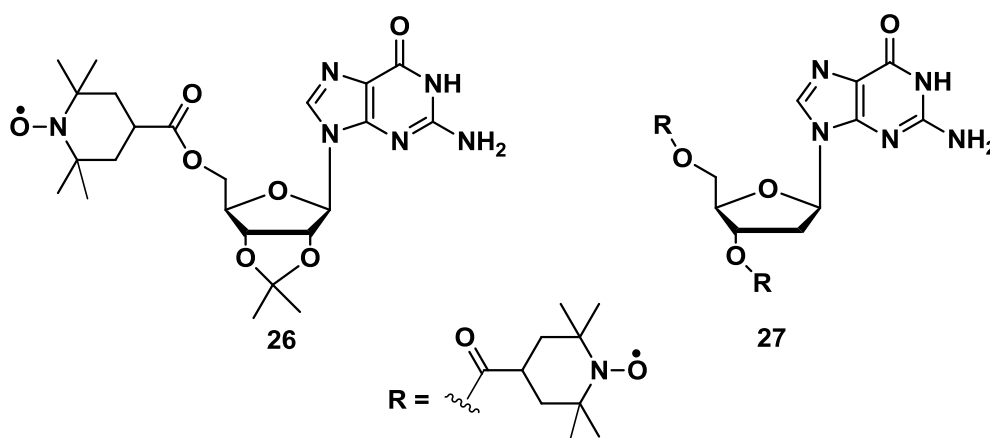
4 Synthesis of a guanosine functionalized as PTM derivative

4.1 Concepts

The work described in this chapter has been done in collaboration with Prof. Jaume Veciana in Barcelona. Among the lines of research of his group, there is one concerning the study of a group of organic radical compounds defined PTM (polychlorotriphenylmethyl derivatives). Organic radicals are open-shell molecules composed of light elements—mostly H, C, N, O and S—with an electronic configuration that makes them very reactive. They are species with an unpaired electron occupying the highest molecular orbital which can easily take part in reactions, such as hydrogen abstraction, dimerization or recombination, leading to the loss of the open-shell character. Nevertheless, it is possible to have persistent organic radicals both by screening the paramagnetic center with bulky substituents, hence protecting it from undesired reactions and taking advantage of electronic delocalization.^[1,2] The polychlorinated trityl radicals,^[3] where the central methyl sp^2 carbon is the spin bearing atom, is one of these persistent radicals. Our group has reported various examples of open-shell moieties organized into a supramolecular architecture showing magnetic properties^[4,5]. These studies have shown that the scaffolding of the persistent radical unit 4-carbonyl-2,2,6,6-tetramethylpiperidine-1-oxyl (TEMPO), can be achieved by taking advantage of the self-assembly templated by potassium ions of the guanosine derivative **26** into a H-bonded network. In the presence of potassium ions, this compound can form in fact a D₄-symmetric octameric assembly $[G26_8K]^+$ containing eight spin centers showing a weak electron spin-spin exchange interaction. Reversible interconversion, fueled by cation release and complexation, allows the switching between discrete quartet-based assemblies and molecularly dissolved **26** (or its ribbon-like supramolecular oligomers), and thus the control of the weak intermolecular spin-spin interactions. This system was the first example of a reversible introduction-suppression of a weak spin-spin exchange in a self-recognizing and self-assembling molecule controlled by the addition/removal of a templating cation.^[6] Instead **27**, despite the presence of two bulky substituents, forms indeed a K^+ -templated octameric assembly giving rise to very strong spin-spin interactions, comparable to those observed in very concentrated monoradical solutions.

Synthesis of a guanosine derivative functionalized as PTM derivative

This finding is consistent with the proposed structure consisting of 16 radical units confined within the complex.



So we have decided to synthesize derivatives **28** and **29** to study the supramolecular aggregates formed by 2',3'-O-isopropylidene-guanosine in the presence of a bulky diamagnetic (α HPTM) **28** or paramagnetic substituent (PTM) **29** and to observe the influence of a chiral substituent on the G-Ace self-assembly.

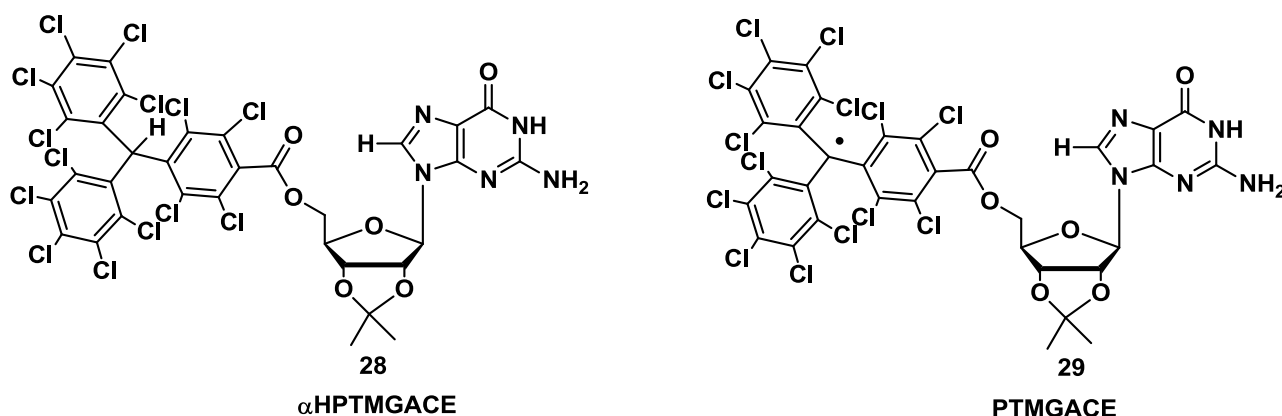


Figure 4.53: Diamagnetic derivative **28** (α HPTM-Gace) and paramagnetic derivative **29** (PTM-Gace)

4.2 Overview of PTM derivatives

Since Gomberg's discovery of the triphenylmethyl radical (fig. 3.52) in 1900^[7] physical properties of neutral radicals have been a source of inspiration for research into molecule-based functional materials.^[8] Magnetism induced by interactions of unpaired electrons is one of the most characteristic properties of organic neutral radicals.^[9] The alignment of spins due to the unpaired electrons with adequate interactions through p electrons or one pair of electrons of heteroatoms in the solid state give place to the obtaining of molecule-based magnetic materials. The molecular skeleton of stable neutral radicals has two important features: one regarding the good stabilization of the spin and the second regarding the modulation and control of electronic structure which in turn will control the intermolecular interactions responsible for the physico-chemical properties of the materials. For designing novel neutral radicals, it is vital to utilize these two aspects effectively.^[10] For example, stabilization of neutral radicals by steric protection not only suppresses the dimerization reaction and the reaction with oxygen, but also greatly influences crystal structures and, thus, intermolecular spin-spin interactions. Triphenylmethyl radicals were the first example of an open-shell organic radical prepared and studied.^[7]

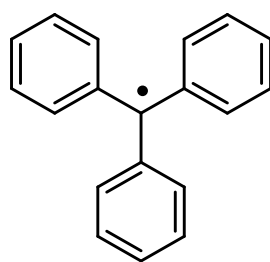


Figure 4.54: Skeleton of triphenylmethyl radical

From then, several derived diradicals and polyradicals have been obtained.^[11] However their high reactivity prevented any practical use. The increase of persistence was achieved by a proper shielding of the central carbon atom leading to a wide variety of derivatives that show longer life.^[12] Among them the polychlorotriphenylmethyl (PTM) radicals are characterized by an extremely high persistence and stability. They are composed of three totally or partially chlorinated phenyl rings connected to a central carbon atom with a sp^2 hybridization (fig. 4.55).^[13] The steric strain that exists in a

hypothetical planar conformation of these derivatives, originated mainly by the bulky chlorine atoms at the ortho positions, is released by the rotation of the aromatic rings around the bonds linking the central to the ipso-carbon atoms of the molecule. This forces the molecule to adopt a *propeller-like conformation*. As a consequence, from the stereochemical point of view, such radicals exist in two different enantiomeric forms that can interconvert at high temperatures with an energy barrier of ca. 23 kcal mol⁻¹.^[14] Following the Cahn–Ingold–Prelog nomenclature,^[15] the two atropisomeric forms are called *Plus* (P), when the rings present a clockwise torsion, and *Minus* (M) when the torsion is the opposite one.

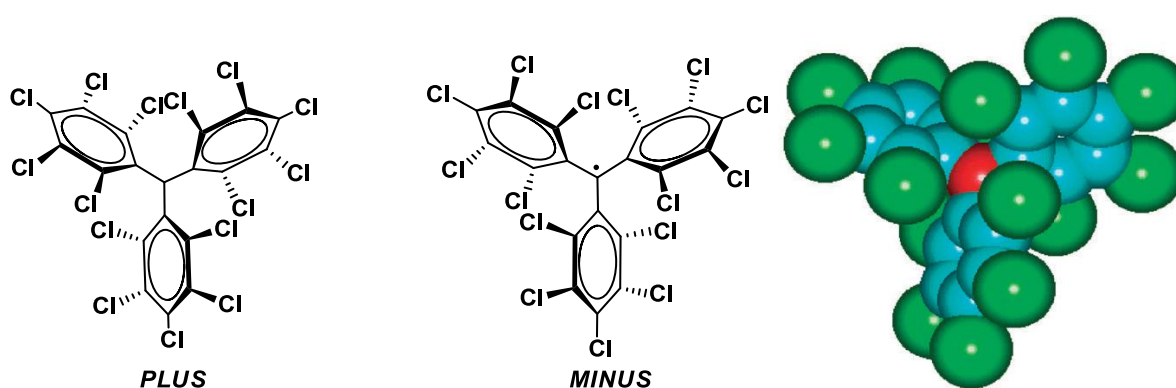


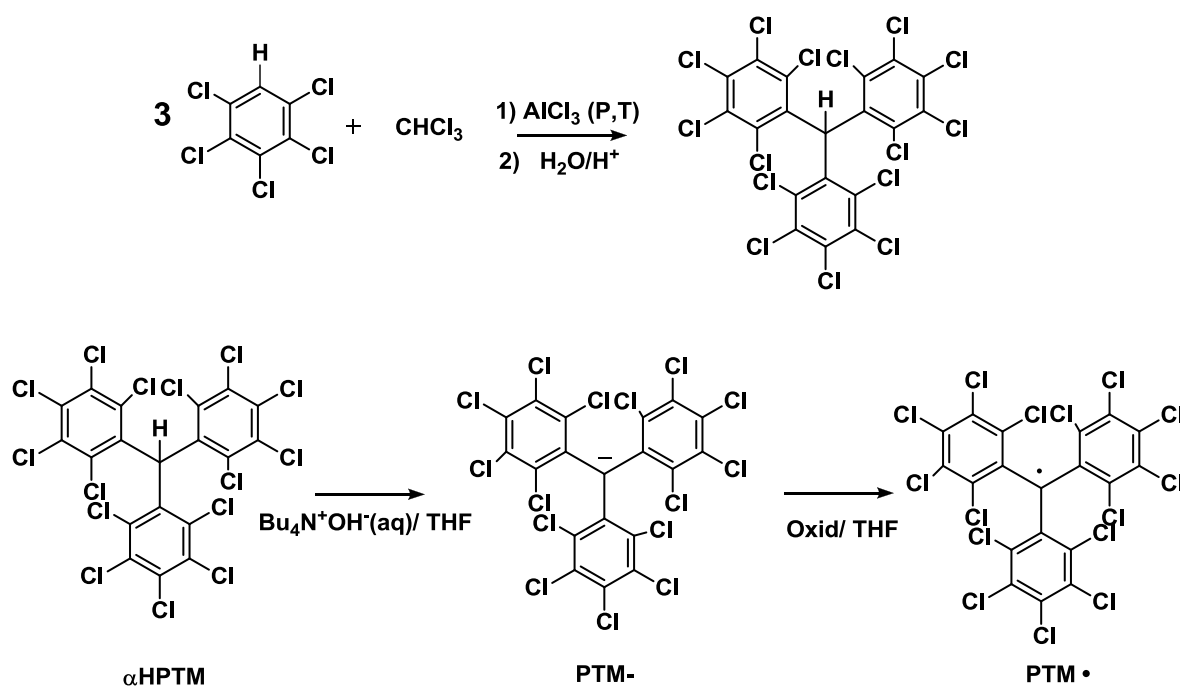
Figure 4.55: Left: radical (PTM) showing the high steric shielding of the central carbon atom (in red) surrounded by the six bulky chlorine atoms at the ortho positions. Right: representation of the *Plus* (P) and *Minus* (M) atropisomeric forms of perchlorotriphenylmethyl radical.^[9]

Besides the generation of a *propeller-like* conformation, the presence of the bulky chlorine atoms at the ortho positions and the three phenyl groups provide the main source of steric protection of the central carbon atom, which is the atom with the major spin density. In fig. 4.55 is shown a molecular model of the perchlorotriphenylmethyl radical showing that the central carbon atom is surrounded and protected by three ortho-chlorine atoms at each side of the molecule. Indeed, the protection of the methyl carbon is translated into a large persistence and a very high chemical and thermal stability for this family of radicals.^[3,16–19] Thus, differently from the non-chlorinated analogue, which dimerizes very quickly and is so reactive towards oxygen to hamper its isolation as radical, PTM radicals in solution are perfectly inert to oxygen and to many other aggressive reagents, decomposing only in the presence of light in solution due to the loss of two of the *ortho* chlorine atoms with formation of a fluorene type derivative.^[20]

Consequently as long as they are kept in the dark, such radicals behave as classical organic compounds and they can be used as intermediates in many reactions and treated with usual purification techniques, such as chromatography, crystallization, sublimation, etc. These radicals in solid state decompose with high melting points,^[21] usually near 300 °C, and they are indefinitely stable to light and air .^[22]

4.2.1 Synthesis of PTM radicals

The synthesis of PTM radicals is usually achieved from the corresponding polychlorotriphenylmethanes through the formation of their carbanions with a base, e.g. NaOH, followed by oxidation with a weak oxidant, such as p-chloranil, I₂ or Ag⁺. The synthesis of the radical precursors generally consists in a sequence of Friedel-Crafts at high temperature and pressure with an excess of the chlorinatedbenzene derivatives,^[9,3] such as it is depicted in Scheme 6



Scheme 6

The steps to obtain PTM radicals from αHPTM , can be monitored by UV-Vis. αHPTM , PTM anion and PTM radical are characterized by three different absorption bands around 280-300 nm (due to the presence of phenyl rings), 505 nm, and 374 nm respectively. The high persistence of PTM radicals makes it possible their functionalization them at the

meta and para positions (of the aromatic rings). Thanks to the efforts of Ballester and coworkers during the 70s and 80s, these radicals were functionalized using a great variety of reactions,^[23] which in some cases required extreme conditions. One of the first applications of these radicals was the spin labelling of amino acid and peptides.^[24] PTM functionalization has also allowed the use of such radicals as building blocks of molecular materials with specific properties.

4.2.2 PTM properties

PTM radicals, due to their particular structural and electronic characteristics, are classified as inert radicals. The possibility of functionalizing these molecules of different positions with a large variety of substituents, allows the preparation of molecular materials with electroactive, paramagnetic and fluorescent properties. PTM radicals are also interesting because they are electroactive species from which it is possible to generate the corresponding carbanionic and carbocationic species. Indeed, as shown in fig. 4.56, the cyclic voltametry of radical exhibits two reversible waves that correspond to the oxidation and reduction of this radical, giving rise to the corresponding carbanion 1^- and carbocation 1^+ , which are also quite stable species both in solution and in the solid state. The reduction of PTM radicals at low potentials turns out to be more feasible than the corresponding oxidation which requires rather high potentials. Such a fact makes this type of radicals excellent electron-acceptor units in push-pull systems with NLO (non-linear-optical) properties and/or to achieve intramolecular electron transfer in molecular nanowires. Electroactivity of PTM radicals can be used for making switchable multifunctional molecular materials since the magnetic, optical and electronic properties of these open-shell molecules can be switched on and off with an external electrochemical stimulus.^[9]

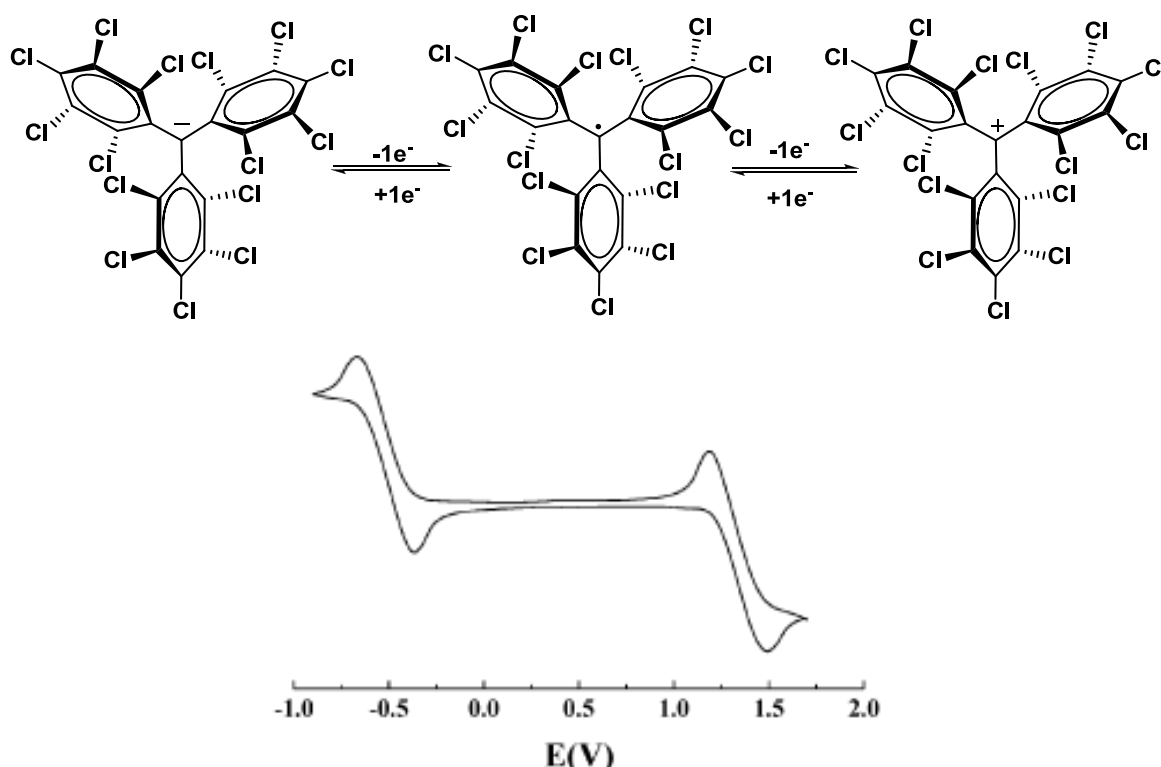


Figure 4.56: Cyclic voltammogram of radical PTM in CH_2Cl_2 , with 0.1 M $n\text{-Bu}_4\text{NPF}_6$ (vs. Ag/AgCl) showing the reversible formation of two different ionic species that correspond to the oxidation and reduction of this radical.

For example PTM anion has been covalently bonded to C_{60} , generating a triad^[25] (fig. 4.57). For this triad, photionduced charge separation was observed in polar and nonpolar solvents trough photoexcitation at room temperature. The efficiency and the rate of the charge separation process were quite high and even though the properties of C_{60} bis-perchlorotriphenylmethide anion were not as good as the best one found in some C_{60} -porphyrins or C_{60} -chloride based dyads,^[26] it was demonstrated a new possibility to fuctionalize fullerenes based on the perchlorotriphenylmethide anion which can be added to other known functional materials based on the parent perchlorotriphenylmethil radicals that works as an acceptor and has permitted the development of multifunctional switchable molecular systems.^[27-28]

Synthesis of a guanosine derivative functionalized as PTM derivative

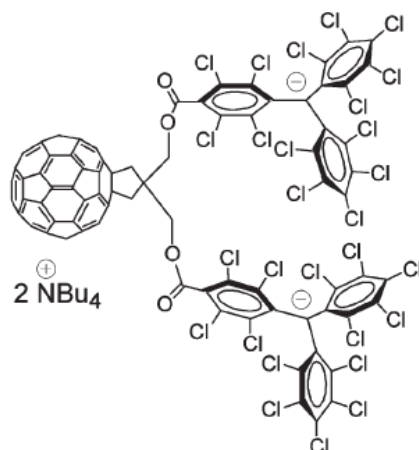


Figure 4.57: Molecular structure of C60-(PTM)₂

Moreover PTM radicals are fluorescent molecules, upon irradiation they emit in the red region at the energy of absorption band (380 nm). When linked to appropriate molecules, such as the carbazole derivatives, their red luminescence makes them candidates for the preparation of electroluminescent devices.^[29-30] Paramagnetism is another property; EPR (electronic paramagnetic resonance) spectra of PTM radicals are characterized by a single narrow line centered at a *g* value between 2.002 and 2.003. The EPR spectrum is also characterized by other two broad and separated lines from the main line: these signals correspond to the coupling of the free electron with the ¹³C nuclei of the triphenylmethyl skeleton. Many studies have been carried out on PTM radicals functionalized with one or more carboxylic groups in *para* and *meta* position. For example they have been used to obtain purely / organic molecular magnetic materials.^[31] Molecules investigated were PTMMC (monocarboxylic derivative), PTMDC (dicarboxylic derivative), PTMTC (tricarboxylic derivative) and PTMHC (hexacarboxylic derivative) (fig.4.58).

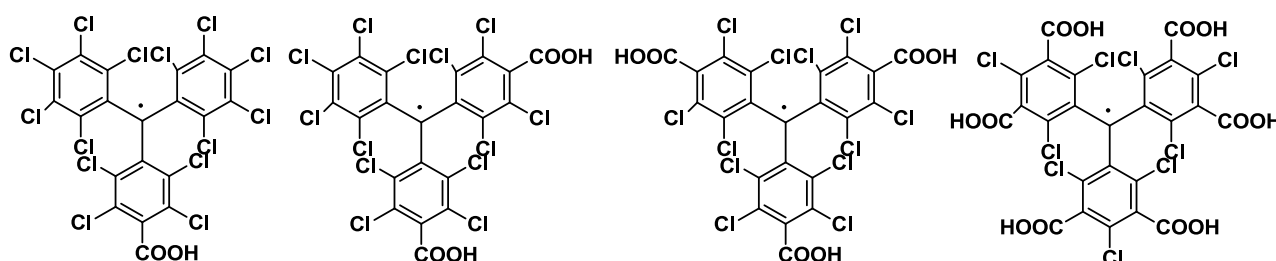


Figure 4.58

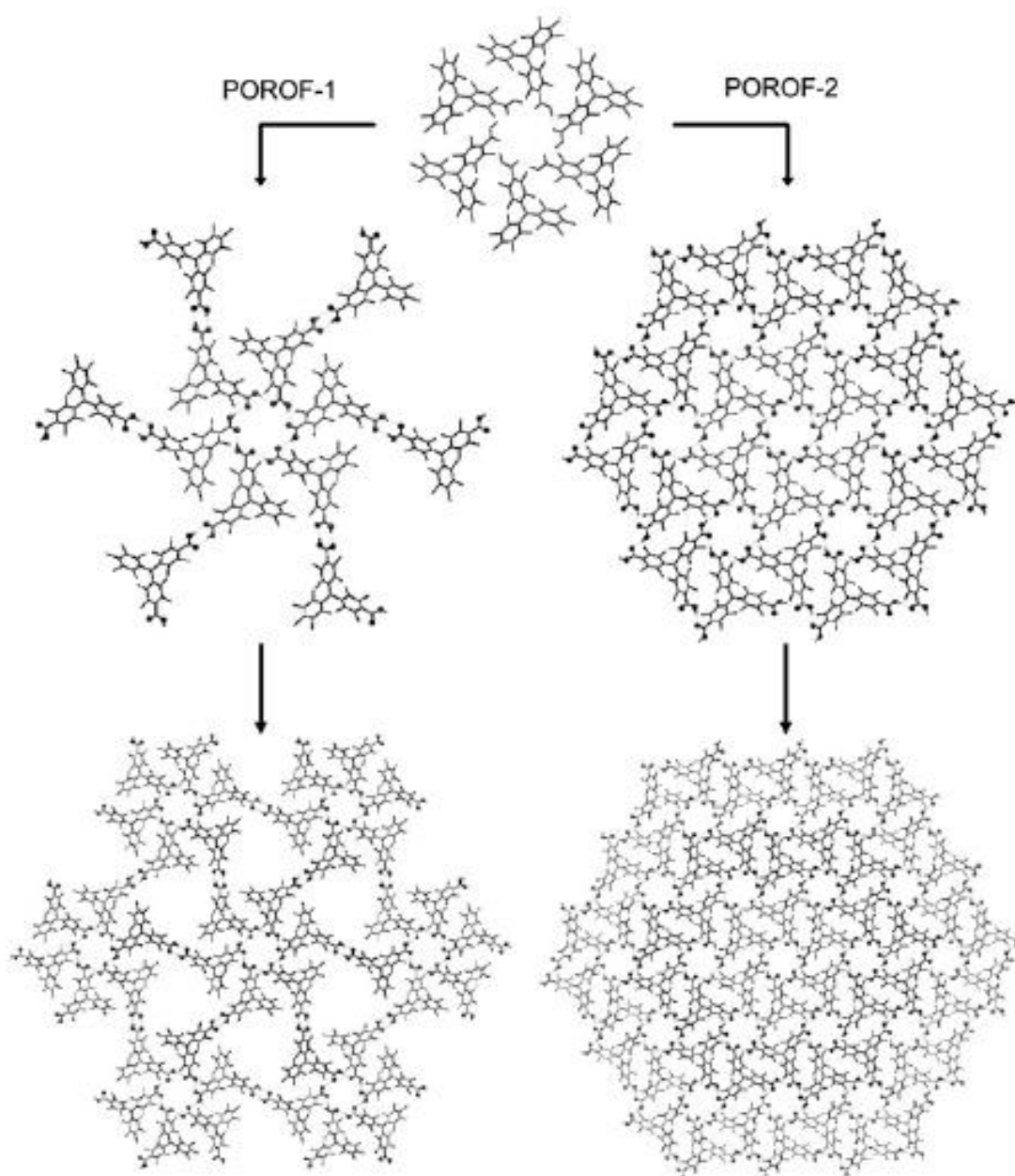


Figure 4.59 : Crystal structures of POROF-1 and POROF-2

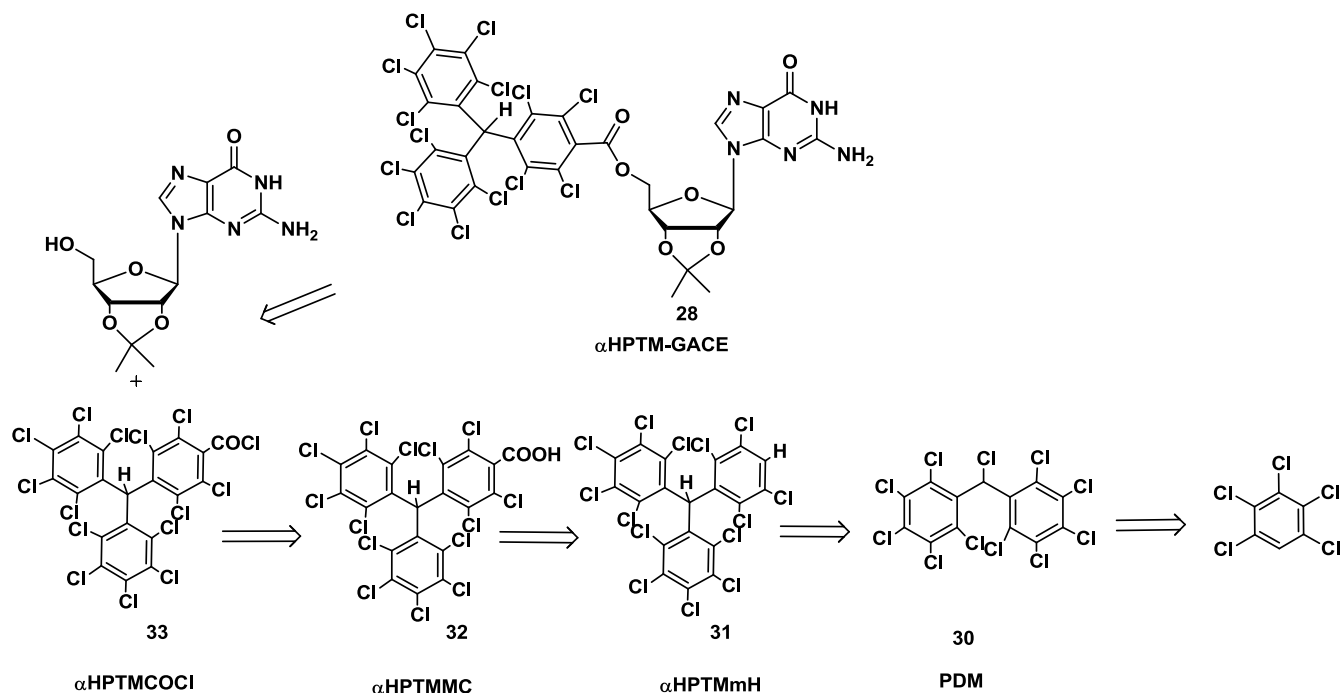
It was observed that self-assembly of PTMMC yields to the formation of supramolecular dimers and to the onset of weak ferromagnetic interactions between the radical units, while increasing the number of carboxylic acid functions as in PTMDC and in PTMTC, has allowed the observation of the first examples of purely organic-radical open frameworks (POROF-1 and POROF-2, fig 4.59), where astonishing structural characteristics are associated with relevant magnetic properties. Two key points emerge from the study of POROF: first, carboxylic groups on PTM radicals have been shown as superexchange pathways for attaining magnetic couplings and, second the geometry and

Synthesis of a guanosine derivative functionalized as PTM derivative

the rigidity of the molecules, together with the paramagnetic character of substituted PTM radicals, offer magnetic and porous materials with a purely organic nature. The remarkable properties of POROF materials can be exploited to address several challenging aspects both in crystal engineering and molecular magnetism. In the latest years, the possibility to functionalize gold,^[32-33] graphite, indium tin oxide (ITO),^[34] or quartz^[35] surfaces with perchlorinated radical derivatives, and hence transfer their properties to such solid supports, was explored for the preparation of robust switchable devices. One of the last example was the preparation of TiO₂ and SiO₂ porous thin films consisting of tilted nanocolumns. They were prepared by glancing angle physical vapor evaporation (GLAD) and have been infiltrated with perchlorinated trityl radicals.^[36] The main driving forces for infiltration from aqueous solutions of the carboxylate-substituted radical derivatives were the electrostatic interactions between their negative charge and the net positive charges induced on the film pores. The infiltrated composite thin films were robust and easy to handle thanks to the physical protection exerted by the film columns. They also keep the multifunctionality of the used guests, as confirmed by electron paramagnetic resonance (EPR), UV-Vis spectroscopy and fluorescence spectroscopy. To prove the electroactivity of the infiltrated porous films, a porous TiO₂ host layer was supported onto conductive indium tin oxide (ITO). By application of an appropriate redox potential, the guest radical molecules have been reversibly switched from their open-shell electronic configuration to their diamagnetic state and hence were changed their optical properties.

4.3 α HPTM-GACE: synthetic approach

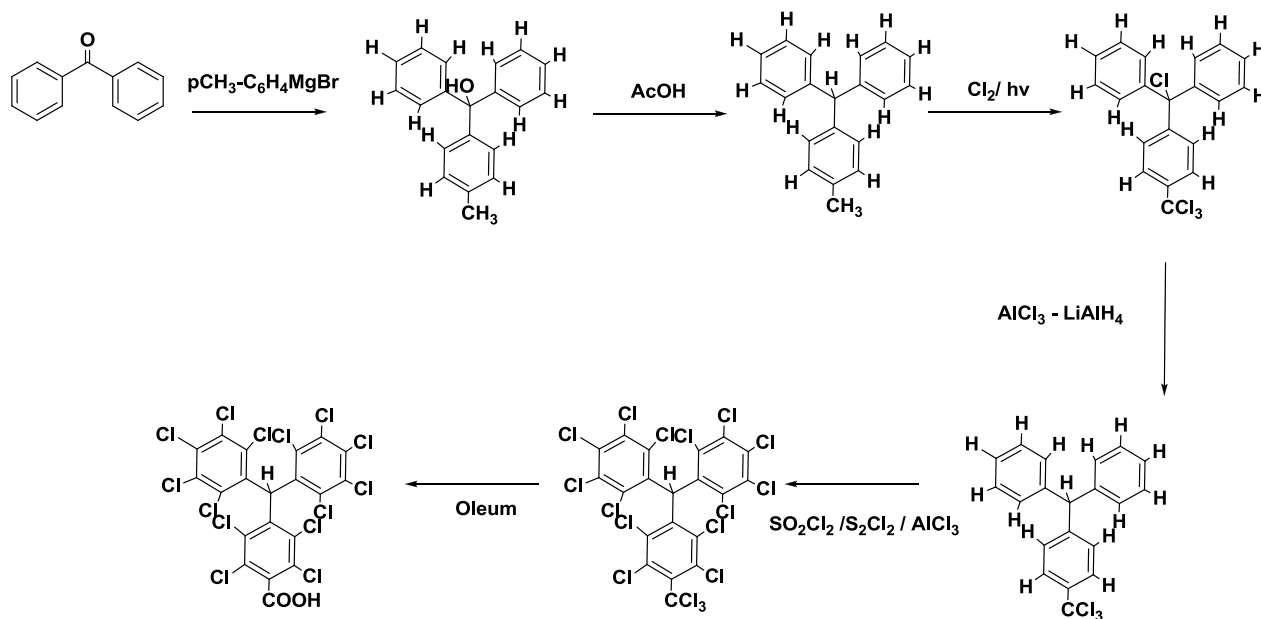
The synthesis of derivative **28** has been carried out following the synthetic route of scheme 7.



Scheme 7

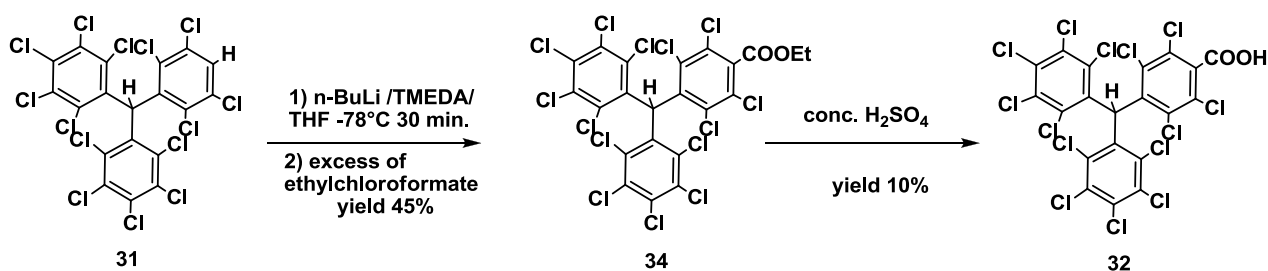
The first steps necessary to obtain the triphenyl methane skeleton (**31** α HPTMmH) were carried out following a procedure described in literature.^[3] The reaction conditions have been reported in Scheme 6 (see 4.2.1). Different synthetic approaches were used for the synthesis of monocarboxylic derivative (**32** α HPTMMC). The synthesis reported in the scheme **8** was described in literature^[37] and it involves five crucial points: (i) the formation of the triphenyl methane skeleton *via* a Grignard reaction followed by the reduction of the triphenylcarbinol derivative obtained from this reaction; (ii) the chlorination of the methyl group, which is accompanied by the chlorination of the central carbon atom that makes it necessary an additional step for removing this chlorine; (iii) the chlorination of the three phenyl rings, to obtain the perchlorinated skeleton; (iv) the conversion of the trichloromethyl group into carboxylic acid (α HPTMMC) **32**.

*Synthesis of a guanosine derivative
functionalized as PTM derivative*



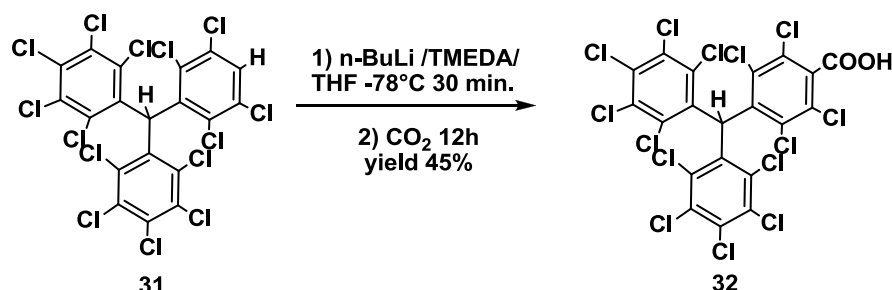
Scheme 8

In order to avoid this large number of steps and to obtain higher yields, PTMMC was synthesized with a new synthetic route through the formation of a lithiated intermediate. The lithiation reaction was already described by Dang and coworkers^[38] to prepare the α HPTM tricarboxylic derivative. They used *n*-BuLi as organometallic reagent in THF at -78°C with tetramethylethylenediamine (TMEDA) to obtain the lithiated intermediate and the ethyl chloroformate as electrophilic reagent to obtain a α HPTM substituted in *ortho* position with three ethyl ester functions. These were hydrolyzed with sulphuric acid to give the tricarboxylic compound with high yield. Starting from **31** (Scheme 9) and following the same procedure described above, we have tried to carry out synthesis of **32** but the hydrolysis of the ester provides a low yield.



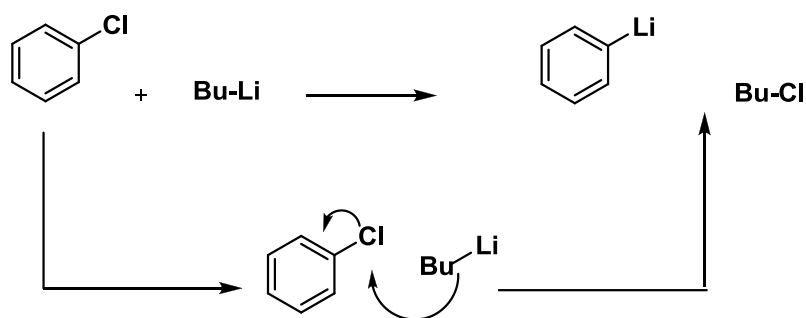
Scheme 9

Thereby we have synthesized the monocarboxylic acid by a direct carbonation of the organo-lithium intermediate (Scheme 10): to a solution of **31** in THF (-78°C) was added n-BuLi, then carbon dioxide gas was bubbled through the mixture, followed by acidification with hydrochloric acid to pH 1. (see experimental part).



Scheme 10

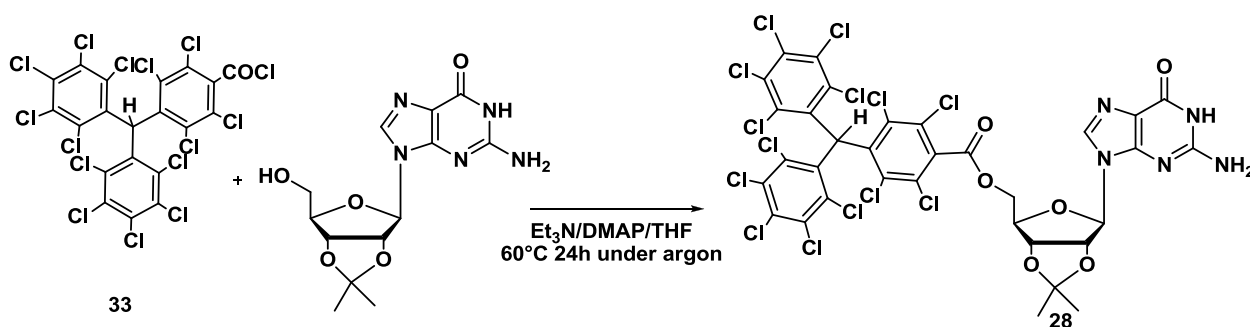
This alternative synthesis of α HPTMMC (**32**) is easier than the method described in literature, but yields suffer from side reactions leading to the formation of monocarboxylic compounds where one chlorine has been replaced by hydrogen. Indeed organolithium compounds can also remove halogen atoms from alkyl and aryl halides in a reaction known as *halogen-metal exchange*. Halogens and the lithium simply swap places. As with many of these organometallic processes, the mechanism is not altogether clear, but it can be represented as a nucleophilic attack on halogen by butyllithium. (scheme 11)



Scheme 11

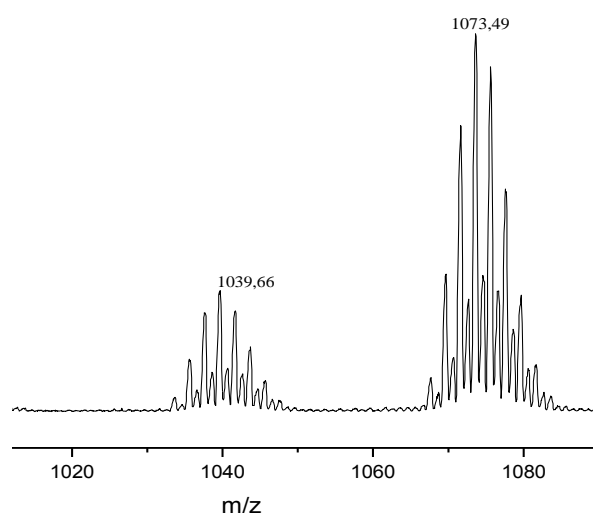
Acid chloride (**33**) was prepared with thionyl chloride refluxing for 24h following the procedure described in literature^[39] and the coupling with 2',3'-O-isopropylidenguanosine to obtain derivative **28** was carried out in THF under the conditions described in the scheme 12 with a yield of 40 %.

Synthesis of a guanosine derivative functionalized as PTM derivative



Scheme 12

Chlorine atom has two stable isotopes, ³⁵Cl and ³⁷Cl present in a percentage of 75,77% and 24,23% respectively. In the presence of more than one chlorine, taking in the account the relative percentage, characteristic multiplets are observed, of which each m/z peak intensity is predictable on the basis of the total number of chlorine present. The most intense peak in the ESI-MS spectrum of **28** was obtained at a m/z= 1073,49 with an isotopic distribution corresponding to 14 chlorine atoms, in the spectrum it can be observe another peak corresponding to the loss of one and chlorine atom (fig. 4.60).



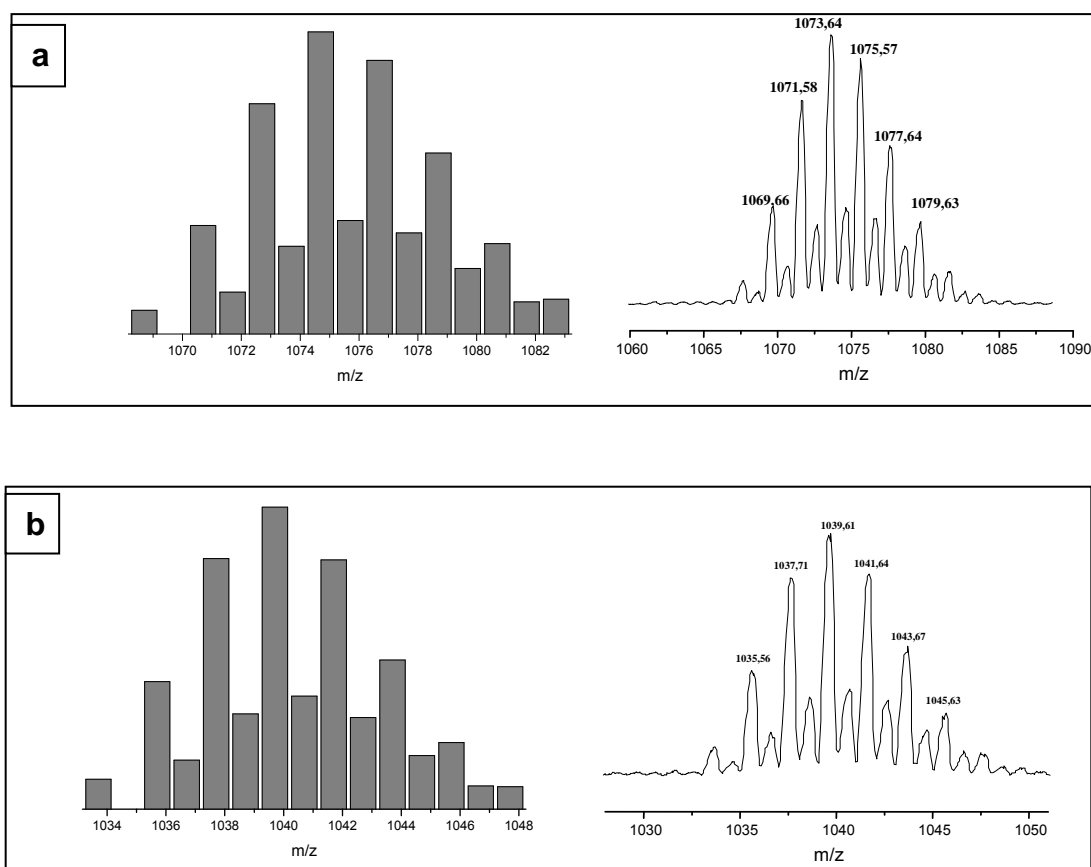


Figure 4.60. ESI-MS spectrum of **28** at the top. In the panel **a** it is represented the simulation of experimental spectrum on left of compound **28** and the ESI-MS spectrum of **28** on right, in the panel **b** is represented the simulation of experimental spectrum of **28** with a loss of a chlorine atom on left and the ESI-MS spectrum on right.

The interesting properties of PTM radical derivatives have led us to try the synthesis of radical compound **29** (PTM-Gace). We have explored two different synthetic approaches: (a) coupling between acid chloride radical (PTMCOCl) and 2',3'-O-isopropylidene-guanosine following the same procedure described above; (b) deprotonation of **28** with tetrabutylammonium hydroxide to obtain carbanion **28a** followed by one-electron oxidation with iodine. The acid radical (PTMMC) was synthesized as reported in scheme **6** (see also experimental part derivative **35**), that is, using sodium hydroxide as base to form the anion followed by oxidation with iodine to form the radical. Due to the stability of these molecules, starting from PTMMC, it has been possible to form the acid chloride (**33**) using thionyl chloride. These reactions were carried out in the dark because PTM radicals in solution are not stable but they can form

Synthesis of a guanosine derivative functionalized as PTM derivative

a fluorene type derivatives, due to the loss of chlorine atoms from the ortho position. The coupling between PTMCOCl radical and guanosine did not work neither under the coupling conditions described above for **28** nor under different conditions (solvent, temperature and reaction time), in all cases it was recovered from the reaction only the started materials (PTMMC and Gace) and byproducts which analyzed by MALDI –TOF mass spectroscopy didn't correspond to PTM-Gace (**29**). In the second approach HPTM-Gace (**28**) was treated with a base to obtain the corresponding anion.

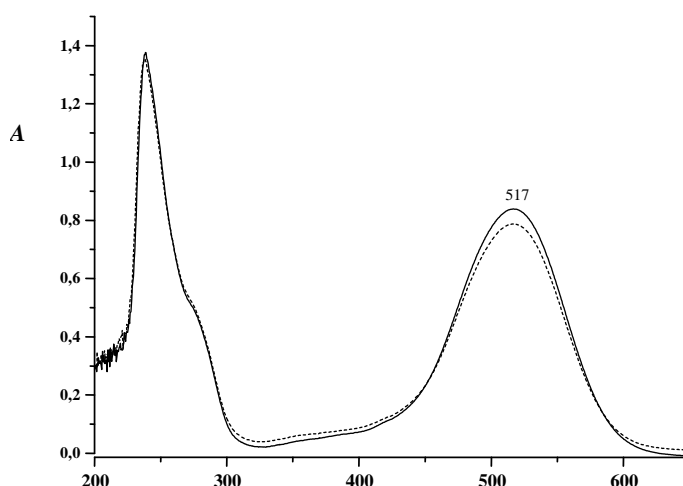
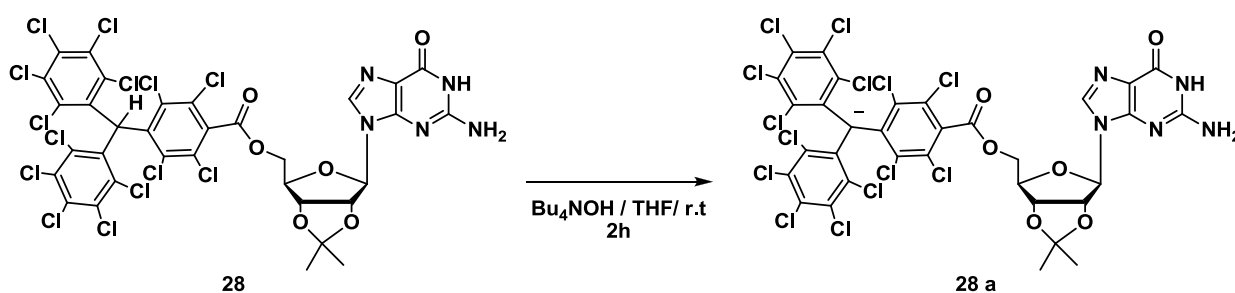


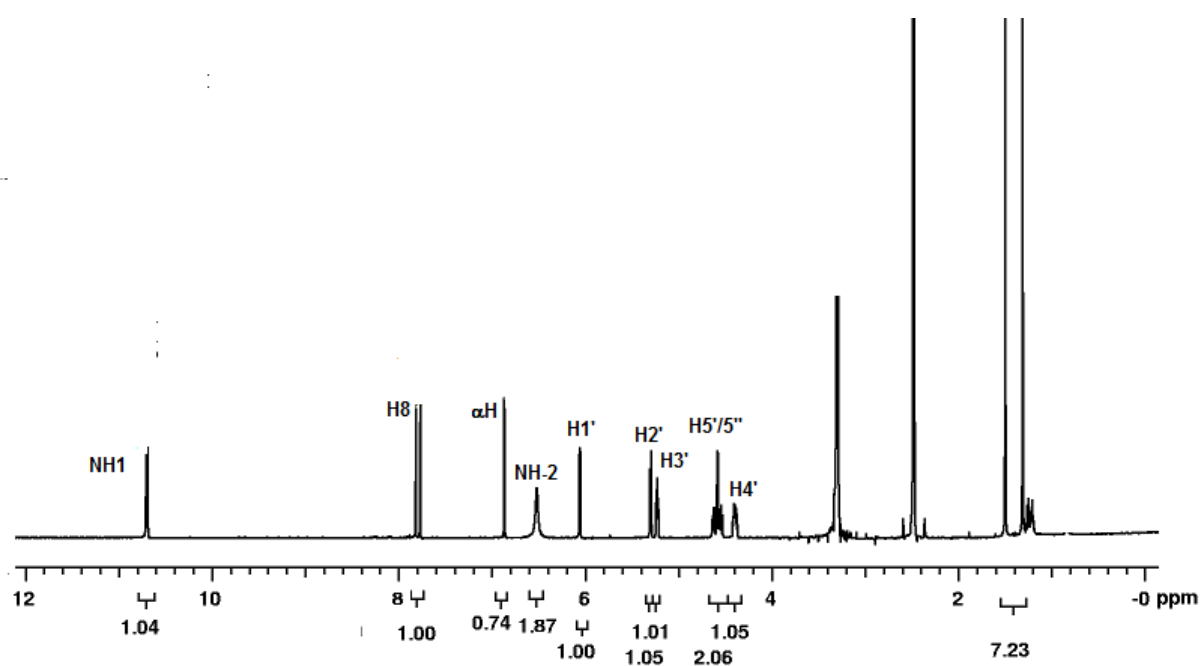
Figure 4.61: UV spectra obtained during the formation of the anion **28 a** in THF after one hour (dashed line) and two hours from the addition of tetrabutylammonium hydroxide

The formation of the anion was followed the reaction by UV spectroscopy. The spectra reported in fig. 4.61 show the presence of the anion: a band at ca. 505 nm typical NMR experiments (^1H and DOSY) confirm the presence of the anion. However the imino proton signal of guanosine is not present in these spectra, and it has been supposed that the tetrabutylammonium hydroxide can remove this proton, thus depriving the nucleobase of a

fundamental hydrogen involved in the formation of G-quartets structure. All compounds described in this chapter have been characterized by NMR, IR spectroscopy and ESI-MS (experimental part).

4.4 α HPTM-GACE: studies in solution

α HPTM-GACE (**28**) was studied in solution in order to observe the different supramolecular aggregates that this compound can form. As described in chapter 2, lipophilic guanosines, depending on the presence or the absence of cations, can form G-quartet assemblies or ribbon-like structures, respectively. The methods used to characterize these aggregates are NMR spectroscopy (mono- and bidimensional experiments such as NOESY, DOSY; HMBC; HSQC) and circular dichroism (CD). Generally, the first step to study LipoG's self-assembly is the characterization of the molecule in its disaggregated state: this is normally done by recording NMR and CD spectra in a solvent like dimethylsulphoxide (DMSO). Indeed DMSO solvent competes for hydrogen bonds, inhibiting the formation of guanosine aggregates. ^1H NMR of **28** in DMSO- d_6 , shows a double set of signals for all the protons of guanosine and also for the central hydrogen of PTM (fig. 4.62).



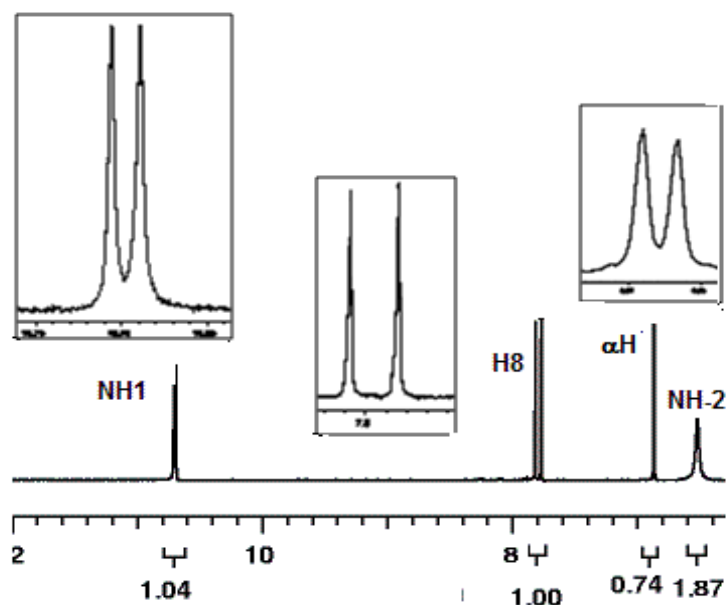


Figure 4.62: ¹H-NMR spectrum of **28** in DMSO-d₆ recorded at r.t. (top); ¹H NMR spectrum enlargement of imino (NH-1), H8 and αH protons (bottom)

The presence of a chiral racemic moiety (PTM) linked to optically pure guanosine (Gace) implies the existence in solution of two diastereoisomeric forms. Indeed PTM derivatives exist in two atropisomeric forms (Plus and Minus) due to the rotation of the aromatic rings around the bonds linking the central to the ipso-carbon atoms of the molecule. Assuming that guanosine, due to the steric hindrance of the PTM group, adopts an *anti* conformation around the glycosidic bond when it is not involved in the formation of supramolecular aggregates, the two sets of signals can be attributed to the two diastereoisomeric forms arising from PTM atropisomers. ¹H NMR spectra recorded at different temperatures, starting from a room temperature up to 390° K, confirm the presence of two diastereoisomers (Plus-αHPTMGace and Minus αHPTMGace) as they show (fig. 4.63) coalescence of all protons of the guanosine and also of the hydrogen on the α carbon of PTM substituent.

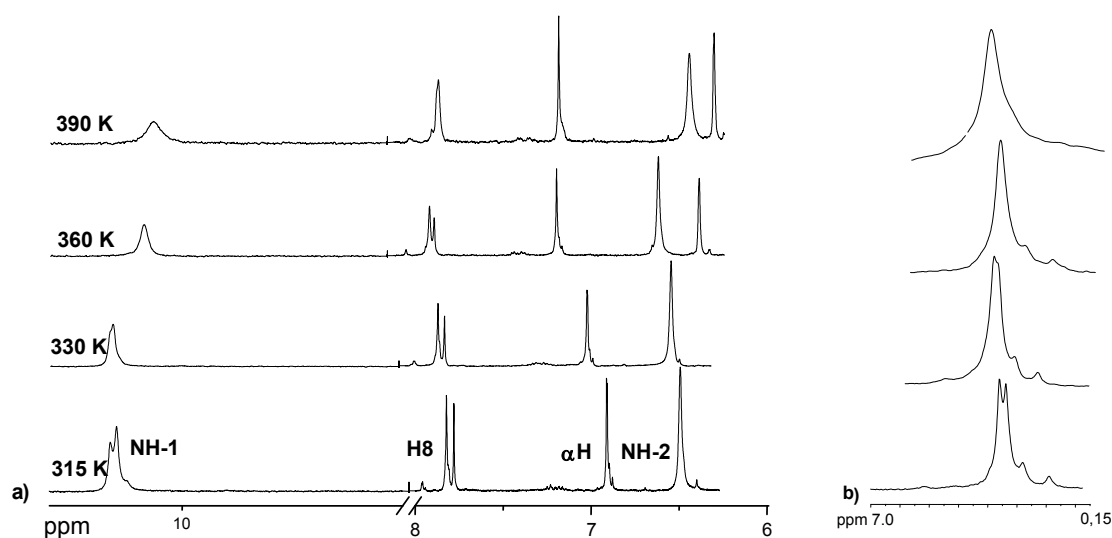


Figure 4.63: a) Region of ^1H -NMR spectra of **28** recorded in DMSO-d_6 at different temperatures; b) ^1H -NMR signal of the αH proton of **28** at different temperatures

The study of the supramolecular behaviour of $\alpha\text{HPTMGACE}$ **28** was carried out first by means of circular dichroism. Spectra were recorded before and after the addition of cations, namely potassium picrate (K^+pic^-) and strontium picrate ($\text{Sr}^{2+}\text{pic}_2^-$), to evaluate the ability of **28** to produce in chloroform aggregates due to the formation and stacking of G-quartets (fig. 4.64).

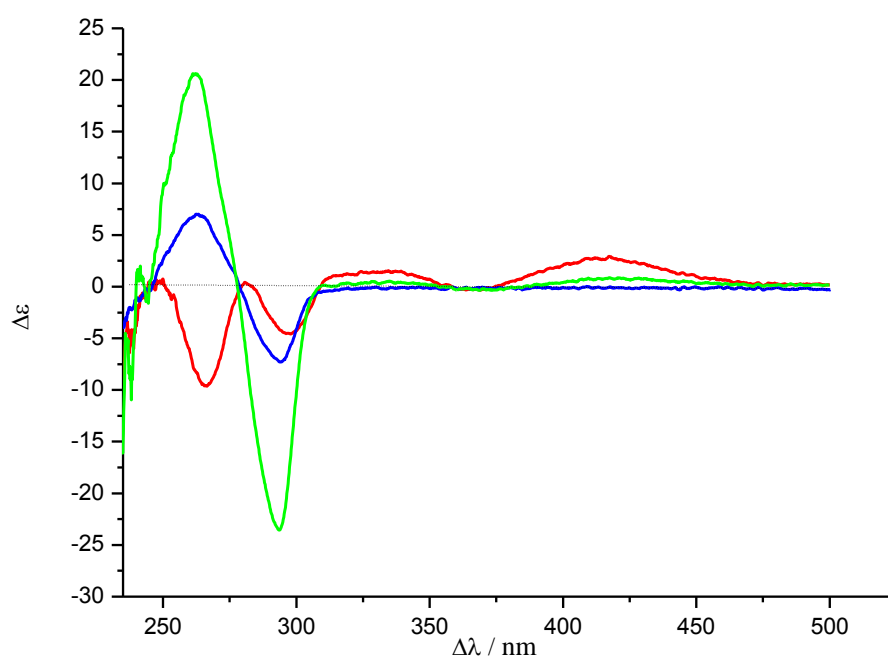


Figure 4.64. CD spectra of **28** 10 mM in chloroform: before the addition of cations (blue line), after the addition of potassium picrate (8:1) (green line); after the addition of strontium picrate (8:1) (red line).

Synthesis of a guanosine derivative functionalized as PTM derivative

Before the addition of salts, a low intensity exciton CD spectrum, characterized by two bands centered at 261 nm and 294 nm, is observed. It is known that 2',3'-O-isopropylidene-guanosine (Gace) derivatives can coordinate cations much more easily than other guanosine derivatives and the spectrum observed is suggestive of the presence in the sample of stacked G-quartets templated by a small amount of cations residual of the synthetic work-up. This is confirmed by the observation that dilution of the mother solution of **28** with methanol, a solvent competing for hydrogen bonds, produces the disappearance of the CD signal. When a weighted (1/8 mol/mol) amount of potassium picrate is added to a chloroform solution of **28** a solid-liquid extraction occurs and the intensity of CD spectrum increases: this spectrum is typical of a columnar structure composed of two stacked G-quartets.^[40] In particular this spectrum is suggestive of an head to tail octamer with *D*₄ symmetry (fig. 2.19). When to a solution of **28** in chloroform is added strontium picrate (bivalent cation), a different CD spectrum can be observed, where two negative bands centered to 267 and 296 nm are present. Even in this case, these bands are indicative of the presence of a stacked structure in solution. Both the spectra recorded after the extraction of cations showed two induced bands at 368 and 415 nm, which correspond to an induced CD on the picrate chromophore.

A more detailed information on the structure of cation-templated supramolecular aggregates arising from **28** can be obtained by NMR experiments: in particular ¹H-NMR, COSY, HMBC, HSQC and DOSY have been used.

¹H-NMR spectra were recorded in dimethyl sulphoxide and in chloroform (after and before addition of cations) to confirm the presence of supramolecular aggregates (fig. 4.65). In DMSO-d₆ amino (NH₂) and imino protons, (NH-1), not involved in the formation of hydrogen bonds, appear at 6.4 ppm and 10.3 ppm, respectively (fig 4.65 a). When the ¹H-NMR spectrum of **28** is recorded in chloroform (10 mM) (fig 4.65 b) it is possible to distinguish the presence of two supramolecular species, octamer (●) and ribbon (◆) (vide infra). Compared with spectrum a, two broad imino-proton (NH-1) signals appear at higher frequencies (δ 12.1(◆) and δ 12.4 ppm (●)), corresponding to hydrogen-bonded NH-1 of the two aggregate respectively. The amino protons (NH-2) show a broad signal at δ 6,4 ppm for the ribbon structure ◆ while for the octamer ● it is

possible observe only one amino proton at δ 9.8 ppm (this deshielding is due to its involvement in the hydrogen bond responsible for the formation of G-quartets (fig. 2.19).

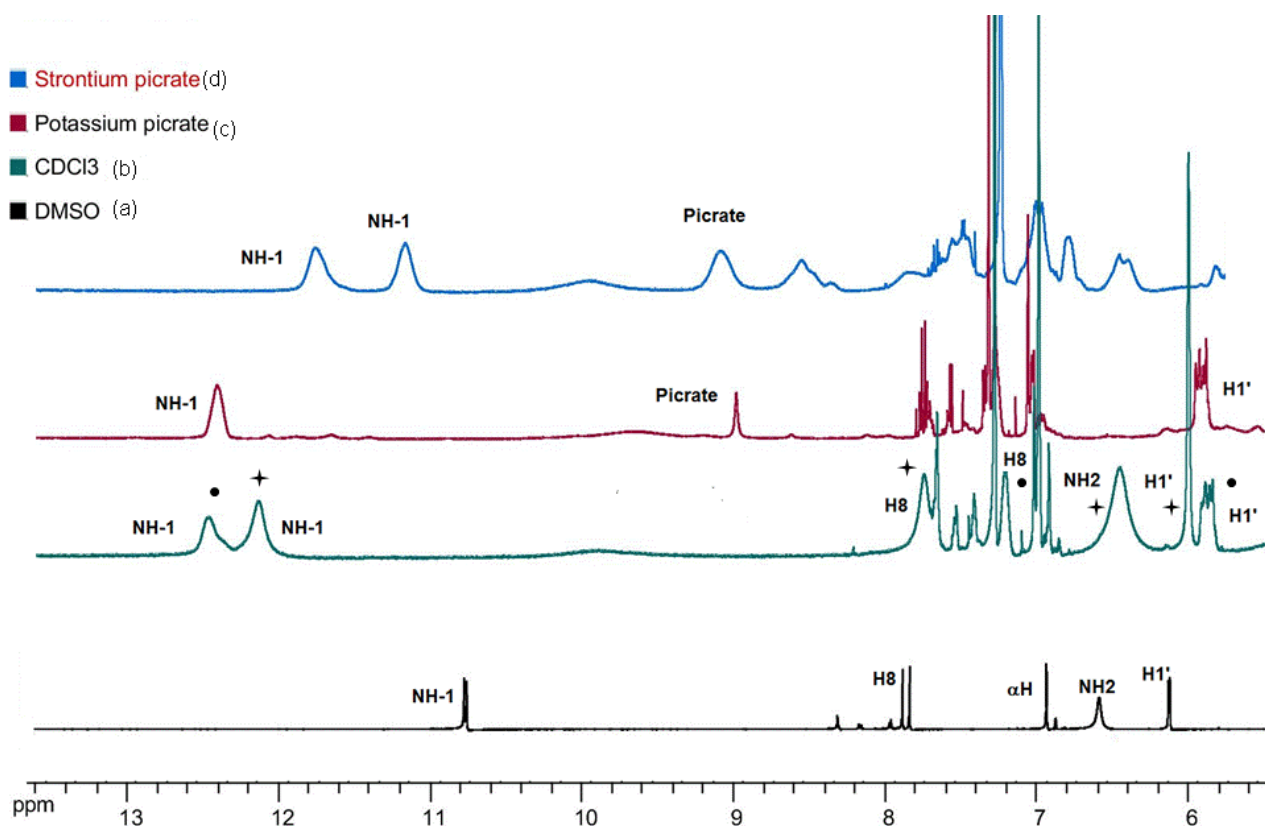


Figure 4.65:Regions of ^1H NMR spectra of **28** in: **a**) DMSO- d_6 , **b**) solution of chloroform (10mM), **c**) solution of chloroform 10 mM with potassium picrate (8:1), **d**) solution of chloroform 10 mM with strontium picrate (8:1)

Besides CD (see above), the presence of two different aggregates in the chloroform solution has been confirmed by DOSY experiments. The Dosy technique is a method used for measuring diffusion rates and provides information about the size of molecules in solution.^[41] It is also used to study the self-association of natural products,^[42] peptides,^[43] and proteins^[44] and can be regarded as a powerful tool in supramolecular chemistry. Indeed diffusion NMR has been used to define the aggregation state of ion pairs and other organometallic assemblies.^[45] For example Davis and colleagues used this method to distinguish between the possible structures, of identical sub-unit composition, formed by a lipophilic G-derivative and to better understand the self-assembly process, with respect to the role of cation, anion and solvent.^[46] Analysis of H8 \bullet peak at

*Synthesis of a guanosine derivative
functionalized as PTM derivative*

δ 7.18 ppm and H8 \blacklozenge peak at δ 7.71 ppm provided two different diffusion coefficients $D_{\bullet} = 2.25 \pm 0.013 \cdot 10^{-10} \text{ m}^2 \text{ s}^{-1}$ and $D_{\blacklozenge} = 2.9 \pm 0.016 \cdot 10^{-10} \text{ m}^2 \text{ s}^{-1}$.

After the addition of a weighted (1/8 mol/mol) amount of potassium picrate to the solution of **28** (10mM) in chloroform, the ^1H -NMR spectrum shows a predominant species (fig 4.65 c), whose signals resonate at the same frequencies as those marked with \bullet in the above discussed spectrum (fig 4.65 b). Taking into account also the above mentioned changes observed in the CD spectrum (blue line and green line in fig 4.64), this confirms the existence of octameric aggregate $[(\text{G28})_8 \text{K}](\text{pic})$ also in the chloroform solution before the extraction probably due to the presence of sodium or potassium residual of the synthetic work-up. In particular, observing the ^1H -NMR spectrum after potassium picrate extraction, integration of the picrate (8.94 ppm) and H8 (7.14 ppm) signals supports a 8:1 stoichiometry for the complex (typical of an octamer). A single set of signals (although broad) for the imino NH-1, H8, amino NH-2 protons and an upfield shift for H8 with respect to its resonance in the absence of cations, are a peculiarity of an head-to-head or tail-to-tail octamer (D_4 symmetry). The broadening of all signals is due to the contribute of the two different diastereoisomeric forms of **28** to the supramolecular aggregate. In the formation of the octamer no self-recognition between Plus and Minus $\alpha\text{HPTMGace}$ occurs so recorded peaks are due to a statistic distribution of the two diastereoisomers in the octamers. CD spectra, above mentioned, confirm the presence of D_4 -octamer. NOESY spectrum recorded on the same sample shows a cross peak between H8 proton and H1', indicative of the existence in the two stacked G-quartets of guanosine all in a *syn*-conformation. (fig.4.66).

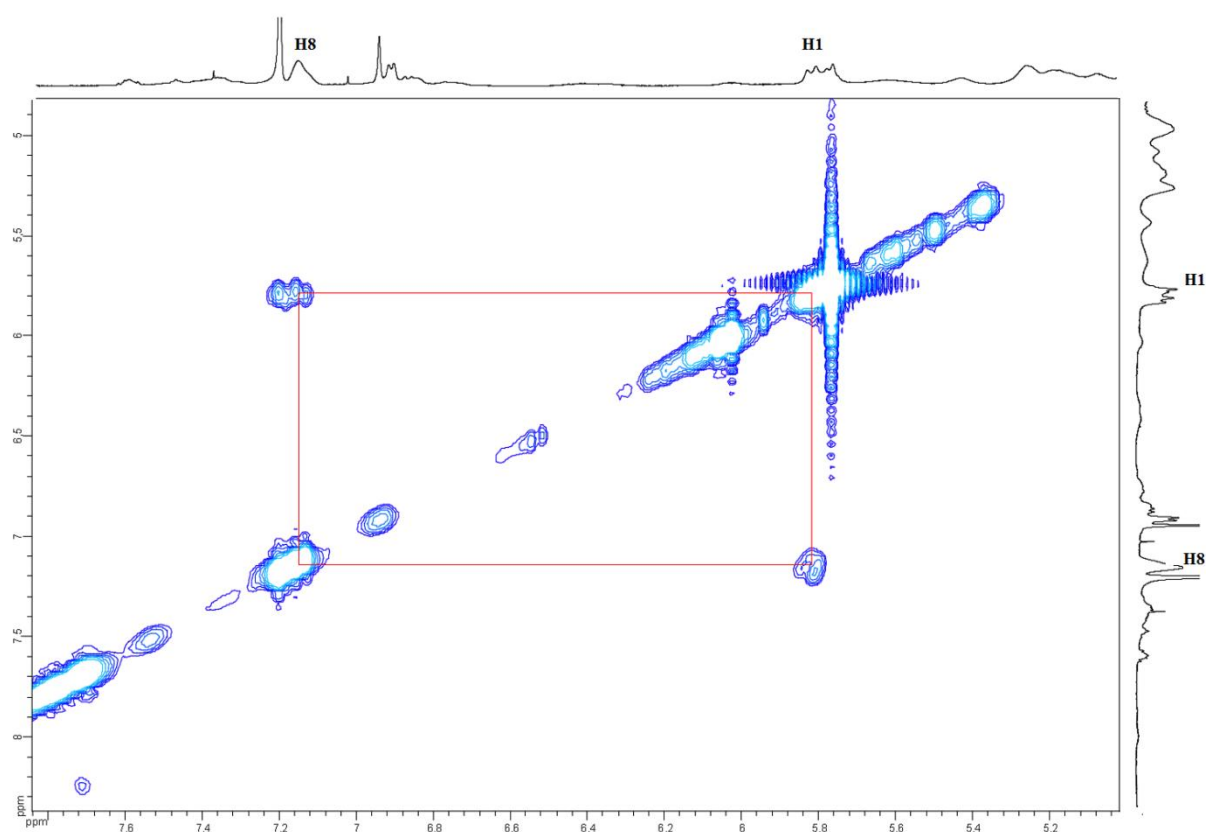


Figure 4.66: Portion of NOESY spectrum of **28** in CDCl_3 (10 mM) with potassium picrate 8:1.

Diffusion NMR spectra recorded on $[(\text{G28})_8 \text{K}](\text{pic})$, and in particular the analysis of NH-1 peak at δ 12.43 ppm and H8 peak at δ 7.18 ppm, show diffusion coefficients of $D_{\bullet} = 1.72 \pm 0.018 \cdot 10^{-10} \text{ m}^2 \text{ s}^{-1}$ and $1.81 \pm 0.022 \cdot 10^{-10} \text{ m}^2 \text{ s}^{-1}$ respectively. If these values are normalized over the solvent diffusion coefficient measured on the same sample, they can be compared with the corresponding values obtained analogously from the other samples, under the same conditions. As reported in table 4, these values agree with those obtained for the octameric structure (\bullet) observed in mother chloroform solution.

When a weighted (1/8 mol/mol) amount of strontium (Sr^{++}) picrate was added to a solution of **28** in chloroform, a spectrum different from **c** was observed (fig.4.65 d): for instance, two signals are present for the imino proton (11.76 ppm and 11.18 ppm). Supramolecular characterization of this new aggregate was not possible by bidimensional NMR experiments, due to broad signals. Signals broadening can be caused by the high molecular weight of this species and/or, in this case, by the inhomogeneous

Synthesis of a guanosine derivative functionalized as PTM derivative

stereochemical composition of the aggregate, due to the presence of the two diastereoisomers of **28**. However, some information can be extracted from DOSY experiments. The diffusion coefficient for NH-1 peak at δ 11.76 ppm normalized for solvent diffusion, provides a value of $D/D_s = 0.10$. This value suggests that the complex formed by solid-liquid extraction with strontium picrate is an higher order aggregate than the octamer observed after K^+ extraction (table 4). It has been reported in the literature^[47] that divalent cations such as Sr^{++} or Ba^{++} can give D_4 -symmetric hexadecamers of formula $[(G)_{16}M_2]4Pic$ where the four picrate anions use their phenolate oxygen atoms and their two ortho-substituted nitro groups to form bifurcated hydrogen bonds to the $N2H_B$ amino protons that protrude from the two “inner” G4-quartets, thus linking two octamers together (fig. 4.67).

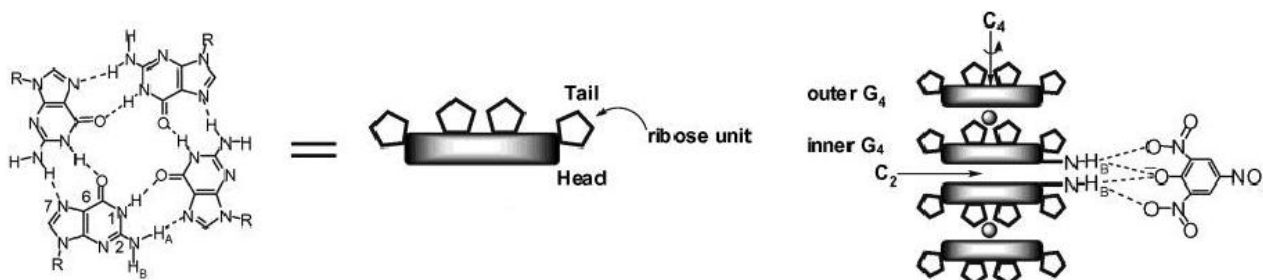


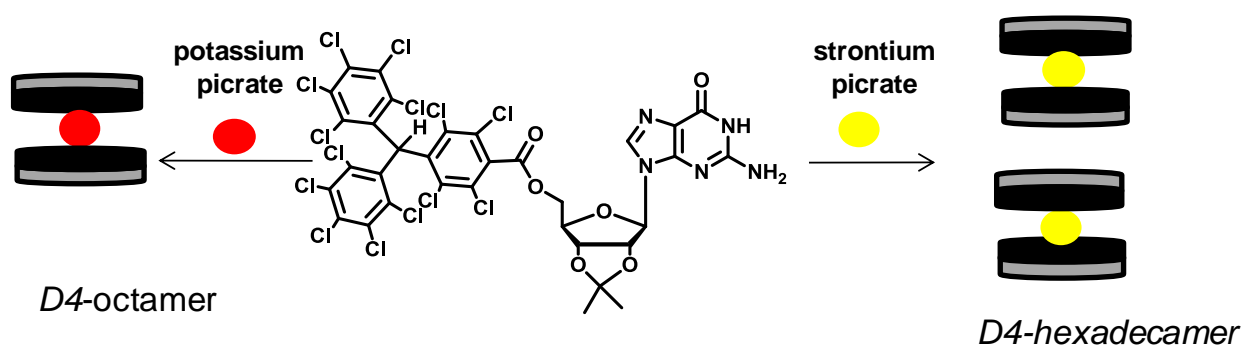
Figure 4.67: Schematic representation of the formation of an hexadecamer as reported in the ref 11

By comparison with the data reported in the literature,^[46] it is reasonable to assume that the supramolecular aggregate formed in the presence of strontium picrate is an hexadecamer with formula $[(G28)_{16}Sr_2]4Pic$ as represented in fig.4.67. Signals at δ 11.7 and δ 11.18 could be the NH-1 peaks of outer and inner G-quartets; the broad signals in the region comprised between δ 8.2 ppm and 10 ppm are probably due to the amino protons of inner and outer quartets involved in intra-quartet hydrogen. CD spectra (red line fig.4.64), which show the presence of stacked G-quartets in a supramolecular structure different from octameric complex, further support this assumption.

	δ ppm	Diffusion coefficient (D) $10^{-10} \text{ m}^2 \text{ s}^{-1}$	D/D _{solvent}
H8 _{ribbon}	7.71	2.91 ± 0.016	0.16
H8 _{octamer}	7.18	2.25 ± 0.013	0.12
H8 _{octamer}	7.18	1.81 ± 0.022	0.12
NH-1 _{octamer}	12.43	1.72 ± 0.018	0.13
NH-1 _{hexad}	11.76	2.00 ± 0.020	0.10

Tab.4

Although no conclusive evidence about the structure of this aggregate is available, NMR and circular dichroism confirm the formation of two different structures (octamer or hexadecamer) depending on the nature of cation. The monovalent cation potassium induces mainly the stacking of two G-quartet, while the divalent cation strontium seems to promote a further stacking with the formation of a more complex supramolecular aggregate. The supramolecular behaviour observed for **28** is summarized in figure 4.68.



Bibliography

1. (a) A. Caneschi, D. Gatteschi and P. Rey, *Prog. Inorg. Chem.*, **1991**, 39, 331; (b) O. Kahn, *Magnetism: A Supramolecular Function*, Kluwer, Dordrecht, **1996**; (c) P. M. Lahti, *Magnetic Properties of Organic Materials*, Marcel Dekker, New York, **1999**; (d) K. Itoh and M. Kinoshita, *Molecular Magnetism*, Kodansha (Gordon and Breach), Tokyo, **2000**; (e) *Magnetism: Molecules to Materials*, ed. J. S. Miller and M. Drillon, Wiley-VCH, Weinheim, **2001–2005**, vol. I–V; (f) B. D. Koivisto and R. G. Hicks, *Coord. Chem. Rev.*, **2005**, 249, 2612; (g) D. Luneau and P. Rey, *Coord. Chem. Rev.*, **2005**, 249, 2591; (h) K. E. Vostrikova, *Coord. Chem. Rev.*, **2008**, 252, 1409.
2. (a) P. P. Power, *Chem. Rev.*, **2003**, 103, 789; (b) R. G. Hicks, *Org. Biomol. Chem.*, **2007**, 5, 1321.
3. O. Armet, J. Veciana, C. Rovira, J. Riera, J. Castañer E. Molins J. Rius, C. Miravittles, S. Olivella and J. Brichfeus, *J. Phys. Chem.*, **1987**, 91, 5608.
4. C. Graziano, S. Masiero, S. Pieraccini, M. Lucarini, G. P. Spada *Org. Lett.* **2008**, 10, 1739-1742
5. P. Neviani, E. Mileo, S. Masiero, S. Pieraccini, M. Lucarini, G. P. Spada *Org. Lett.*, **2009**, 11, 3004
6. Self-assembled spin cage containing four radical centers have also been reported: Nakabayashi, K.; Ozaki, Y.; Kawano, M.; Fujita, M. *Angew. Chem., Int. Ed.* **2008**, 47, 2046–2048.
7. M. Gomberg, *J. Am. Chem. Soc.*, **1900**, 22, 757; (b) M. Gomberg, *J. Am. Chem. Soc.*, **1901**, 23, 496; (c) M. Gomberg, *Chem. Rev.*, **1924**, 1, 91.
8. (a) D. Griller and K. U. Ingold, *Acc. Chem. Res.*, **1976**, 9, 13; (b) A. R. Forrester and J. M. Hay and R. H. Thomson, *Organic Chemistry of Stable Free Radicals*, Academic Press, London and New York, **1968**; (c) *Metal–Organic and Organic Molecular Magnets*, ed. P. Day and A. E. Underhill, *The Royal Society of Chemistry*, Cambridge, **1999**; (d) *Supramolecular Engineering of Synthetic Metallic Materials*, ed. J. Veciana, C. Rovira and D. B. Amabilino, Kluwer Academic Publishers, Dordrecht, **1999**; (e) *Molecular Magnets: Recent Highlights*, ed. W. Linert and M. Verdaguer, Springer-Verlag, Vienna, **2003**; (f)

- Carbon-Based Magnetism, ed. T. L. Makarova and F. Palacio, Elsevier B. V. Amsterdam, **2006**.
9. I. Ratera and J. Veciana* *Chem. Soc. Rev.*, **2012**, *41*, 303–349
 10. *Stable Radicals: Fundamentals and Applied Aspects of Odd-Electron Compounds*, ed. R. Hicks, Wiley, New York, **2010**
 11. (a) A. Rajca, J. Wongsriratanakul and A. Rajca, *Science*, **2001**, *294*, 1503; (b) A. Rajca, K. Lu and S. Rajca, *J. Am. Chem. Soc.*, **1997**, *119*, 10335; (c) A. Rajca, J. Wongsriratanakul and S. Rajca, *J. Am. Chem. Soc.*, **2004**, *126*, 6608; (d) A. Rajca, *Adv. Phys. Org. Chem.*, **2005**, *40*, 153; (e) A. Rajca, S. Utamapanya and S. Thayumanavan, *J. Am. Chem. Soc.*, **1992**, *114*, 1884; (f) A. Rajca, *Chem. Rev.*, **1994**, *94*, 871.
 12. W. P. Neumann, A. Penenory, U. Stewen and M. Lehning, *J. Am. Chem. Soc.*, **1967**, *89*, 2054.
 13. M. Ballester, *Acc. Chem. Res.*, **1985**, *18*, 380.
 14. J. Veciana and M. I. Crespo, *Angew. Chem., Int. Ed. Engl.*, **1991**, *30*, 74
 15. R. S. Cahn, C. Ingold and V. Prelog, *Angew. Chem., Int. Ed. Engl.*, **1966**, *5*, 385
 16. N. Ventosa, D. Ruiz, C. Rovira and J. Veciana, *Mol. Cryst. Liq. Cryst.*, **1993**, *232*, 333.
 17. M. Ballester, *Adv. Phys. Org. Chem.*, 1989, *25*, 267.
 18. M. Ballester, I. Pascual, J. Riera and J. Castañer, *J. Org. Chem.*, **1991**, *56*, 217
 19. V. M. Domingo and J. Castañer, *Chem. Commun.*, **1995**, 895.
 20. M. A. Fox., E. Gaillard and C. C. Chen *J. Am. Chem. Soc.*, **1987**, *109*, 7088
 21. Rius, C. Miravittles, E. Molins, M. I. Crespo and J. Veciana, *Mol. Cryst. Liq. Cryst.*, **1990**, *187*, 155.
 22. M. Ballester, J. Riera, J. Castañer, C. Badia and J. M. Monso´, *J. Am. Chem. Soc.*, **1971**, *93*, 2215.
 23. (a) M. Ballester, J. Riera, J. Castañer, C. Rovira and O. Armet, *Synthesis*, **1986**, *64*; (b) M. Ballester, J. Veciana, J. Riera, J. Castañer, C. Rovira and O. Armet, *J. Org. Chem.*, **1986**, *51*, 2472.
 24. M. Ballester, J. Riera, J. Castañer, C. Rovira, J. Veciana and C. Onrubia, *J. Org. Chem.*, **1983**, *48*, 3716

25. S. Chopin, J. Cousseau*, E. Levillain, C. Rovira, J. Veciana, A. S. D. Sandanayaka, Y. Araki O. Ito *J. Mater Chem.*, **2006**, *16*, 112
26. (a) M. Yamazaki, Y. Araki, M. Fujitsuka and O. Ito, *J. Phys. Chem. A*, **2001**, *105*, 8615; (b) F. D'Souza, G. R. Deviprasad, M. E. Zandler, V. T. Hoang, A. Klykov, M. E. El-Khouly, M. Fujitsuka and O. Ito, *J. Phys. Chem. B*, **2002**, *106* 4952.
27. C. Sporer, I. Ratera, D. Ruiz-Molina, Y. Zhao, J. Vidal-Gancedo, K. Wurst, P. Jaitner, K. Clays, A. Persoons, C. Rovira and J. Veciana, *Angew. Chem., Int. Ed.*, **2004**, *43*, 5266.
28. I. Ratera, D. Ruiz-Molina, J. Vidal-Gancedo, J. J. Novoa, K. Wurst, J.-F. Letard, C. Rovira and J. Veciana, *Chem. Eur. J.*, **2004**, *10*, 603; (b) I. Ratera, D. Ruiz-Molina, F. Renz, J. Ensling, K. Wurst, C. Rovira, G. Philipp and J. Veciana, *J. Am. Chem. Soc.*, **2003**, *125*, 1462.
29. V. Gamero, D. Velasco, S. Latorre, F. Lopez Calahorra, E. Brillas and L. Julia *Tetrahedron Lett.*, **2006**, *47*, 2305
30. S. Castellanos, D. Velasco, F. Lopez-Calahorra, E. Brillas and L. Julia *J. Org. Chem.*, **2008**, *73* , 3759.
31. N. Roques, D. Maspoch, A. Dactu, K. Wurst, D. Ruiz-Molina, C. Rovira, J. Veciana, *Polyhedron*, **2007**, *26*, 1934
32. N. Crivillers, M. Mas-Torrent, J. Vidal-Gancedo, J. Veciana, C. Rovira, *J. Am. Chem. Soc.* **2008**, *130*, 5499.
33. V. Mugnaini, M. Fabrizioli, I. Ratera, M. Mannini, A. Caneschi, D. Gatteschi, Y. Manassen, J. Veciana, *Solid State Sci.* **2009**, *11*, 956.
34. C. Simao, M. Mas-Torrent, N. Crivillers, V. Lloveras, J. Veciana, C. Rovira, *Nature Chem.*, **2011**, *3*, 359
35. N. Crivillers, M. Mas-Torrent, S. Perruchas, N. Roques, J. Vidal-Gancedo, J. Veciana, C. Rovira, L. Basabe-Desmonts, B. Jan Ravoo, M. Crego-Calama, D. N. Reinhoudt, *Angew. Chemie Int. Ed.* **2007**, *46*, 2215.
36. M. Oliveros, L. Gonzalez-García, V. Mugnaini, F. Yubero, N. Roques, J. Veciana, A.R. Gonzalez-Elipe, C. Rovira *Langmuir* **2011**, *27*, 5098–5106

37. (a) M. Ballester, J. Castañer, J. Riera, A. Ibañez, J. Pujades, *J. Org. Chem.*, **1982**, 47 259;
(b) V.M. Domingo, J. Castañer, J. Riera, A. Labarta, *J. Org. Chem.* **1994**, 59, 2604;
(c) S. Lopez, J. Carilla, L. Fajari, L. Julia, E. Brillas, A. Labarta, *Tetrahedron* **1995**, 51, 730
38. V. Dang, J. H. Wang, S. Feng, C. Buron, F. A. Villamena, P. G. Wang and P. Kuppusamy *Bioorganic & Medicinal Chemistry Letters*, **2007**, 17,4062
39. S. Chopin, J. Cousseau, E. Levillain, C. Rovira, J. Veciana, A. S. D. Sandanayaka, Y. Araki and O. Ito *J. Mater. Chem.*, **2006**, 16, 112-121
40. M. S. Kaucher, Y. F. Lam, S. Pieraccini, G. Gottarelli, J. T. Davis, *Chem. Eur. J.*, **2005**, 11, 164
41. For some reviews on the technique, see: a) W. S. Price, *New Advances in Analytical Chemistry (Ed.: E. Atta-ur-Rahman)*, Gordon and Breach Science, Amsterdam, **2000**, pp. 31–72; b) P. Stilbs, *Prog. Nucl. Magn. Reson. Spectrosc.* **1987**, 19, 1–45; c) W. S. Price, *Concepts Magn. Reson.* **1997**, 9, 299–336; d) W. S. Price, *Concepts Magn. Reson.* **1998**, 10, 197–237; e) C. S. Johnson, *Prog. Nucl. Magn. Reson. Spectrosc.* **1999**, 34, 203–25
42. a) M. C. Lo, J. S. Helm, G. Sarngadharan, I. Pelczer, S. Walker, *J. Am. Chem. Soc.* **2001**, 123, 8640–8641; b) A. H. Daranas, J. J. Fernandez, E. Q. Morales, M. Norte, J. A. Gavin, *J. Med. Chem.* **2004**, 47, 10–13; c) K. Shikii, S. Sakamoto, H. Seki, H. Utsumi, K. Yamaguchi, *Tetrahedron* **2004**, 60, 3487–3492.
43. a) K. H. Mayo, E. Ilyina, H. Park, *Protein Sci.* **1996**, 5, 1301–1315; b) S. G. Yao, G. J. Howlett, R. S. Norton, *J. Biomol. Nucl. Magn. Reson.* **2000**, 16, 109–119.
44. a) P. R. Wills, Y. Georgalis, *J. Phys. Chem.* **1981**, 85, 3978–3984; b) A. S. Altieri, D. P. Hinton, R. A. Byrd, *J. Am. Chem. Soc.* **1995**, 117, 7566–7567; c) V. V. Krishnan, *J. Magn. Reson.* **1997**, 124, 468–473; d) E. Ilyina, V. Roongta, H. Pan, C. Woodward, K. H. Mayo, *Biochemistry* **1997**, 36, 3383–3388; e) W. S. Price, F. Tsuchiya, Y. Arata, *J. Am. Chem. Soc.* **1999**, 121, 11503–11512.

*Synthesis of a guanosine derivative
functionalized as PTM derivative*

45. For a review: M. Valentini, H. Ruegger, P. S. Pregosin, *Helv. Chim. Acta* **2001**, *84*, 2833 –2853.
46. M. S. Kaucher , Y.F. Lam, S. Pieraccini, G. Gottarelli, and J. T. Davis *Chem. Eur. J.* **2005**, *11*, 164 – 173
47. X. Shi, K. M. Mullaugh, J. C. Fettinger, Y. Jiang, S. A. Hofstadler, J. T. Davis *J. AM. CHEM. SOC.* **2003**, *125*, 10830-10841

5 Experimental Part

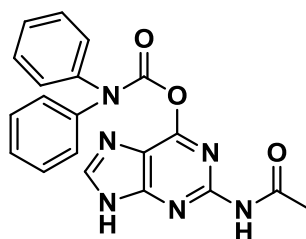
5 Experimental part

General

All reactions were carried out under magnetic or mechanical stirring. Reactions requiring anhydrous conditions were carried out in oven-dried glassware under dry argon atmosphere. For TLC analyses, Baker IB2-F silica gel plates were used. Column chromatography was performed on Aldrich silica gel 230-400 mesh. Reagents and solvents, including dry solvents, were purchased from Aldrich, Fluka or Alfa Aesar.

NMR spectra were recorded with Varian (Gemini 200, Inova 400, Mercury 600 MHz) and Bruker (Avance 400 MHz) instruments; decoupled ¹³C NMR spectra were usually recorded. To assign carbons, DEPT spectra (multiplicity 1.5) were recorded. All NMR spectra were referenced relative to residual solvent peaks. Electrospray (ES) ionization mass spectra were obtained with a Micromass ZMD 4000. High resolution mass spectra (electronic impact) were recorded with a Thermo Finnigan MAT 95 XP spectrometer. CD spectra were recorded on a JASCO J-710 Spectropolarimeter (cell path length = 0.01 cm).

Derivative 8: 2-acetamido-6,9-dihydro-1H-purin-6-yl diphenylcarbamate



Acetic anhydride¹ (10 ml) was added to a suspension of 2-amino-1H-purin-6(9H)-one (6 g, 39,8 mmol dried over P₂O₅ under vacuum 2h at 55°C) in dimethylacetamide (DMAC, 50 mL). The resulting suspension was stirred seven hours at 160°C. The crude material was filtered and the white compound (**8a**) was washed with ethanol and dried under vacuum 2h.

ESI-MS: m/z (%): 236.20 (100) [1+H]

To a solution of **8a** (6.3g, 27 mmol) in pyridine (130 ml) were added *N,N*-diisopropylethylamine (DIPEA 9.3 mL) and *N,N*-diphenylcarbamoyl chloride (DPC-

Cl 6.8 g 29mmol).The reaction mixture was stirred for 2.5 h at r.t, a pink solution was formed. H₂O (11.6 ml) was added and the mixture was stirred for other 10 minutes. All solvents were removed under reduced pressure and the oil obtained was co-evaporated three time with toluene to remove the traces of pyridine and dried under the vacuum. A solution of H₂O/EtOH 50% was added and It was heated at reflux temperature for 1.5 h and a precipitate began to separate. After heating the reaction mixture was allowed to cool to a r.t. The pink solid was filtered, washed several times with EtOH, and dried under the vacuum.

Yield: 80%

¹H-NMR (600 MHz DMSO-d₆): δ 13.56 (s, 1H, 9-NH), 10.62 (s, 1H, 2-NH), 8.48 (s, 1H, H8), 7.44 (t, J = 7.7 Hz, 8H, ar-CH), 7.31 (t, J = 7.4 Hz 2H,ar-CH), 2.16 (s, 3H, acetyl-CH₃).

ESI-MS: m/z (%): 411.1 (100) [1+Na]

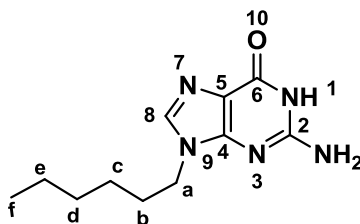
N⁹-Alkylguanines 13-15, 19-24. General procedure.

Mitsunobu coupling of **8** with linear (**a-h**) and chiral alcohols(**i-m**) was carried out according to the procedure described in literature.^[2]

Protected guanine **8** (1.1mmol) was added to a solution of primary alcohol (1.15 mmol) and PPh₃ (triphenylposphine 1.15 mmol) in anhydrous THF (20 mL) under N₂ atmosphere. Diisopropyl-azodicarboxilate (DIAD 1.15mmol). was added to the resulting suspension. The reaction mixture was stirred at 70°C for 6 hrs; then a second equivalent of alcohol (1.15 mmol), PPh₃ (1.15 mmol) and DIAD (1.15 mmol) were added. The mixture was stirred for further 6 hrs at the same temperature. After cooling down, the reaction mixture was poured into a saturated sodium chloride solution (25 mL) and extracted with dichloromethane (3x50 mL) . The combined organic layers were washed with water and dried over anhydrous magnesium sulfate. The solvent was removed under reduced pressure and the crude reaction mixture was purified by chromatography on silica gel affording the protected N-9 alkylated guanine **8b** The protected N-9 alkylated

guanine (0,20 mmol) was dissolved in a mixture of 30% ammonia/methanol (1:1) (60 mL). The resulting solution was heated at 60°C for 2 hrs. The solvent was then removed under reduced pressure and the crude reaction mixture was purified by chromatography on silica gel to give the expected N-9 alkylguanine as a white solid **8c**.

Derivative 13: 9-Hexylguanine



The general procedure described above was followed. Petroleum ether/ethyl acetate 1:1 was used for the purification of the protected N-9 hexyl guanine. Dichloromethane/methanol 98:2 was used for the purification of the title compound.

Yield 42%

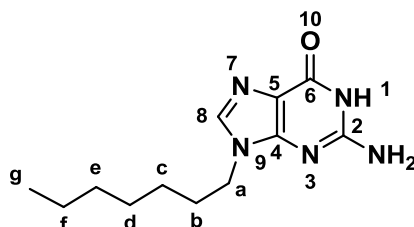
¹H-NMR (400 MHz DMSO-d₆): δ 10.53 (s, 1H, 1-NH), 7.67 (s, 1H, H8), 6.43 (s, 2H, NH₂), 3.91 (t, J = 7.1 Hz, 2H,a-CH₂), 1.70 (m, 2H,b-CH₂), 1.23 (m, c-e 6H), 0.93–0.75 (t, 3H, f-CH₃).

¹³C-NMR (400 MHz DMSO- d₆): δ 157,72, 154.35, 152.04, 138.35, 117.48, 43.52, 31.59, 30.28, 26.54, 22.87, 14.74.

ESI-MS: m/z (%): 234.1 (100) [1-H]-

Elemental analysis calcd (%) for C₁₁H₁₇N₅O: C 56.15, H 7.28, N 29.76; found C 56.02, H 7.27, N 29.76

Derivative 20: 9-Heptylguanine



The general procedure described above was followed. Petroleum ether/ethyl acetate 6:4 was used for the purification of the protected N-9 heptylguanine. Dichloromethane/methanol 94:6 was used for the purification of the title compound.

Yield 34%

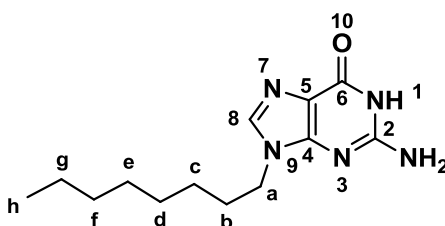
$^1\text{H-NMR}$ (400 MHz DMSO- d_6): δ 10.52 (s, 1H, 1-NH), 7.67 (s, 1H, H8), 6.42 (s, 2H, NH_2), 3.91 (t, $J = 7.1$ Hz, 2H, a- CH_2), 1.70 (m, 2H, b- CH_2), 1.23 (m, c-f 8H), 0.93 – 0.75 (t, $J = 7.0$ 3H, g- CH_3).

$^{13}\text{C-NMR}$ (400 MHz DMSO- d_6): δ 157.74, 154.36, 152.05, 117.49, 43.54, 32.05, 30.33, 28.07, 26.86, 22.56, 14.82.

ESI-MS: m/z (%): 248.1(100) [1-H^+]

Elemental analysis calcd (%) for $\text{C}_{12}\text{H}_{19}\text{N}_5\text{O}$: C 57.81, H 7.68, N 28.09; found C 57.94, H 7.69, N 28.16

Derivative 21: 9-Octylguanine



The general procedure described above was followed. Petroleum ether/ethyl acetate 6:4 was used for the purification of the protected N-9 octylguanine. Dichloromethane/methanol 94:6 was used for the purification of the title compound.

Yield 20%

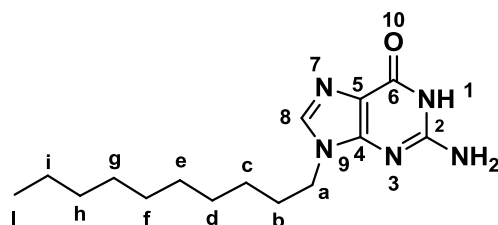
$^1\text{H NMR}$ (600 MHz, DMSO- d_6): δ 10.49 (s, 1H, NH), 7.67 (s, 1H, H8), 6.40 (s, 2H), 3.91 (t, $J = 7.2$ Hz, 2H, a- CH_2), 1.77 – 1.66 (m, 2H, b- CH_2), 1.29 – 1.16 (m, 10H, c-g CH_2), 0.84 (t, $J = 7.0$ Hz, 3H, h- CH_3).

$^{13}\text{C-NMR}$ (400 MHz DMSO- d_6): δ 157.71, 154.32, 152.04, 138.36, 117.49, 43.53, 32.04, 30.28, 29.45, 29.34, 26.87, 22.93, 14.82.

ESI-MS: m/z (%): 262.1 (100) [1-H^+]

Elemental analysis calcd (%) for C₁₃H₂₁N₅O: C 59.29, H 8.04, N 26.59.; found C 59.43, H 8.02, N 26.54

Derivative 14: 9-Decylguanine



The general procedure described above was followed. Petroleum ether/ethyl acetate 1:1 was used for the purification of the protected N-9 decyl guanine. The title compound was obtained through recrystallization from methanol.

Yield 51%

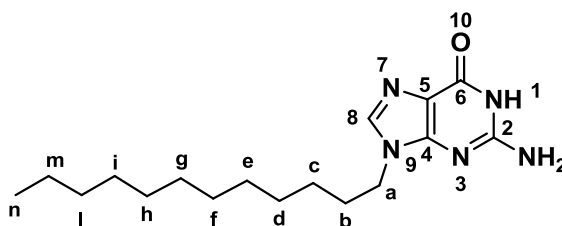
¹H NMR (600 MHz, DMSO-d₆) δ 10.9 (s, 1H, NH), 7.67 (s, 1H, H8), 6.40 (s, 2H), 3.91 (t, *J* = 7.2 Hz, 2H, a-CH₂), 1.77 – 1.66 (m, 2H, b-CH₂), 1.29 – 1.16 (m, 10H, c-g CH₂), 0.84 (t, *J* = 7.0 Hz, 3H, h-CH₃).

¹³C-NMR (400 MHz DMSO- d₆): δ 157.71, 154.32, 152.04, 138.36, 117.49, 43.53, 32.04, 30.28, 29.45, 29.34, 26.87, 22.93, 14.82.

ESI-MS: *m/z* (%): 290.1 (100) [1-H]⁻.

Elemental analysis calcd (%) for C₁₅H₂₅N₅O: C 61.83, H 8.65, N 24.03; found C 61.94, H 8.64, N 24.04

Derivative 22: 9-Dodecylguanine



The general procedure described above was followed. Petroleum ether/ethyl acetate 1:1 was used for the purification of the protected N-9 dodecyl guanine. Dichloromethane/methanol 94:6 was used for the purification of the title compound.

Yield 54 %

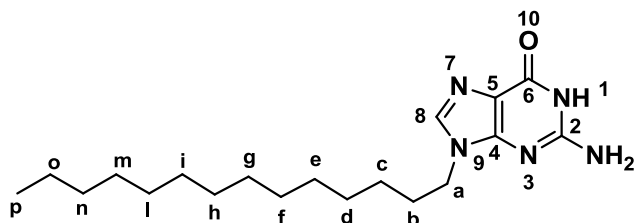
$^1\text{H-NMR}$ (600 MHz DMSO- d_6): δ 10.50 (s, 1H, 1-NH), 7.67 (s, 1H, H8), 6.41 (s, 2H, NH_2), 3.90 (t, $J = 7.1$ Hz, 2H, a- CH_2), 1.82 (m, 2H, b- CH_2), 1.22 (s, 18H, c-m CH_2), 0.93 – 0.77 (t, $J = 7.0$ 3H, n- CH_3).

$^{13}\text{C-NMR}$ (400 MHz DMSO- d_6): δ 157.71, 154.34, 152.04, 138.35, 117.49, 43.53, 32.20, 30.30, 29.91, 29.89, 29.61, 29.41, 26.88, 23.00, 14.86.

ESI-MS: m/z (%): 318.1 (100) [1-H] $^+$

Elemental analysis calcd (%) for $\text{C}_{15}\text{H}_{25}\text{N}_5\text{O}$: C 63.92, H 9.15, N 21.92; found C 63.87, H 9.16, N 21.95.

Derivative 23: 9-Tetradecylguanine



The general procedure described above was followed. Petroleum ether/ethyl acetate 1:1 was used for the purification of the protected N-9 tetradecyl guanine. Dichloromethane/methanol 96:4 was used for the purification of the title compound.

Yield 20 %

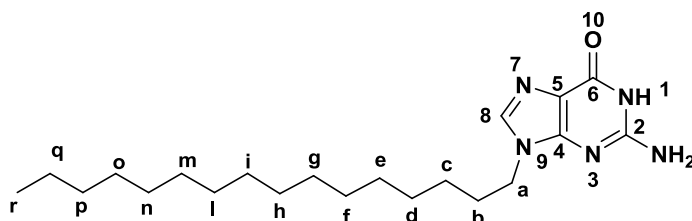
$^1\text{H-NMR}$ (200 MHz DMSO- d_6): δ 11.13 (s, 1H, 1-NH), 7.64 (s, 1H, H8), 6.69 (s, 2H, NH_2), 3.90 (t, $J = 7.1$ Hz, 2H, a- CH_2), 1.70 (m, 2H, b- CH_2), 1.22 (s, 22H, c-o CH_2), 0.93 – 0.77 (t, $J = 7.0$ 3H, p- CH_3).

$^{13}\text{C-NMR}$ (200 MHz DMSO- d_6): δ 158.04, 154.01, 152.09, 138.08, 117.45, 43.48, 32.21, 31.88, 30.32, 29.93, 29.61, 29.29, 26.91, 26.59, 24.94, 23.01, 22.67, 14.87, 14.54.

ESI-MS: m/z (%): 346.1 (100) [1-H]⁻

Elemental analysis calcd (%) for C₁₉H₃₃N₅O: C 65.67, H 9.57, N 20.15; found C 65.85, H 9.59, N 20.20

Derivative 24: 9-Hexadecylguanine



The general procedure described above was followed. Petroleum ether/ethyl acetate 1:1 was used for the purification of the protected N-9 hexadecyl guanine. Dichloromethane/methanol 94:6 was used for the purification of the title compound.

Yield 26 %

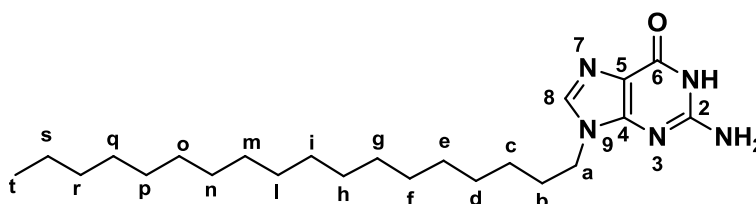
¹H-NMR (400 MHz DMSO-d₆): δ 10.50 (s, 1H, 1-NH), 7.67 (s, 1H, H8), 6.41 (s, 2H, NH₂), 3.90 (t, $J = 7.1$ Hz, 2H, a-CH₂), 1.70 (m, 2H, b-CH₂), 1.22 (s, 24H, c-p CH₂), 0.93 – 0.77 (t, $J = 7.0$ 3H, r-CH₃).

¹³C-NMR (400 MHz DMSO- d₆): δ 157.70, 154.33, 152.03, 138.33, 117.47, 43.53, 32.19, 30.29, 29.94, 29.91, 29.82, 29.60, 29.40, 26.88, 22.99, 14.86.

ESI-MS: m/z (%): 374.1 (100) [1-H]⁻

Elemental analysis calcd (%) for C₂₁H₃₇N₅O: C 67.16, H 9.93, N 18.65 ; found C 67,00, H 9.95, N 18.61

Derivative 15: 9-Octadecylguanine



The general procedure described above was followed. Petroleum ether/ethyl acetate 1:1 was used for the purification of the protected N-9 octadecylguanine. The title compound was obtained through recrystallization from methanol.

Yield 60%

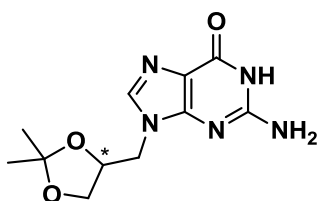
$^1\text{H-NMR}$ (400 MHz DMSO- d_6): δ 10.50 (s, 1H, 1-NH), 7.68 (s, 1H, H8), 6.40 (s, 2H, NH₂), 3.92 (t, $J = 7.1$ Hz, 2H, a-CH₂), 1.68 (m, 2H, b-CH₂), 1.22 (s, 30 H, c-s CH₂), 0.93 – 0.77 (t, $J = 7.0$ 3H, t-CH₃).

$^{13}\text{C-NMR}$ (400 MHz DMSO- d_6): δ 157.43, 154.13, 151.09, 137.82, 117.58, 43.36, 31.87, 29.95, 29.56, 29.49, 29.23, 29.10, 26.67, 22.61, 14.38.

ESI-MS: m/z (%): 402.1 (100) [1-H]⁺

Elemental analysis calcd (%) for C₂₁H₃₇N₅O: C 68.45, H 10.24, N 17.35; found C 68.62, H 10.22, N 17.38.

Derivative 16a: 2-amino-9-(((S)-2,2-(dimethyl-1,3-dioxolan-4-yl)methyl)-guanine



Protected guanine **8** (1.54 mmol) was added to a solution of alcohol **i** (1.15 mmol) and PPh₃ (1.46 mmol) in anhydrous THF (20 mL) under N₂ atmosphere. Diisopropylazodicarboxylate (DIAD 1.46 mmol) was added to the resulting suspension.

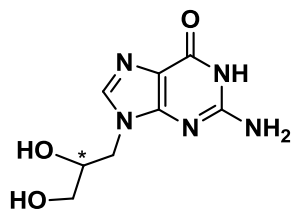
The reaction mixture was stirred at 70°C for 6 hrs; then a second equivalent of alcohol (1.15 mmol), PPh₃ (1.54 mmol) and DIAD (1.54 mmol) were added. The mixture was stirred for further 6 hrs at the same temperature. After cooling down, the reaction mixture was poured into a saturated sodium chloride solution (25 mL) and extracted with dichloromethane (3x50 mL). The combined organic layers were washed with water and dried over anhydrous magnesium sulfate. The solvent was removed under reduced pressure and the crude reaction mixture was purified by chromatography on silica gel (petroleum ether/ethyl acetate 1:1) affording the protected product.

The protected N-9 alkylated guanine was dissolved in a mixture of 30% ammonia/methanol (1:1) (60 mL). The resulting solution was heated at 60°C for 2 hrs. The solvent was then removed under reduced pressure and the crude reaction mixture was purified by chromatography on silica gel (dichlorometane/methanol 96:4)

Yield 29%

ESI-MS: m/z (%): 264.1(100) [1-H]⁻

Derivative 16 b: 2-amino-9-(((S)-2,3-(dihydroxypropyl)-guanine

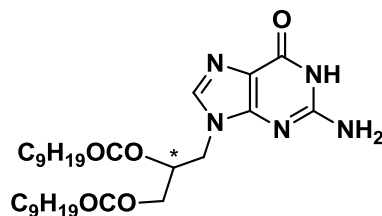


16 was dissolved in methanol (12 ml) and it was added HCl 1N (3 ml). The resulting solution was stirred for 2 hrs at room temperature. The solvent was removed under reduced pressure and the product **11b** was recrystallized from methanol and washed with dichloromethane.

Yield 95%

ESI-MS: m/z (%): 224.1(100) [1-H]⁻

Derivative 16: 9-(((S)-2,3-(decanoyloxy)propyl)-guanine



16b (0.35mmol dried over P₂O₅ under vacuum 2h at 55°C) was dissolved in dry CH₃CN (4 mL). To the solution was added TEA (triethylamine 2.4 eq., 0.87 mmol), decanoic anhydride (2.2 eq., 0.79 mmol) and DMAP (dimethylaminopyridine, catalytic amount)

The mixture was stirred overnight and the suspension was filtered and washed with CH₃CN. **16** was recrystallized from ethanol

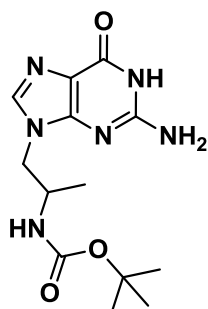
Yield 87%

¹H NMR (600 MHz, DMSO-d₆): δ 10.53 (s, 1H), 7.62 (s, 1H), 6.43 (s, 2H), 5.33 (tt, *J* = 7.3, 3.7 Hz, 1H), 4.29 (dd, *J* = 12.2, 3.2 Hz, 1H), 4.22 – 4.14 (m, 2H), 4.04 (dd, *J* = 12.2, 6.8 Hz, 1H), 2.27 (t, *J* = 7.4 Hz, 2H), 2.19 (t, *J* = 7.3 Hz, 2H), 1.48 (t, *J* = 7.2 Hz, 2H), 1.38 (m, 2H), 1.29 – 1.15 (m, 22H), 1.13 (t, *J* = 7.6 Hz, 2H), 0.85 (m, 6H).

¹³C-NMR (400 MHz DMSO- d₆): δ 173.18, 172.67, 157.73, 152.10, 138.30, 117.00, 69.82, 63.08, 40.84, 34.08, 33.97, 31.96, 29.55, 29.51, 29.41, 29.35, 29.09, 28.98, 25.03, 24.94, 22.77, 14.62.

ESI-MS: *m/z* (%): 532.2 (100) [1-H]⁻

Derivative 17: **9-((S)-tert-butyl isopropylcarbamate)-guanine**



The general procedure described for derivative **16** was followed. The primary alcohol used for Mitsunobu coupling was (S)-(+)-2-aminopropan-1-ol (**m**) previously protected with a *tert*-butyloxycarbonyl³ (BOC) group.

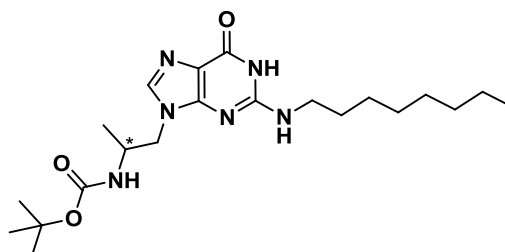
The crude reaction mixture wasn't purified by chromatography on silica gel (petroleum ether/ethyl acetate) but the protected N-9 alkylated guanine was directly dissolved in a mixture of 30% ammonia/methanol (1:1). Dichloromethane/methanol 98:2 and 94:6 was used for the purification of the title compound.

Yield 40%

¹H NMR (200 MHz, DMSO-d₆): δ 10.51 (s, 1H), 7.49 (s, 1H), 6.92 (d, *J* = 6.8 Hz, 1H), 6.43 (s, 2H), 3.85 (m, 3H), 1.31 (s, 8.7 H), 1.17 – 0.95 (m, 3H).

ESI-MS: *m/z* (%): 307.3 (100) [1-H]⁻

Derivative 17a: 9-((S)-tert-butyl isopropylcarbamate)-N₂C8-guanine



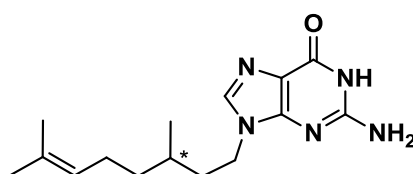
To a suspension of derivative⁴ **18** (98 mg, 0.304 mmol) and NaBH₃CN (114 mg, 6eq.) in dry methanol was added octanaldehyde (0.190 mL, 4 eq.), the mixture was heated at 50°C under argon. After 3 days it was added another portion of aldehyde (1.eq) and NaBH₃CN (1 eq.). The solvent was removed under reduced pressure after 96 h, the residue was acidified with HCl 1N. The resulting solution was purified by silica gel chromatography eluting with: acetone/dichloromethane (9:1), dichloromethane/ methanol (94:6).The title compound was recrystallized from methanol.

Yield 15%

¹H NMR (200 MHz, DMSO-d₆) :δ 10.39 (s, 1H), 7.51 (s, 1H), 6.89 (d, *J* = 6.8 Hz, 1H), 6.33 (t, *J* = 5.5 Hz, 1H), 3.37 – 3.18 (m, 2H), 1.61 – 1.45 (m, 2H), 1.30 (m, 19H), 1.28(s, 3H), 1.01 (d, *J* = 5.4 Hz, 3H), 0.97 – 0.77 (m, 3H).

ESI-MS: *m/z* (%): 419.28 (100) [1-H]⁻.

Derivative 18: 9-((S)-3,7-(dimethyl-6-octen))-guanine



The general procedure described for derivative **16** was followed. The primary alcohol used for Mitsunobu coupling was (S)-3,7 dimethyl-6-octen-1-ol.**(1)** Petroleum ether/ethyl

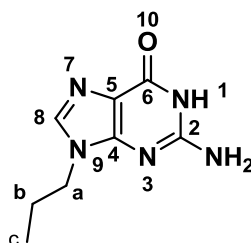
acetate 1:1 was used for the purification of the protected N-9-((S)-3,7-(dimethyl-6-octen))-guanine. Dichloromethane/methanol 96:4 and recrystallization from ethanol was used for the purification of the title compound.

Yield 50%

^1H NMR (400 MHz, DMSO- d_6): δ 10.50 (s, 1H), 7.68 (s, 1H), 6.39 (s, 2H), 5.02 (tt, $J = 7.1, 1.6$ Hz, 1H), 4.03 – 3.85 (m, 2H), 1.95 – 1.84 (m, 2H), 1.82 – 1.69 (m, 2H), 1.64 – 1.47 (m, 6H), 1.37 – 1.25 (m, 2H), 1.13 (m, 1H), 0.90 (d, $J = 6.3$ Hz, 3H).

ESI-MS: m/z (%): 288.2 (100) [1-H] $^-$

Derivative 25a: 9-Propylguanine



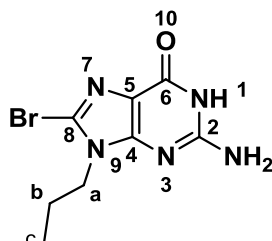
The general procedure described for 9-alkylguanines was followed. Petroleum ether/ethyl acetate 1:1 was used for the purification of the protected N-9-propylguanine. Dichloromethane/methanol 90:1 was used for the purification of the title compound.

Yield 60%

^1H -NMR (200 MHz DMSO- d_6) δ 10.53 (s, 1H, 1-NH), 7.67 (s, 1H, H8), 6.58 (s, 2H, NH_2), 3.89 (t, $J = 7.9$ Hz, 2H, a- CH_2), 1.70 (m, 2H, b- CH_2), 0.87 (t, 3H, c- CH_3).

ESI-MS: m/z (%): 192.1 (100) [1-H] $^-$.

Derivative 25 b: 8-bromo-9-propylguanine



The preparation of **25 b** was carried out according this synthetic procedure.^[5]

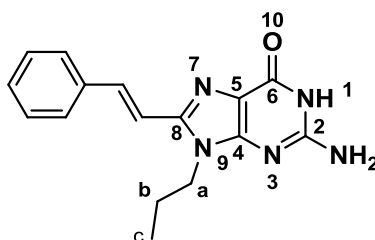
To a stirred mixture of 9-propylguanine (186 mg, 0.96 mmol) in glacial acetic acid (2 mL), heated to 50°C, was added bromine (50 mL 0.96 mmol). The mixture was allowed to stand 3-5h at 110°C under stirring. The reaction mixture was then poured into 10 ml of ice-water with stirring and allowed to stand at room temperature for a few hours. The precipitated was filtered, washed with water and dried. The crude product was recrystallized from methanol to give **25b**

Yield 70%

¹H NMR (200 MHz, DMSO-d₆) δ 10.66 (s, 1H), 6.58 (s, 2H, NH₂), 3.89 (t, *J* = 7.3, 2H), 1.84 – 1.56 (m, 2H), 0.87 (t, *J* = 7.4 Hz, 3H).

ESI-MS: *m/z* (%): 271.1 (100) [1-H]⁻

Derivative 25: 8-bromo-9-(propyl)-guanine



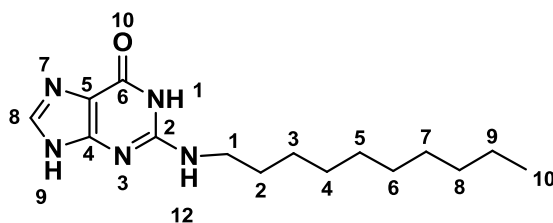
Suzuki-Miyaura cross-coupling reaction was carried out following the synthetic procedure published by the Shaughnessy group.^[6] To a flask containing **25 b** (176 mg, 0.65 mmol) in dry DMF (24 mL), it was added (*E*)-2-phenylvinylboronic acid (115 mg, 1.2 eq.) and Et₃N (361 μl, 4 eq.) under argon. The mixture was stirred for 5 min. at a room temperature. To the suspension was added Pd(PPh₃)₄ (tetrakis(triphenylphosphine)palladium 37 mg 0.05 eq) and the mixture was stirred for 48 h at 110°C. The solvent was concentrated in vacuo washed with water and purified by silica gel chromatography (ethyl acetate/methanol 99:1). The product was recrystallized from ethanol to give **21**.

Yield 10%

¹H NMR (200 MHz, DMSO-d₆) δ 10.55 (s, 1H), 7.79 – 7.16 (m, 7H), 6.50 (s, 2H), 4.10 (t, *J* = 7.3 Hz, 2H), 1.69 (q, *J* = 7.5 Hz, 2H), 0.87 (t, *J* = 7.3 Hz, 4H).

ESI-MS: *m/z* (%): 294.3 (100) [1-H]⁻

Derivative 9: 2-(decylamino)-guanine



The preparation of **22** was carried out according to this synthetic procedure described in literature⁷.

A stirred solution of 2-bromohypoxanthine (100 mg, 0.4 mmol) and decylamine (0.240 ml 3.0 eq) in a mixture of 2-methoxyethanol (2.4 mL) was heated at reflux. After 24 h, the mixture was chilled in an ice bath, and the precipitate was filtered and washed with concentrated aqueous ammonia and methanol. The product was purified by dissolving the precipitate (yellow solid) in hot 1 N sodium hydroxide. The hot mixture was filtered, acidified with glacial acetic acid, washed with methanol, and dried over phosphorus pentoxide.

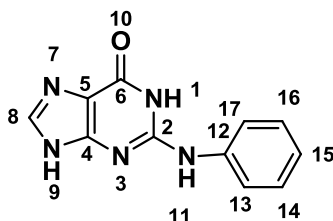
The product was purified by silica gel chromatography dichloromethane/methanol 94:6.

Yield 25%

¹H NMR (200 MHz, DMSO-d₆) δ 12.7 (broad s, 1H, 9-NH), 10.55 (s, 1H, 1-NH), 7.67 (s, 1H, H8), 6.34 (t, 1H, NH), 3.18 (m, 2H, 1-CH₂), 1.69 (m, 2H, 2-CH₂), 1.34 (m, 4H, 2-CH₂), 0.97 (t, 3H).

ESI-MS: *m/z* (%): 290.3 (100) [1-H]⁺.

Derivative 10: 2-(phenylamino)-guanine



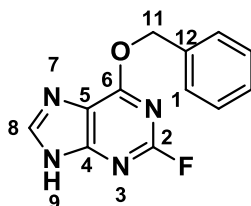
The preparation of **23** was carried out according to the synthetic procedure followed above

Yield 70%

^1H NMR (200 MHz, DMSO- d_6) δ 12.82 (s, 1H, 9-NH), 10.53 (s, 1H, 1NH), 8.66 (s, 1H, 11-NH), 7.85 (s, H8), 7.63 (d, $J = 7.9$ Hz, 2H, (12-13 CH)), 7.34 (t, $J = 7.8$ Hz, 2H (14-16 CH)), 7.03 (t, $J = 7.3$ Hz, 1H, (15-CH)).

ESI-MS: m/z (%): 290.3 (100) $[1-\text{H}]^-$

Derivative 11: 2-fluoro-6-benzyloxypurine



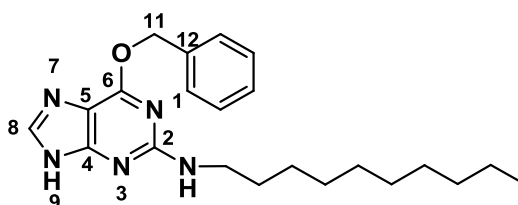
2-amino-6-benzyloxypurine^[8] (140 mg, 0.58 mmol) synthesised as described in literature^[9], was dissolved in HBF_4 40% (2mL) and the suspension was cooled to -15°C . An aqueous solution of NaNO_2 0.4 M (2mL) was added dropwise to a cooled suspension, it was vigorously stirred for 30 min., recooled to -15°C and neutralized to $\text{PH} = 6.0$ with aqueous NaOH (50% in H_2O). The water was removed in vacuo and the resulting orange solid chromatographed on silica gel (96:4 dichloromethane/methanol)

Yield 40%

^1H NMR (200 MHz, DMSO- d_6) δ 12.82 (s, 1H, 9-NH), 7.85 (s, H8), 7.34-7.63 (m, 5H, ArH), 5.26 (s, 2H, OCH_2).

ESI-MS: m/z (%): 243.3 (100) $[1-\text{H}]^-$.

Derivative 12: 6-(benzyloxy)-N-decyl-guanine



A stirred solution of **11** (40mg, 0.4 mmol) and decylamine (0.100 ml 3.eq) in a mixture of 2-methoxyethanol(2.5 mL) was heated at reflux. After 3 h, the mixture was chilled in an ice bath, and the precipitate was filtered and washed with concentrated aqueous

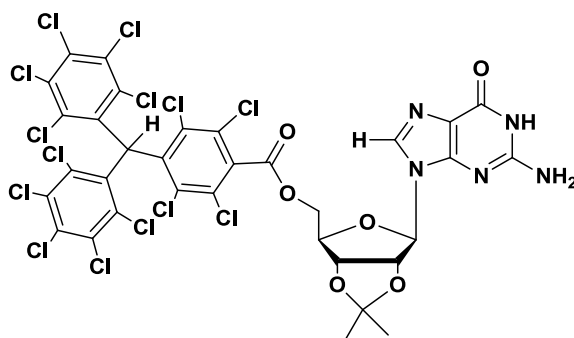
ammonia and methanol. The product was purified by dissolving the precipitate (yellow solid) in hot 1 N sodium hydroxide. The hot mixture was filtered, acidified with glacial acetic acid washed with methanol, and dried over phosphorus pentoxide. The product was purified by silica gel chromatography eluting with: dichloromethane and dichloromethane /methanol 93:7.

Yield 40%

^1H NMR (200 MHz, DMSO- d_6) δ 12.82 (s, 1H, 9-NH), 7.85 (s, H8), 7.34-7.63 (m, 5H, ArH), 6.5 (t, 1H, NH) 5.26 (s, 2H, OCH₂) 3.09 (dt 2H, NHCH₂), 1.4 (m, 2H, CH₂), 1.2 (m, 16H) 0.87 (t, 3H).

ESI-MS: m/z (%): 380.1 (100) [1-H]⁺

Derivative 28: **α HPTMGACE**



To a suspension of **29** (669 mg, 0.85 mmol) in dry THF (20 mL) was added distilled TEA (117 μ L, 1 eq.) Sigma Aldrich 2',3'-O-isopropylidene-guanosine (GAce 274 mg, 0.85 mmol) and a catalytic amount of DMAP. The pink mixture was stirred under argon for 24h at 80°C. After this time it was added HCl 1N (2 mL), the solvent was evaporated under vacuo and the solid was dissolved in dichloromethane and extracted three times with HCl 1N and water. The organic phase was collected and dried with anhydrous MgSO₄. The title compound was purified by silica chromatographic column using a mixture of dichloromethane/methanol 98:2

R_f = 0.5 (CH₂Cl₂/CH₃OH 96:4)

Yield 40 %

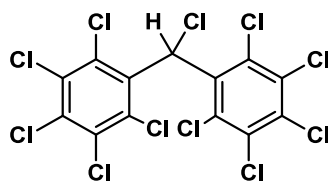
^1H NMR (600 MHz, DMSO- d_6): δ 10.72 (br. s 1H, NH) 7.83 (s, 1H, H8) 6.9 (s, 1H, αH), 6.5 (br. s, 2H, NH_2) 6.08 (s, 1H, H_1' -sugar), 5.32(d, 1H, H_2' -sugar), 5.27 (m, 1H, H_3' -sugar), 4.59 (m, 2H, $\text{H}_5'/$

H_5'' -sugar), 4.42 (m, 1H, H_4'), 1.51/1.31 (s, 6H, $(\text{CH}_3)_2$).

^{13}C (300 MHz, DMSO- d_6): δ 162.29 (C), 156.68 (C), 153.67 (C), 150.35 (C), 138.57 (C), 136.35 (CH), 135.60 (C), 135.48 (C), 134.44 (C), 134.36 (C), 134.30 (C), 133.53 (C), 133.50 (C), 133.15 (C), 132.98 (C), 131.86 (C), 129.69 (C), 128.67 (C), 117.0 (C), 113.28 (C), 113.20 (C), 88.72 (CH), 84.20 (CH), 83.72 (CH), 81.23 (CH), 66.88 (CH_2), 55.96 (CH), 26.90 (CH_3), 25.26 (CH_3).

ESI-MS: m/z (%): 1073.8. (100) [1-H] $^-$ 1039.7 (100) [$\text{M}-35$].

Derivative 30: **6,6'-(chloromethylene)bis(1,2,3,4,5-pentachlorobenzene)**



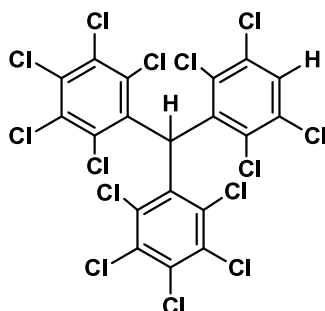
The synthesis of **30** (PDM) was carried out according the literature.^[10] A mixture of 1,2,3,4,5-pentachlorobenzene (10 g, mmol 39,9), chloroform (1.6 mL, 2 eq.) and aluminium chloride (2,6 g, 2eq) was heated at 130°C for 3,5h in a glass pressure vessel. The mixture was poured on to ice /HCl 1N and extracted with chloroform. The organic layer was washed with water dried with sodium sulfate and evaporated. The product was recrystallized from chloroform.

Yield 80%

^1H NMR (200 MHz, CDCl_3): δ 7.12 (s, 1H, αH).

ESI-MS: m/z (%): 546.3.3 (100) [1-H] $^-$.

Derivative 31: 6,6((2,3,5,6,tetrachlorophenyl)methylene)bis(1,2,3,4,5pentachlorobenzene)



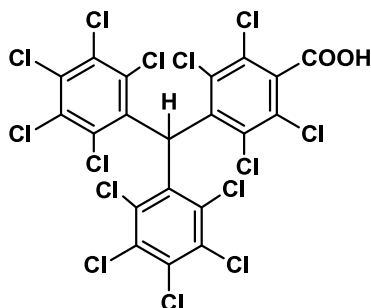
The synthesis of **31** (α HPTMmH) was carried out according the literature.^[10] A mixture of **30** (5 g, mmol 9.1), tetrachlorobenzene (3.9 g, 2eq.) and aluminium chloride (1,2 g, 2eq.) was heated at 150°C for 1,5h in a glass pressure vessel. The mixture was poured on to ice /HCl 1N and extracted with chloroform. The organic layer was washed with water dried with sodium sulfate and evaporated. The raw material by silica gel chromatography eluting with hexane Unreacted tetrachlorobenzene was separated from the title compound by sublimation.

Yield 70%

¹H NMR (200 MHz, CDCl₃): δ 6.90 (s, 1H, α H), 7.65 (s, 1H, ar-H).

ESI-MS: m/z (%): 725.3.3 (100) [1-H]⁻ 690.3 (100) [M-35]

Derivative 32: 4-(bis(perchlorophenyl)methyl)-2,3,5,6,tetrachlorobenzoic acid



A mixture of **31** α HPTMmH (1.3 g, 1.8 mmol) and TMEDA (286 μ l, 1 eq.) were dissolved in dry THF (40 mL), under a slight flux of argon at low temperature (-78°). To the mixture was added n-butyl lithium 1.6M in hexane (1.1 mL, 1.05 eq.). The reaction

was kept at low temperature for 30 min..Then an excess of CO₂ was added , the reaction was stirred under CO₂ pression for 24 h. After this period the solvent was evaporated and the product was dissolved in ether and extracted with water, the aqueous phase was acidified with HCl 37% and extracted with ether three times.The organic layer was dried with anhydrous magnesium sulphate. The product (α HPTMMC) was purified by silica chromatographic column using a mixture of dichlorometane/methanol 90:1

Yield 46 %

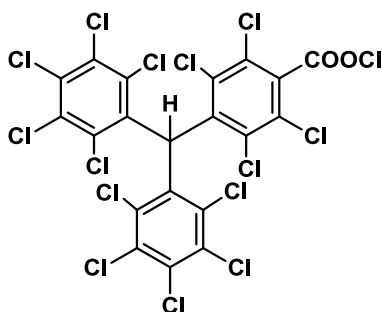
IR-ATR ν (cm⁻¹): 3455, 1713, 1563, 1441, 1372, 1337, 1296, 1239, 1215, 935, 864, 811.

¹H NMR (600 MHz, DMSO-d₆): δ 6.90 (s, 1H, α H).

¹³C (600 MHz, DMSO-d₆): δ 163.79, 137.22, 137.14, 135.09, 135.02, 134.18, 134.07, 133.81, 133.61,133.49, 133.43, 133.45, 133.01, 132.46, 132.39, 128.80, 127.92, 56.49.

ESI-MS: m/z (%): 769.3. (100) [1-H] 725.3 (100) [M-45]

Derivative 33: 4-(bis(perchlorophenyl)methyl)-2,3,5,6,tetrachlorobenzoyl chloride



A solution of **32** (α HPTMMC 1 g, 1.3 mmol) in thionyl chloride (5 mL) was refluxed for 24 h.^[11]Excess of SOCl₂ was removed by distillation. The resulting solid was washed with pentane and purified by chromatography (silica gel, chloroform).

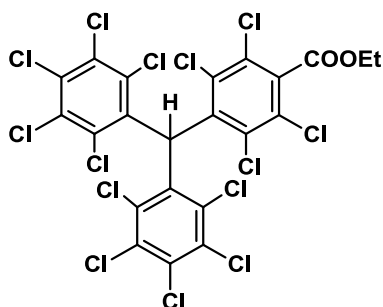
Yield 80%

IR-ATR ν (cm⁻¹):2924, 1772, 1563, 1441, 1372, 1337, 1296, 1239, 1215, 935, 864, 811.

¹H NMR (600 MHz, DMSO-d₆): δ 6.90 (s, 1H, α H).

ESI-MS: m/z (%): 788.3. (100) [1-H] 753.3 (100) [M-35].

Derivative 34: Ethyl-4-(bis(perchlorophenyl)methyl)2,3,5,6,tetrachlorobenzoate



A mixture of **31** α HPTMmH. (0.800 g, 1.10 mmol) and TMEDA (tetramethylethylenediamine 163 μ l, 1.10 eq.) were dissolved in dry THF (50 mL), under a slight flux of argon at low temperature (-78°). To the mixture was added n-butyl lithium 1.6M in hexane (0.690 mL, 1.05 eq.).^[12] The reaction was kept at low temperature for 30 min. Then an excess of ethylchloroformiate (20 mL) was added, the reaction was stirred for 12h. The solvent was evaporated and the raw amterial was dissolved in dichlorometane and extracted three times with water.The organic layer was collected and dried with anhydrous magnesium sulphate.The product was purified by silica chromatographic column using a mixture of hexane/ethylacetate (97:3).

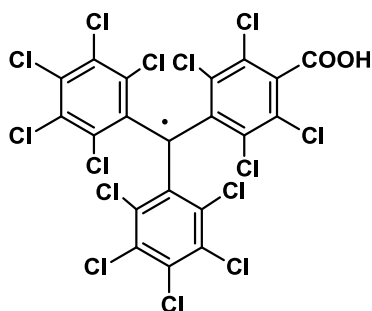
Yield 45 %

ESI-MS: m/z (%): 797.6. (100) [1-H]⁻ 763.3 (100) [M-35]

¹H NMR (200 MHz, DMSO-d₆): δ 6.90 (s, 1H, α H), 4.21 (q, $J = 7.2$ Hz, 2H, -OCH₂), 1.09 (t, $J = 7.1$ Hz, 3H, CH₃).

ESI-MS: m/z (%): 797.6. (100) [1-H]⁻ 763.3 (100) [M-35].

Derivative 35: 4-(bis(perchlorophenyl)methyl)-2,3,5,6,tetrachlorobenzoic acid radical

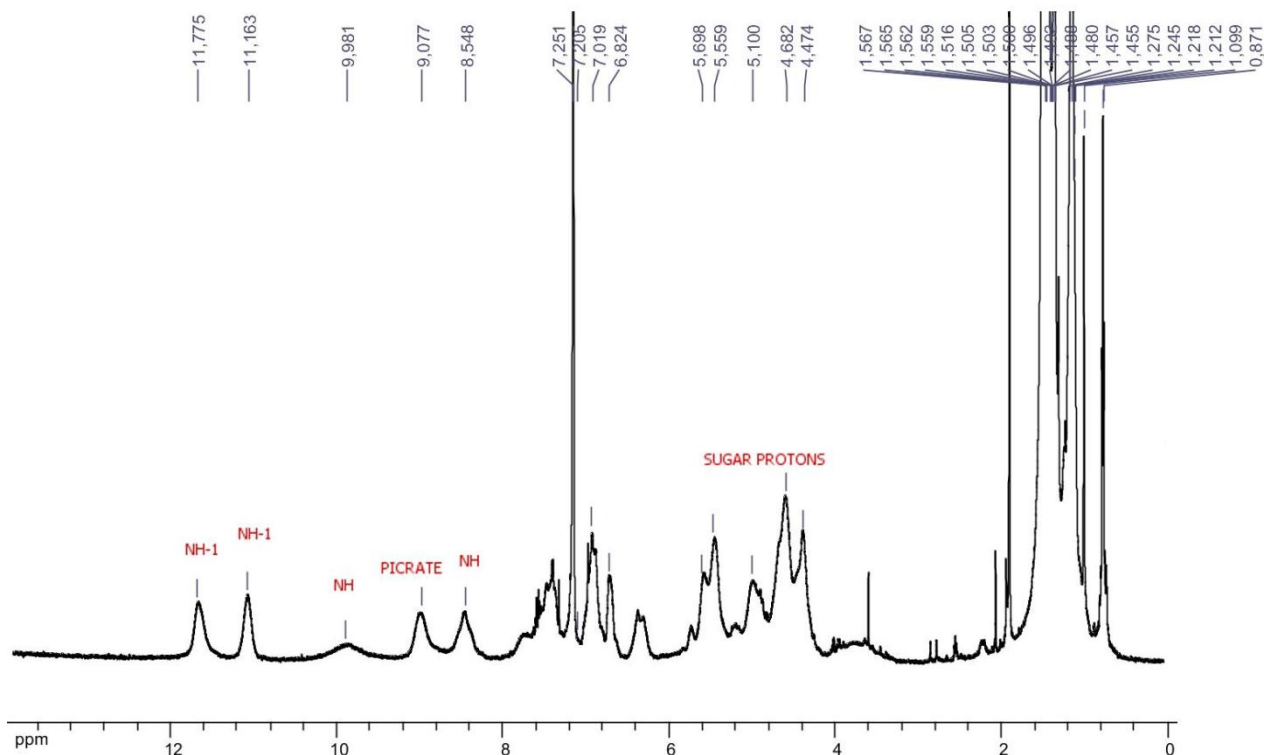


A mixture of acid **32** (264 mg, 0.34 mmol) and NaOH (1g, 25 mmol), was dissolved in a solution of ether (130 ml) and DMSO (25 ml) and stirred for 96 hs in the dark. The mixture was filtered and solid iodine (1.17 eq.) was added into the solution which was left undisturbed in the dark room for 30 min. after which it was washed with a solution of sodium hydrogen sulphite and then acidified with HCl to obtain a red precipitate. Such a solution was extracted with Et₂O. The organic phase was dried with anhydrous magnesium sulphate, filtered and then solvent evaporated under vacuum. The collected red solid was the pure compound **35**.

Yield 40%

IR-ATR ν (cm⁻¹): 3455, 1713, 1563, 1441, 1372, 1337, 1296, 1239, 1215, 935, 864, 811.

ESI-MS: m/z (%): 769.3. (100) [1-H]⁻ 725.3 (100) [M-45]



$^1\text{H-NMR}$ spectra (600 MHz) of **28** (10mM) recorded in CDCl_3 , in CDCl_3 with potassium picrate 8:1(octamer), in CDCl_3 with strontium picrate 8:1 (hexadecamer).

STM investigation

STM measurements were performed using a Veeco scanning tunneling microscope (multimode Nanoscope III, Veeco) in constant current mode at the interface between highly oriented pyrolytic graphite (HOPG) and a supernatant solution. Diluted solutions of all guanine derivatives were applied to the basal plane of the surface. For STM measurements the substrates were glued on a magnetic disk and an electric contact is made with silver paint (Aldrich Chemicals). The STM tips were mechanically cut from a Pt/Ir wire (90/10, diameter 0.25 mm). The raw STM data were processed through the application of background flattening and the drift was corrected using the underlying graphite lattice as a reference. The latter lattice was visualized by lowering the bias voltage to 20 mV and raising the current to 65 pA. All of the models were minimized with Chem3D at the MM2 level, which includes potentials for H-bonds and torsion

potentials for describing rotations around single bonds. It was decided to use MM2 force field since is a rather inexpensive method from the computational time viewpoint which has been proven to be successfully employed to describe poly-atomic structures based on H-bonding. Mother solution of alkylated guanine derivatives were dissolved in DMSO at 95°C and diluted with 1,2,4-trichlorobenzene (TCB) to give 1mM solutions. Monolayer pattern formation was achieved by applying 4 μ L of solution onto freshly cleaved HOPG. Then STM images were recorded only after achieving a negligible thermal drift.

Bibliography

1. R. Zou and M. J. Robins, *Can. J. Chem.* **1987**, *65*, 1436-1437
2. A. Ciesielski, R. Perone, S. Pieraccini, G. P. Spada, P. Samorì, *Chem. Commun.*, **2010**, *46*, 4493-4495
3. Myllymaki, V. T.; Lindvall, M. K.; Koskinen, A. M. P. *Tetrahedron Lett.* **2001**, *57*, 4629-4635
4. M. Sako,* H. Kawada, and K. Hirota *J. Org. Chem.* **1999**, *64*, 5719-5721
5. M. A. Michael, H. B. Cottam, D. F. Smee, R. K. Robins and G. D. Kini *J. Med. Chem.* **1993**, *36*, 3431-343.
6. E. C. Western, J. R. Daft, E. M. Johnson, P. M. Gannett, K. H. Shaughnessy, *J. Org. Chem.* **2003**, *68*, 6767-6774
7. G. E. Wright, L. W. Dudycz, *J. Med. Chem.* **1984**, *27*, 175-181
8. Beach, J. Warren; Kim, Hea O.; Jeong, Lak S; Nampalli, Satyanarayana; Islam, Qamrul et al. *J. Org. Chem.* **1992**, *54*, 3887-3894
9. W02008/101514 A1, *NANODREAM S.R.L. UNIPERSONAL*, 2008
10. M. Ballester, J. Riera, J. Castañer, C. Rovira and O. Armet *Synthesis-Stuttgart*, **1986**, *1*, 64-66
11. S. Chopin, J. Cousseau, E. Levillain, C. Rovira, J. Veciana, A. S. D. Sandanayaka, Y. Araki and O. Ito *J. Mater. Chem.*, **2006**, *16*, 112-121
12. V. Dang, J. H. Wang, S. Feng, C. Buron, F. A. Villamena, P. G. Wang and P. Kuppusamy *Bioorganic & Medicinal Chemistry Letters*, **2007**, *17*, 4062